

Oncology and Translational Medicine

Volume 6 • Number 6 • December 2020

Comparable outcomes but higher risks of prolonged viral RNA shedding duration and secondary infection in cancer survivors with COVID-19: A multi-center, matched retrospective cohort study

Hui Peng, Sheng Wang (Co-first author), Qi Mei, Yuhong Dai, Jian Li, Ming Li, Kathrin Halfter, Xueyan Jiang, Qin Huang, Lei Wang, Wei Wei, Ru Liu, Zhen cao, Motuma Yigezu Daba, Fangfang Wang, Bingqing Zhou, Hong Qiu, Xianglin Yuan 237

Identification of potential immune-related prognostic biomarkers of lung cancer using gene co-expression network analysis

Aixia Chen, Shengnan Zhao, Fei Zhou, Hongying Lv, Donghai Liang, Tao Jiang, Rui Liu, Lijin Zhu, Jingyu Cao, Shihai Liu, Hongsheng Yu 247

Silencing Neuropilin 1 gene reverses TGF- β 1-induced epithelial mesenchymal transition in HGC-27 gastric cancer cell line

Weiguo Xu, Xin Yang, Qiqi Zhan, Guanyi Ding, Shang Guo, Bing Zhu, Hong Xu, Xiangmei Liu 258

Oncology and Translational Medicine

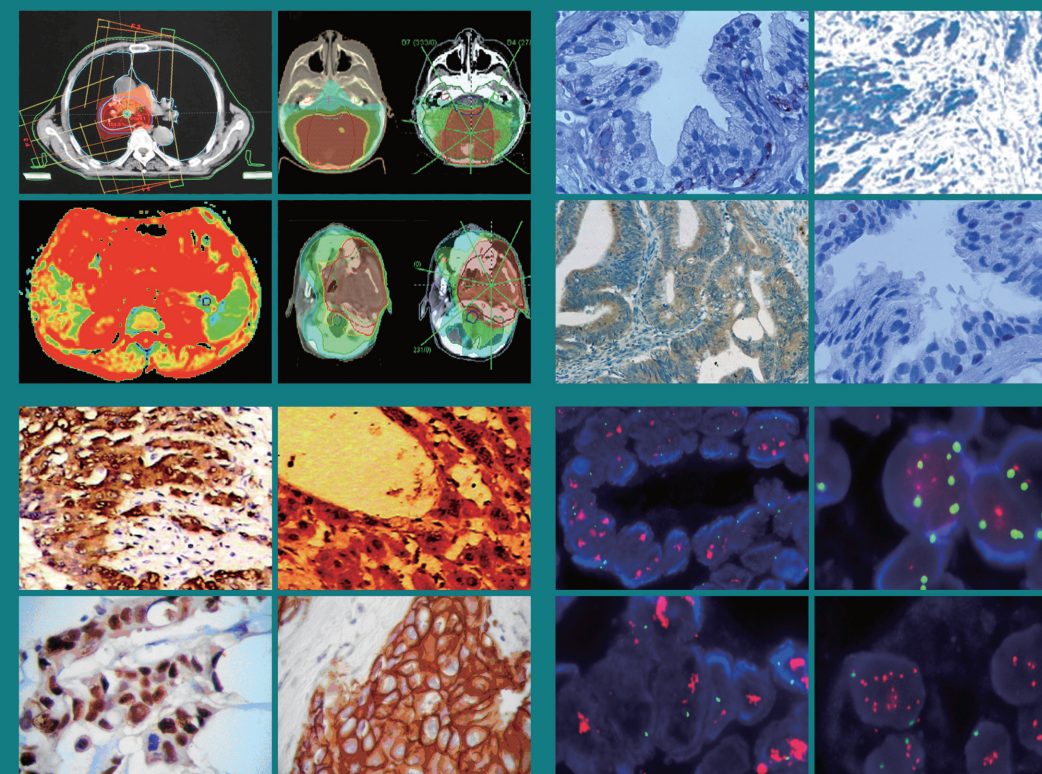
Volume 6 • Number 6 • December 2020

pp 237-281

Oncology and Translational Medicine

肿瘤学与转化医学（英文）

ISSN 2095-9621
CN 42-1865/R



Online First
Immediately Online

otm.tjh.com.cn

Faster
publication!

邮发代号: 38-121

ISSN 2095-9621



9 772095 962204



GENERAL INFORMATION
» otm.tjh.com.cn

Volume 6
Number 6
December 2020





Honorary Editors-in-Chief

W.-W. Höpker (Germany)
Mengchao Wu (China)
Yan Sun (China)

Editors-in-Chief

Anmin Chen (China)
Shiying Yu (China)

Associate Editors

Yilong Wu (China)
Shukui Qin (China)
Xiaoping Chen (China)
Ding Ma (China)
Hanxiang An (China)
Yuan Chen (China)

Editorial Board

A. R. Hanauske (Germany)
Adolf Grünert (Germany)
Andrei Iagaru (USA)
Arnulf H. Hölscher (Germany)
Baoming Yu (China)
Bing Wang (USA)
Binghe Xu (China)
Bruce A. Chabner (USA)
Caicun Zhou (China)
Ch. Herfarth (Germany)
Changshu Ke (China)
Charles S. Cleeland (USA)
Chi-Kong Li (China)
Chris Albanese (USA)
Christof von Kalle (Germany)
D Kerr (United Kingdom)
Daoyu Hu (China)
Dean Tian (China)
Di Chen (USA)
Dian Wang (USA)
Dieter Hoelzer (Germany)
Dolores J. Schendel (Germany)
Dongfeng Tan (USA)
Dongmin Wang (China)
Ednin Hamzah (Malaysia)
Ewerbeck Volker (Germany)
Feng Li (China)
Frank Elsner (Germany)
Gang Wu (China)
Gary A. Levy (Canada)
Gen Sheng Wu (USA)
Gerhard Ehninger (Germany)
Guang Peng (USA)
Guangying Zhu (China)
Gunther Bastert (Germany)
Guoan Chen (USA)

Guojun Li (USA)
Guoliang Jiang (China)
Guoping Wang (China)
H. J. Biersack (Germany)
Helmut K. Seitz (Germany)
Hongbing Ma (China)
Hongtao Yu (USA)
Hongyang Wang (China)
Hua Lu (USA)
Huaqing Wang (China)
Hubert E. Blum (Germany)
J. R. Siewert (Germany)
Ji Wang (USA)
Jiafu Ji (China)
Jianfeng Zhou (China)
Jianjie Ma (USA)
Jianping Gong (China)
Jihong Wang (USA)
Jilin Yi (China)
Jin Li (China)
Jingyi Zhang (Canada)
Jingzhi Ma (China)
Jinyi Lang (China)
Joachim W. Dudenhausen (Germany)
Joe Y. Chang (USA)
Jörg-Walter Bartsch (Germany)
Jörg F. Debatin (Germany)
JP Armand (France)
Jun Ma (China)
Karl-Walter Jauch (Germany)
Katherine A. Siminovitch (Canada)
Kongming Wu (China)
Lei Li (USA)
Lei Zheng (USA)
Li Zhang (China)
Lichun Lu (USA)
Lili Tang (China)
Lin Shen (China)
Lin Zhang (China)
Lingying Wu (China)
Luhua Wang (China)
Marco Antonio Velasco-Velázquez (Mexico)
Markus W. Büchler (Germany)
Martin J. Murphy, Jr (USA)
Mathew Casimiro (USA)
Matthias W. Beckmann (Germany)
Meilin Liao (China)
Michael Buchfelder (Germany)
Norbert Arnold (Germany)
Peter Neumeister (Austria)
Qing Zhong (USA)
Qinghua Zhou (China)

Qingyi Wei (USA)
Qun Hu (China)
Reg Gorczynski (Canada)
Renyi Qin (China)
Richard Fielding (China)
Rongcheng Luo (China)
Shenjiang Li (China)
Shenqiu Li (China)
Shimosaka (Japan)
Shixuan Wang (China)
Shun Lu (China)
Sridhar Mani (USA)
Ting Lei (China)
Ulrich Sure (Germany)
Ulrich T. Hopt (Germany)
Ursula E. Seidler (Germany)
Uwe Kraeuter (Germany)
W. Hohenberger (Germany)
Wei Hu (USA)
Wei Liu (China)
Wei Wang (China)
Weijian Feng (China)
Weiping Zou (USA)
Wenzhen Zhu (China)
Xianglin Yuan (China)
Xiaodong Xie (China)
Xiaohua Zhu (China)
Xiaohui Niu (China)
Xiaolong Fu (China)
Xiaoyuan Zhang (USA)
Xiaoyuan (Shawn) Chen (USA)
Xichun Hu (China)
Ximing Xu (China)
Xin Shelley Wang (USA)
Xishan Hao (China)
Xiuyi Zhi (China)
Ying Cheng (China)
Ying Yuan (China)
Yixin Zeng (China)
Yongjian Xu (China)
You Lu (China)
Youbin Deng (China)
Yuankai Shi (China)
Yuguang He (USA)
Yuke Tian (China)
Yunfeng Zhou (China)
Yunyi Liu (China)
Yuquan Wei (China)
Zaide Wu (China)
Zefei Jiang (China)
Zhangqun Ye (China)
Zhishui Chen (China)
Zhongxing Liao (USA)

Oncology and Translational Medicine

December 2020 Volume 6 Number 6

Contents

Comparable outcomes but higher risks of prolonged viral RNA shedding duration and secondary infection in cancer survivors with COVID-19: A multi-center, matched retrospective cohort study

Hui Peng, Sheng Wang (Co-first author), Qi Mei, Yuhong Dai, Jian Li, Ming Li, Kathrin Halfter, Xueyan Jiang, Qin Huang, Lei Wang, Wei Wei, Ru Liu, Zhen cao, Motuma Yigezu Daba, Fangfang Wang, Bingqing Zhou, Hong Qiu, Xianglin Yuan 237

Identification of potential immune-related prognostic biomarkers of lung cancer using gene co-expression network analysis

Aixia Chen, Shengnan Zhao, Fei Zhou, Hongying Lv, Donghai Liang, Tao Jiang, Rui Liu, Lijin Zhu, Jingyu Cao, Shihai Liu, Hongsheng Yu 247

Silencing Neuropilin 1 gene reverses TGF- β 1-induced epithelial mesenchymal transition in HGC-27 gastric cancer cell line

Weiguo Xu, Xin Yang, Qiqi Zhan, Guanyi Ding, Shang Guo, Bing Zhu, Hong Xu, Xiangmei Liu 258

Influence of lymph node micrometastasis on the staging system for gastric cancer

Lixiong Gao, Xiankun Ren, Guiquan Li, Benhua Wu, Xuan Chen 266

Salvage treatments for prostate-specific antigen relapse of cT₃N₀M₀ prostatic adenocarcinoma after radical prostatectomy combined with neoadjuvant androgen deprivation

Lufang Zhang, Dongliang Pan, Ludong Liu, Yunjiang Zang, Ningchen Li 272

Intervention for oxaliplatin-induced hypersensitivity in China: a cross-sectional internet-based survey

Min Li, Wei Li, Yue Wang, Xiaofang Shangguan, Rui Huang, Dong Liu, Chengliang Zhang 277

Oncology and Translational Medicine

Volume 6 • Number 6 • December 2020

Aims & Scope

Oncology and Translational Medicine is an international professional academic periodical. The Journal is designed to report progress in research and the latest findings in domestic and international oncology and translational medicine, to facilitate international academic exchanges, and to promote research in oncology and translational medicine as well as levels of service in clinical practice. The entire journal is published in English for a domestic and international readership.

Copyright

Submission of a manuscript implies: that the work described has not been published before (except in form of an abstract or as part of a published lecture, review or thesis); that it is not under consideration for publication elsewhere; that its publication has been approved by all co-authors, if any, as well as – tacitly or explicitly – by the responsible authorities at the institution where the work was carried out.

The author warrants that his/her contribution is original and that he/she has full power to make this grant. The author signs for and accepts responsibility for releasing this material on behalf of any and all co-authors. Transfer of copyright to Huazhong University of Science and Technology becomes effective if and when the article is accepted for publication. After submission of the Copyright Transfer Statement signed by the corresponding author, changes of authorship or in the order of the authors listed will not be accepted by Huazhong University of Science and Technology. The copyright covers

the exclusive right and license (for U.S. government employees: to the extent transferable) to reproduce, publish, distribute and archive the article in all forms and media of expression now known or developed in the future, including reprints, translations, photographic reproductions, microform, electronic form (offline, online) or any other reproductions of similar nature.

Supervised by

Ministry of Education of the People's Republic of China.

Administered by

Tongji Medical College, Huazhong University of Science and Technology.

Submission information

Manuscripts should be submitted to:
<http://otm.tjh.com.cn>
dmedizin@sina.com

Subscription information

ISSN edition: 2095-9621
CN: 42-1865/R

■ Subscription rates

Subscription may begin at any time. Remittances made by check, draft or express money order should be made payable to this journal. The price for 2020 is as follows: US \$ 30 per issue; RMB ¥ 28.00 per issue.

Database

Oncology and Translational Medicine is abstracted and indexed in EMBASE, Index Copernicus, Chinese Science and Technology Paper Citation Database (CSTPCD), Chinese Core Journals Database, Chinese Journal Full-text Database (CJFD), Wanfang

Data; Weipu Data; Chinese Academic Journal Comprehensive Evaluation Database.

Business correspondence

All matters relating to orders, subscriptions, back issues, offprints, advertisement booking and general enquiries should be addressed to the editorial office.

Mailing address

Editorial office of
Oncology and Translational Medicine
Tongji Hospital
Tongji Medical College
Huazhong University of Science and Technology
Jie Fang Da Dao 1095
430030 Wuhan, China
Tel.: +86-27-69378388
Email: dmedizin@sina.com

Printer

Changjiang Spatial Information
Technology Engineering Co., Ltd.
(Wuhan) Hangce Information
Cartography Printing Filial, Wuhan,
China
Printed in People's Republic of China

Editors-in-Chief

Anmin Chen
Shiyong Yu

Managing director

Jun Xia

Executive editors

Jing Chen
Jun Xia
Yening Wang
Qiang Wu

Comparable outcomes but higher risks of prolonged viral RNA shedding duration and secondary infection in cancer survivors with COVID-19: A multi-center, matched retrospective cohort study*

Hui Peng¹, Sheng Wang² (Co-first author), Qi Mei¹, Yuhong Dai¹, Jian Li³, Ming Li⁴, Kathrin Halfter⁵, Xueyan Jiang¹, Qin Huang¹, Lei Wang⁶, Wei Wei⁷, Ru Liu⁸, Zhen cao⁹, Motuma Yigezu Daba¹, Fangfang Wang¹, Bingqing Zhou¹, Hong Qiu¹ (✉), Xianglin Yuan¹ (✉)

¹ Department of Oncology, Tongji Hospital, Tongji Medical College, Huazhong University of Science and Technology, Wuhan 430030, China

² Department of Radiotherapy, Zhongda Hospital, Medical College of Southeast University, Nanjing 210009, China

³ Institute of Experimental Immunology, University Clinic of Rheinische Friedrich-Wilhelms-University, Bonn 53127, Germany

⁴ Department of Oncology, Wuhan Pulmonary Hospital, Wuhan 430030, China

⁵ Tumor Register Munich, Ludwig-Maximilian-University, Munich 81377, Germany

⁶ Dangyang People's Hospital, Yichang 444100, China

⁷ Department of Medical Affairs, Tongji Hospital, Tongji Medical College, Huazhong University of Science and Technology, Wuhan 430030, China

⁸ Department of Pulmonary Vascular and General Medicine, Fuwai Yunnan Cardiovascular Hospital, Kunming 650102, China

⁹ Wuhan Wuchang Hospital, Wuhan 430030, China

Abstract

Objective To identify the differences in clinical features and outcomes between cancer survivors and non-cancer patients with coronavirus disease 2019 (COVID-19).

Methods In this multicenter, retrospective, and observational cohort study from February 10, 2020 to March 31, 2020 in Wuhan, China, all cancer survivors infected with COVID-19 were screened, and statistically matched with non-cancer patients with COVID-19 using propensity score matching. Demographic, clinical, treatment, and laboratory data were extracted from a standardized medical recording system and underwent review and assessment.

Received: 12 November 2020

Revised: 4 December 2020

Accepted: 15 December 2020

✉ Correspondence to: Hong Qiu. Email: tqiu@163.com;
Xianglin Yuan. Email: xlyuan1020@163.com

* Supported by grants from the SGC's Rapid Response Funding for Bilateral Collaborative Emergence COVID-19 Project between China and Germany (No. C-0065), COVID-19 Emergency Project of Huazhong University of Science and Technology (No. 2020kfyXG-YJ062), and Hepatobiliary and Pancreatic Cancer Grant, Hubei Chen Xiaoping Science and Technology Development Foundation (No. CXPJH12000001-2020344).

© 2020 Huazhong University of Science and Technology

Abstract

Results Sixty-one cancer survivors and 183 matched non-cancer patients were screened from 2,828 COVID-19 infected patients admitted to 4 hospitals in Wuhan, China. The median ages of the cancer survivor cohort and non-cancer patient cohort were 64.0 (55.0–73.0) and 64.0 (54.0–73.5), respectively ($P = 0.909$). Cancer survivors reported a higher incidence of symptom onset than non-cancer patients. Fever (80.3% vs. 65.0%; $P = 0.026$) was the most prevalent symptom, followed by cough (65.6% vs. 37.7%; $P < 0.001$), myalgia, and fatigue (45.9% vs. 13.6%; $P < 0.001$). The risks of the development of severe events (adjusted hazard ratio [AHR] = 1.25; 95% confidence interval [CI]: 0.76–2.06; $P = 0.378$) and mortality (relative risk [RR] = 0.90, 95% CI: 0.79–1.04; $P = 0.416$) in the cancer survivor cohort were comparable to those of the matched non-cancer patient cohort. However, the cancer survivor cohort showed a higher incidence of secondary infection (52.5% vs. 30.1%; RR = 1.47, 95% CI: 1.11–1.95; $P = 0.002$) and a prolonged viral RNA shedding duration (32 days [IQR 26.0–46.0] vs. 24.0 days [IQR 18.0–33.0]; AHR = 0.54; 95% CI: 0.38–0.80; $P < 0.05$).

Conclusion Compared to non-cancer patients, cancer survivors with COVID-19 exhibited a higher incidence of secondary infection, a prolonged period of viral shedding, but comparable risks of the development of severe events and mortality. It is helpful for clinicians to take tailored measures to treat cancer survivors with COVID-19.

Key words: COVID-19; SARS-CoV-2; cancer survivor; prognosis; viral shedding; mortality

Since the beginning of the coronavirus disease 2019 (COVID-19) outbreak in late December 2019, the epidemic has swept the world at an alarming rate. Due to its highly contagious nature and global spread, the World Health Organization (WHO) has declared the coronavirus outbreak a pandemic. Globally, as of 11 November, 2020, there have been 51,251,715 confirmed cases of COVID-19, including 1,270,930 deaths according to the WHO report^[1].

According to a report by the GLOBOCAN 2018, it was estimated that there would be 18.1 million newly diagnosed cancer patients worldwide in 2018^[2]. Given the global spread of COVID-19, the infected population may contain a large number of cancer patients. Currently, patients with cancer are considered to be more susceptible to COVID-19 and at a higher risk for a severe disease course^[3–6]. Studies have suggested that cancer patients have a worse prognosis than individuals without cancer owing to the immunocompromised status caused by malignancy and anti-cancer treatments, including surgery, chemotherapy, radiotherapy, and immunotherapy^[5, 7]. A retrospective analysis of patients in Wuhan showed that cancer patients were 2.3 times more likely to be infected with COVID-19 than the community population⁸. The case-fatality rate among patients with preexisting cancer reached 5.6% compared to 2.3% in general patients^[6]. The small sample size of these studies may have limited the representativeness of the results.

With advances in early diagnosis, improved treatment options, and increased life expectancy, an increasing number of cancer patients are cured and survive^[9–10]. Cancer survivors are a huge population that cannot be ignored in this COVID-19 outbreak. Due to distinctions in nutritional and immune status, it is assumed that cancer survivors and patients may have different outcomes after

COVID-19. A study on COVID-19 patients with cancer showed that non-metastatic cancer patients experienced similar frequencies of severe conditions to those observed in patients without cancer^[11]. However, non-metastatic cancer patients are the same as cancer survivors; nearly half of the patients in the study had received anti-cancer treatment within 40 days, and the interference in outcome could not be ruled out.

Thus, we collected the clinical data of 61 cancer survivors from 4 designated hospitals in Wuhan and compared them with the data of 183 matched non-cancer patients. Our study aimed to determine the clinical characteristics and outcomes of cancer survivors with COVID-19 and identified the difference with non-cancer patients.

Materials and methods

Study design and patients

This retrospective cohort study included two cohorts of adult patients and was conducted in four designated hospitals for COVID-19 patients in Wuhan, including the Optical Valley Branch of Tongji Hospital affiliated with Tongji Medical College of Huazhong University of Science and Technology, Sino-French New Town Branch of Tongji Hospital, Wuhan Pulmonary Hospital, and Wuhan No.1 Hospital. The cancer survivor cohort consisted of cancer survivors who were confirmed to have COVID-19 infection by RNA testing of swab samples, and the non-cancer patient cohort consisted of matched COVID-19 patients without a history of cancer, all of whom were discharged or died between February 10 and March 31, 2020. Each cancer survivor was matched to 3 patients using a propensity score with a caliper value equal to 0.03. This study was approved by the ethics committee

of Tongji Hospital of Huazhong University of Science and Technology (No. TJ-IRB20200409) and was registered in the Chinese Clinical Trial Registry (registration number: ChiCTR2000031327). The requirement for informed consent was waived by the ethics committee.

Data collection and definition

The demographic data, past medical history, onset symptoms, laboratory testing, treatments, and outcome parameters were collected via a standardized electronic medical record. All data were verified by two researchers and reviewed by a third researcher.

The European Organization for Research and Treatment of Cancer (EORTC) Cancer Survivorship Task Force definition of cancer survivors have been adopted in this study, namely, patients who have completed their primary treatment [12]. Restrictions were added on the basis of the EORTC Cancer Survivorship Task Force definition to distinguish between cancer patients and cancer survivors in this study. The included cancer survivors were all diagnosed with malignant tumors, had a treatment-free interval of more than six months, and showed no evidence of disease, while adjuvant endocrine therapy was acceptable.

We defined survival time as the interval between hospital admission and the final events, discharge, or death. Severe events included severe and critical illness, and the time to severe events was defined as the interval between symptom onset and the diagnosis of severe or critical illness by the physician according to the diagnosis standard [13]. Viral RNA shedding duration was defined as the interval between symptom onset and the date of the last severe acute respiratory syndrome coronavirus 2 (SARS-CoV-2) RNA-positive result for naso- or oropharyngeal swabs.

Severe illness was defined as meeting at least one of the following criteria: 1. Shortness of breath, respiratory rate ≥ 30 /min; 2. pulse oxygen saturation (SpO₂) $\leq 93\%$ at rest; 3. partial pressure of arterial oxygen (PaO₂) to fraction of inspired oxygen (FiO₂) ≤ 300 mmHg (1 mmHg = 0.133kPa). Critical illness was defined as meeting at least one of the following criteria: 1. respiratory failure occurred and mechanical ventilation was required; 2. shock; 3. combined with failure of other organs and intensive care unit treatment was required [13].

Acute respiratory distress syndrome (ARDS) was defined according to the Berlin Definition [14], acute kidney injury according to the KDIGO Clinical Practice Guidelines [15], and shock according to the 2016 Third International Consensus Definition [16]. Secondary infection was diagnosed when patients exhibited clinical symptoms of pneumonia or bacteremia, or a new laboratory-confirmed pathogen after admission [16].

Statistical analysis

Descriptive statistical methods were used to analyze the variables. Categorical variables were described as n (%) and the characteristics between cancer and non-cancer were compared using the Chi-square test or Fisher's exact test. Continuous variables are shown as medians with interquartile ranges (IQRs), and the Mann-Whitney U test was conducted to compare the variables between groups. The Kaplan-Meier method was adopted for time-to-event data to estimate the proportion of events. Propensity score matching was used to make the two groups comparable in clinical and demographic characteristics. Cox proportional hazards models were used to estimate the HRs and 95% CIs for cancer survivors and the main outcomes. Model 1 included age (continuous). Model 2 included age and sex (male, female). Model 3, the final multivariate model, was adjusted for age, sex, hypertension (yes or no), D-dimer (continuous), lactate dehydrogenase (LDH) (continuous), high-sensitivity C-reactive protein (hs-CRP) (continuous), and lymphocyte count (continuous). Previous studies have shown that these factors are related to adverse clinical outcomes [2, 17–19]. Therefore, we chose age, sex, hypertension, D-dimer, LDH, hs-CRP, and lymphocyte count to enter the multivariate-adjusted models.

All P values were two-tailed, and P values less than 0.05 were considered statistically significant. All statistical analyses were conducted using SPSS version 23.0 and R version 3.5.2.

Results

Demographic data and Baseline characteristics

Of the 2,828 COVID-19 patients admitted to the 4 hospitals between February 10 and March 31, 2020, in Wuhan, China, 61 cancer survivors and 183 matched non-cancer patients were included in this study. The median age of cancer survivors was 64 years (IQR 55.0–73.0), and 37 (60.7%) cancer survivors were women. Hypertension was the highest in both cohorts. Cancer survivors reported a higher incidence of symptom onset than non-cancer patients. Fever (80.3% vs. 65.0%, $P = 0.026$) was the most prevalent symptom in both cohorts, followed by cough (65.6% vs. 37.7%; $P < 0.001$), myalgia, and fatigue (45.9% vs. 13.6%; $P < 0.001$) (Table 1). Cancer survivors had histories of 15 different types of cancer: 14 (23.0%) with thyroid cancer, 12 (19.7%) with breast cancer, 12 (19.7%) in the urinary system, 8 (13.1%) in the intestinal tract, 7 (11.4%) had lung cancer, 3 (4.9%) had lymphoma, and 6 (9.8%) had other cancers (Fig. 1a). Moreover, 51 patients (83.6%) had stage I or stage II disease among all cancer survivors. The previous anti-cancer treatments in the cancer cohort consisted of surgery for 37 (60.7%) patients, chemotherapy and/or radiotherapy for 8 (13.1%)

patients, endocrine therapy for 5 (8.2%), targeted therapy for 1 (1.6%), and conservative therapy for 1 (1.6%).

Laboratory findings

Major laboratory results on admission were recorded, and patients in the non-cancer cohort had more prominent laboratory abnormalities than those in the cancer survivor cohort. Lymphocytopenia and anemia were present in 49.2% and 82.0% of the cancer survivors, compared with 68.3% and 56.3% of the non-cancer cohort, respectively, indicating significant differences ($P < 0.05$; Table 2). Compared to the cancer cohort, non-cancer patients showed significantly higher levels of D-dimer (median [IQR], 0.73 [0.39–3.51] vs. 0.58 [0.22–1.68]; $P = 0.002$), LDH (319.0 [241.5–399.0] vs. 218.0 [170.5–373.0]; $P < 0.001$), and hs-CRP (51.7 [14.8–98.0] vs. 25.2 [1.8–59.2]; $P < 0.001$; Table 2). Among patients with available data, non-cancer patients had significantly higher levels of interleukin (IL) 6, IL-10, and IL-1 β than cancer survivors, while the level of ferritin was much lower.

Therapeutic methods

In both cohorts, the majority of patients received antiviral treatment and antibiotics. The application of both treatments was based on empirical experience, except for the secondary infection of the identified pathogen. Among cancer survivors, 16 (26.2%) were prescribed lopinavir/ritonavir (400 mg/day) and 9 (14.9%) arbidol (200 mg/day). In comparison to non-cancer patients, significantly fewer cancer survivors received corticosteroids (22 [36.1%] vs. 132 [72.1%]; $P < 0.001$) and interferon atmotherapy (12 [19.7] vs. 82 [44.8%]; $P < 0.001$; Table 1). It is notable that fewer patients received oxygen therapy in the cancer survivor cohort, which tended to receive simpler respiratory support.

Clinical outcomes and complications

The risks of the development of severe events (HR = 0.73, 95% CI: 0.48–1.11; $P = 0.141$) and survival (HR =

0.62, 95% CI: 0.31–1.23; $P = 0.169$) of cancer survivors were comparable to those of 183 matched non-cancer patients (Fig. 1b, 1d; Table 3). Both cohorts had a comparable mortality rate (15.6% vs. 24.6%; RR = 0.90, 95% CI: 0.79–1.04; $P = 0.416$). During hospitalization, the rates of development of severe and critical illness in the course of disease were comparable between the two cohorts. However, the median duration of viral RNA shedding was longer in the cancer cohort than in the non-cancer cohort (32.0 days [IQR, 26.0–46.0] vs. 24.0 days [IQR, 18.0–33.0]; HR = 0.49, 95% CI: 0.35–0.68; $P < 0.001$; Fig. 1c). The timelines of viral RNA shedding of 61 cancer survivors and 61 randomly selected non-cancer patients are displayed in Fig. 2. During the follow-up after discharge, 4.9% of the cancer survivors retested positive in the SARS-CoV-2 RNA testing, which was slightly higher than that of the non-cancer cohort without a statistical difference (Table 3).

In terms of complications, 32 (52.5%) cancer survivors had secondary infection, which was significantly higher than that of the non-cancer patients (33 [52.5%] vs. 55 [30.1%]; RR = 1.47, 95% CI:MM 1.11–1.95; $P = 0.002$). Other complications, including ARDS and acute cardiac injury, showed no difference between both cohorts (Table 2).

The univariate-adjusted and multivariate-adjusted relationships between cancer survivor status and the main outcomes, including survival time, time to severe events, and viral RNA shedding duration, are presented in Table 4. No significant association was found between cancer survivors and the increasing survival time in the fully adjusted model (AHR = 0.36; 95% CI: 0.11–1.20; $P = 0.096$) between cancer survivors and time to severe events (AHR = 1.25; 95% CI: 0.76–2.06; $P = 0.378$). However, compared to the non-cancer patients, cancer survivors were positively associated with the prolonged duration of virus RNA shedding in the age-adjusted model (HR = 0.49; 95% CI: 0.35–0.68; $P < 0.05$). Adjusting the additional factors including sex, hypertension, and other

Table 1 Baseline characteristics between cancer survivor and non-cancer cohorts

Characteristics	Overall	Cancer survivor	Non-cancer	<i>P</i> value
Number of patients	244	61	183	
Age (years)	64.0 (55.0–72.4)	64.0 (55.0–73.0)	64.0 (54.0–73.5)	0.909
Gender				1.000
Male	96 (39.3)	24 (39.3)	72 (39.3)	–
Female	148 (60.7)	37 (60.7)	111 (60.7)	–
Body-mass-index	23.8 (21.0–25.2)	24.0 (20.5–25.5)	23.6 (21.3–25.1)	0.899
Smoking	14 (5.7)	3 (4.9)	11 (6.0)	1.000
Comorbidities	144 (59.0)	39 (63.9)	105 (57.4)	0.103
Hypertension	83 (34.0)	21 (34.4)	62 (33.9)	1.000
Cardiovascular diseases	24 (9.8)	6 (9.8)	18 (9.8)	1.000
Diabetics	37 (15.2)	12 (19.7)	25 (13.6)	0.431

Table 2 Clinical characteristics, laboratory findings and complications

	Overall	Cancer survivor	Non-cancer	P value
Clinical characteristics				
Number of patients	244	61	183	
Initial common symptom	220 (90.2)	54 (88.5)	166 (90.7)	0.681
Fever	179 (73.4)	49 (80.3)	119 (65.0)	0.026
Cough	109 (44.7)	40 (65.6)	69 (37.7)	< 0.001
Myalgia or fatigue	53 (21.7)	28 (45.9)	25 (13.6)	< 0.001
Dyspnea	58 (23.8)	22 (36.1)	36 (19.7)	0.015
Admission body temperature (°C)	36.9 (36.5–37.9)	38.3 (38.0–39.0)	37.6 (36.5–38.3)	0.032
Systolic pressure (mm Hg)	128.0 (120.0–143.0)	131.0 (123.0–145.0)	126.0 (118.0–141.2)	0.164
Respiratory rate (breaths per min)	20.0 (20.0–24.0)	20.0 (20.0–25.0)	20.0 (20.0–24.0)	0.984
Pulse rate (beats per min)	88.0 (80.0–97.0)	84.0 (79.0–96.0)	88.0 (80.0–98.0)	0.302
Laboratory findings				
WBC count (× 10 ⁹ /L)	6.28 (4.41–8.91)	6.66 (5.28–8.29)	6.11 (4.13–9.14)	0.175
< 3.5	31 (12.7)	4 (6.6)	27 (14.8)	0.018*
3.5–9.5	160 (65.6)	48 (78.7)	112 (61.2)	–
> 9.5	53 (21.7)	9 (14.8)	44 (24.0)	–
Neutrophil count (× 10 ⁹ /L)	4.36 (2.84–7.64)	4.60 (3.33–6.51)	4.34 (2.57–7.91)	0.637
< 1.8	18 (7.4)	1 (1.6)	17 (9.3)	0.024*
1.8–6.3	148 (60.7)	44 (72.1)	104 (56.8)	–
> 6.3	78 (32.0)	16 (26.2)	62 (33.9)	–
Lymphocyte count (× 10 ⁹ /L)	0.88 (0.64–1.28)	1.12 (0.77–1.75)	0.83 (0.60–1.18)	0.077
< 1.1	155 (63.5)	30 (49.2)	125 (68.3)	< 0.001*
1.1–3.2	86 (35.2)	29 (47.5)	57 (31.1)	–
> 3.2	3 (1.3)	2 (3.3)	1 (0.6)	–
IL-1b (pg/mL)	6.01 (4.21–8.12)	5.67 (2.52–6.31)	6.87 (4.01–9.11)	0.011
< 5.0	118 (48.4)	45 (73.8)	73 (39.9)	< 0.001*
≥ 5.0	126 (51.6)	16 (26.2)	110 (60.1)	–
IL-2R (U/mL)	524.5 (386.2–721.2)	456.0 (397.0–562.0)	562.0 (338.0–730.5)	0.814
< 223	18 (7.4)	5 (8.2)	13 (7.1)	0.304*
223–710	120 (49.2)	34 (55.7)	86 (47.0)	–
> 710	106 (43.4)	22 (36.1)	84 (45.9)	–
IL-6 (pg/mL)	8.2 (4.6–28.6)	4.9 (2.8–28.9)	11.0 (6.8–28.2)	0.008
< 7	112/233 (48.1)	83 (45.4)	29/50 (58.0)	< 0.001*
≥ 7	121/233 (51.9)	100 (54.6)	21/50 (42.0)	–
IL-8 (pg/mL)	11.8 (8.6–17.8)	11.7 (7.7–15.8)	11.8 (9.8–30.5)	0.129
< 62	157 (64.3)	106 (57.9)	51 (83.6)	< 0.001*
≥ 62	87 (35.7)	77 (42.1)	10 (16.4)	–
IL-10 (pg/mL)	7.5 (6.5–10.9)	6.6 (6.3–13.1)	9.1 (7.5–11.7)	0.022
< 9.1	132/239 (55.2)	95 (51.9)	37/56 (66.1)	< 0.001*
≥ 9.1	107/239 (44.8)	88 (48.1)	19/56 (33.9)	–
TNF-α (pg/mL)	8.3 (7.0–12.6)	9.6 (7.3–13.1)	7.5 (6.2–8.5)	0.026
< 8.1	145/241 (60.2)	111 (60.7)	34/58 (58.6)	0.572*
≥ 8.1	94/241 (39.0)	72 (39.3)	24/58 (41.4)	–
Ferritin (μg/L)	715.9 (237.5–960.4)	945.0 (818.0–1079.6)	425.1 (114.7–671.7)	0.011
Hemoglobin (g/L)	125.0 (114.0–135.0)	120.0 (112.0–128.0)	128.0 (114.5–135)	0.023
< 130	153 (62.7)	50 (82.0)	103 (56.3)	< 0.001*
130–175	91 (37.3)	11 (18.0)	80 (43.7)	–
Myoglobin (ng/mL)	62.4 (42.5–81.3)	66.1 (45.2–87.2)	60.3 (41.1–79.1)	0.331
≤ 154.9	195 (79.9)	46 (75.4)	149 (81.4)	0.229*
> 154.9	49 (20.1)	15 (24.6)	34 (18.6)	–
PT (s)	13.5 (12.6–14.8)	13.6 (12.9–14.3)	13.5 (12.6–14.9)	0.897
≤ 16	216 (88.5)	57 (93.4)	159 (86.9)	0.130*
> 16	28 (11.4)	4 (6.6)	24 (13.1)	–

(Continued to the next page)

(Continued from the last page)

	Overall	Cancer survivor	Non-cancer	P value
D-D dimer ($\mu\text{g/mL FEU}$)	0.72 (0.30–2.85)	0.58 (0.22–1.68)	0.73 (0.39–3.51)	0.002
≤ 0.5	100/243 (41.2)	28/60 (46.7)	72 (39.3)	0.243*
> 0.5	143/243 (58.8)	32/60 (53.3)	111 (60.7)	–
ALT (U/L)	22.0 (14.0–37.0)	21.0 (15.0–32.0)	22.0 (14.0–40.0)	0.312
≤ 50	209 (85.7)	57 (93.4)	152 (83.1)	0.031*
> 50	35 (14.3)	4 (6.6)	31 (16.9)	–
AST (U/L)	29.0 (19.0–45.0)	22.0 (17.8–31.0)	33.0 (20.0–49.0)	0.004
≤ 40	169/243 (69.5)	52/60 (86.7)	117 (63.9)	$< 0.001^*$
> 40	74/243 (30.5)	8/60 (13.3)	66 (36.1)	–
LDH (U/L)	298.0 (205.0–399.0)	218.0 (170.5–373.0)	319.0 (241.5–399.0)	< 0.001
≤ 245	93 (38.1)	55 (30.1)	38 (62.3)	$< 0.001^*$
> 245	151 (61.9)	128 (69.9)	23 (37.7)	–
Albumin (g/L)	35.1 (31.3–38.8)	36.6 (32.0–41.0)	34.5 (30.5–38.3)	0.022
< 35	120 (49.2)	26 (42.6)	94 (51.4)	0.170*
≥ 35	124 (50.8)	35 (57.4)	89 (48.6)	–
Total bilirubin ($\mu\text{mol/L}$)	10.1 (6.58–13.51)	8.34 (6.27–12.6)	10.6 (6.90–13.9)	0.061
≤ 21	226 (92.6)	59 (96.7)	167 (91.3)	0.133*
> 21	18 (7.4)	2 (3.3)	16 (8.7)	–
PTH (mg/L)	0.04 (0.04–0.08)	0.05 (0.04–0.11)	0.04 (0.04–0.06)	0.311
High sensitive (CRP, mg/L)	45.0 (10.8–94.0)	25.2 (1.80–59.2)	51.7 (14.8–98.0)	< 0.001
≤ 5.0	46 (18.9)	22 (36.1)	24 (13.1)	$< 0.001^*$
> 5.0	194 (79.5)	35 (57.4)	159 (86.9)	–
Complications				
Coagulopathy	28 (11.4)	4 (6.6)	24 (13.1)	0.245
Acute cardiac injury	84 (34.4)	27 (44.3)	57 (31.1)	0.086
Acute kidney injury	13 (5.3)	5 (8.2)	8 (4.4)	0.321
Acute liver injury	24 (9.8)	7 (11.5)	17 (9.3)	0.623
Secondary infection	87 (35.7)	32 (52.5)	55 (30.1)	0.002

Data are median [IQR], n (%), or n/N (%), where N is the total number of patients with available data. ICU, Intensive care unit; ARDS, Acute respiratory distress syndrome; UOC, Usual oxygen care, including standard nasal catheter and facemask inhalation; HFNC, High-flow nasal cannula oxygen; (N)IMV, (Non-) Invasive mechanical ventilation; ECMO, Extracorporeal membrane oxygenation; WBC, White blood cell; PLT, Blood platelet count; APTT, Activated partial thromboplastin time; PT, Prothrombin time; ALT, Alanine aminotransferase; AST, Aspartate aminotransferase; LDH, Lactate dehydrogenase; ALP, Alkaline phosphatase; γ -GT, gamma-Glutamyl transpeptidase; hs-CRP, high-sensitivity C-reactive protein. * χ^2 test comparing all subcategories

factors in model 3 did not alter the positive association between cancer survivors and the prolonged duration of viral RNA shedding (AHR = 0.54; 95% CI: 0.38–0.80; $P < 0.05$; Table 4).

Discussion

The results of this study suggest that although the prognosis of cancer survivors with COVID-19 was similar to that of non-cancer patients, cancer survivors had prolonged duration of SARS-CoV-2 RNA shedding and a higher incidence of secondary infection.

Cancer survivors, with history of either hematologic or solid tumors, were reported to have an increased risk of infection and mortality due to immunocompromised status compared to the general population, especially from respiratory infections^[20–23]. However, our study of

COVID-19 infection in cancer survivors did not support this view. Our study found that the mortality rate in the cancer survivor group was 15%, which was comparable to the matched non-cancer cohort. In a study involving 106 cancer patients, the mortality rate of cancer patients was 11%^[11], and the incidence of comorbidities such as hypertension and diabetes was lower than that in our study, suggesting that chronic comorbidities may be one of the most important risk factors for survival outcomes, which was consistent with previous studies.

We found that the median duration of SARS-CoV-2 RNA shedding in cancer survivors was 32 days, which was much longer than the 17–20 days reported in the general patients^[17, 24] and 24 days in the non-cancer cohort in this study. In our study, even after balancing or weighting these factors, viral RNA shedding in the cancer survivor cohort was still significantly longer than that in

Table 3 Treatments and outcomes

	Overall	Cancer survivor	Non-cancer	P value
Treatments				
Antibiotics	202 (82.8)	49 (80.3)	153 (83.6)	0.561
Antiviral treatment	239 (98.0)	58 (95.1)	181 (98.9)	0.101
Corticosteroids	154 (63.1)	22 (36.1)	132 (72.1)	< 0.001
Interferon atmotherapy	94 (35.8)	12 (19.7)	82 (44.8)	< 0.001
Intravenous immunogloblin	73 (29.9)	12 (19.7)	61 (33.3)	0.053
Oxygen therapy	221 (86.3)	49 (76.6)	172 (89.6)	0.004
Standard nasal catheter and facemask inhalation	196 (80.3)	34 (53.1)	162 (88.5)	<.001
High-flow nasal cannula oxygen therapy	31 (12.7)	6 (9.8)	25 (13.7)	0.512
Non-invasive mechanic ventilation	72 (29.5)	8 (13.1)	64 (35.0)	0.001
Invasive mechanic ventilation	15 (6.1)	1 (1.6)	14 (7.7)	0.125
Outcomes				
Disease severity status				0.125
Mild-moderate	121 (49.6)	36 (59.0)	85 (46.4)	–
Severe	73 (29.9)	16 (26.2)	57 (31.2)	–
Critical	50 (20.5)	9 (14.8)	41 (22.4)	–
ARDS	88 (36.1)	15 (24.6)	68 (37.2)	0.086
ICU admission	3 (1.2)	3 (4.9)	5 (2.7)	0.416
Deceased	87 (35.7)	10 (15.6)	45 (24.6)	0.218
Duration of viral sheddling after COVID-19 onset, days	27.0 (20.0–34.0)	32.0 (26.0-46.0)	24.0 (18.0–33.0)	< 0.001
Re-positive of COVID-19 diagnosis	11 (4.5)	3 (4.9)	7 (3.8)	0.716

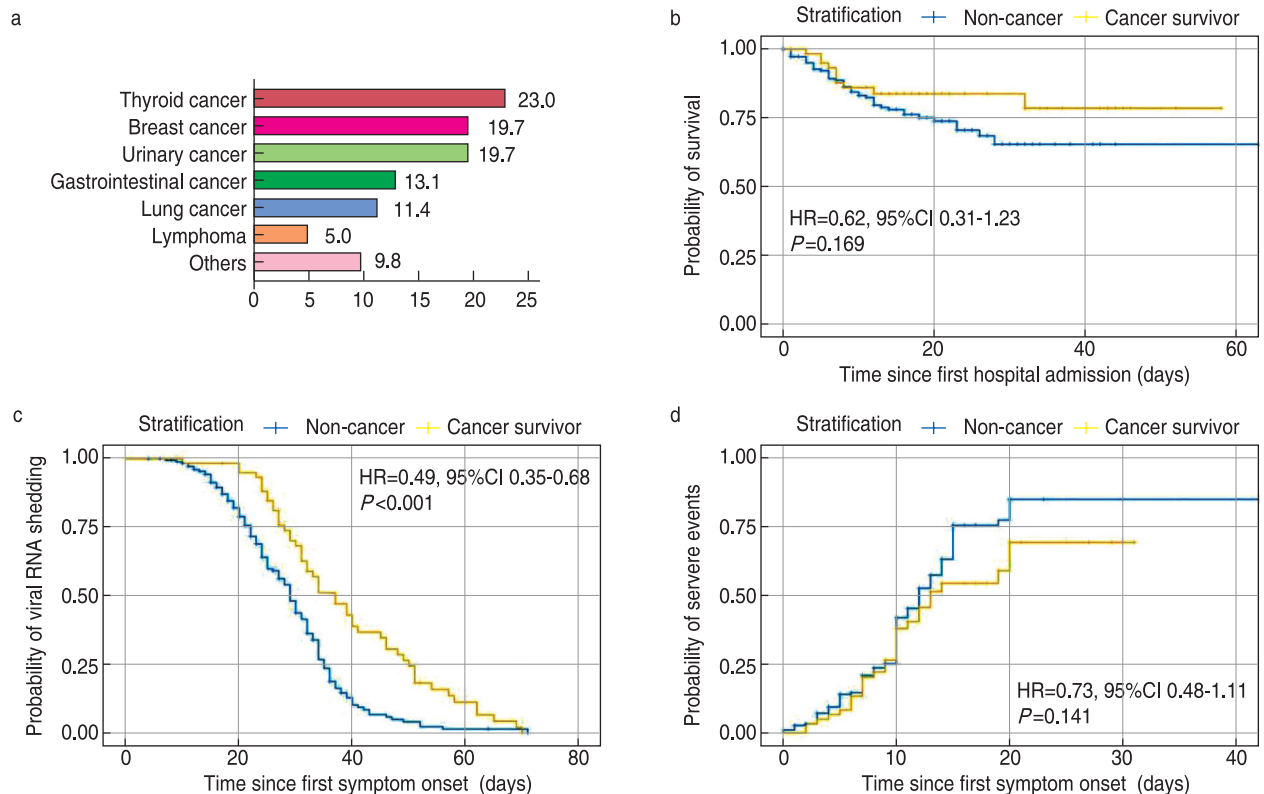


Fig. 1 Tumor categories of cancer survivors (a). The probabilities of survival (b), viral RNA shedding (c) and severe events (d) of the cancer survivors were compared to the non-cancer patients

Table 4 Hazard ratios of survival, viral RNA shedding and severe events for cancer survivor

Survival probability				Model 1			Model 2			Model 3		
	Crude HR	95% CI	P	HR	95% CI	P	HR	95% CI	P	HR	95% CI	P
Cancer survivor Yes vs. No	0.62	0.31–1.23	0.169	0.52	0.26–1.04	0.064	0.53	0.27–1.06	0.074	0.36	0.11–1.20	0.096
Viral RNA Shedding Probability				Model 1			Model 2			Model 3		
	Crude HR	95% CI	P	HR	95% CI	P	HR	95% CI	P	HR	95% CI	P
Cancer survivor Yes vs. No	0.49	0.35–0.68	<0.001	0.49	0.35–0.68	<0.001	0.49	0.35–0.68	<0.001	0.54	0.38–0.80	0.002
Severe events probability				Model 1			Model 2			Model 3		
	Crude HR	95% CI	P	HR	95% CI	P	HR	95% CI	P	HR	95% CI	P
Cancer survivor Yes vs. No	0.73	0.48–1.11	0.141	0.73	0.49–1.11	0.144	0.72	0.47–1.08	0.118	1.25	0.76–2.06	0.378

Model 1 adjusted for age; Model 2 adjusted for age and gender; Model 3 adjusted for age, gender, hypertension, D-dimer, LDH, high sensitive CRP, and lymphocyte count. P value was calculated using cox proportional hazard model.

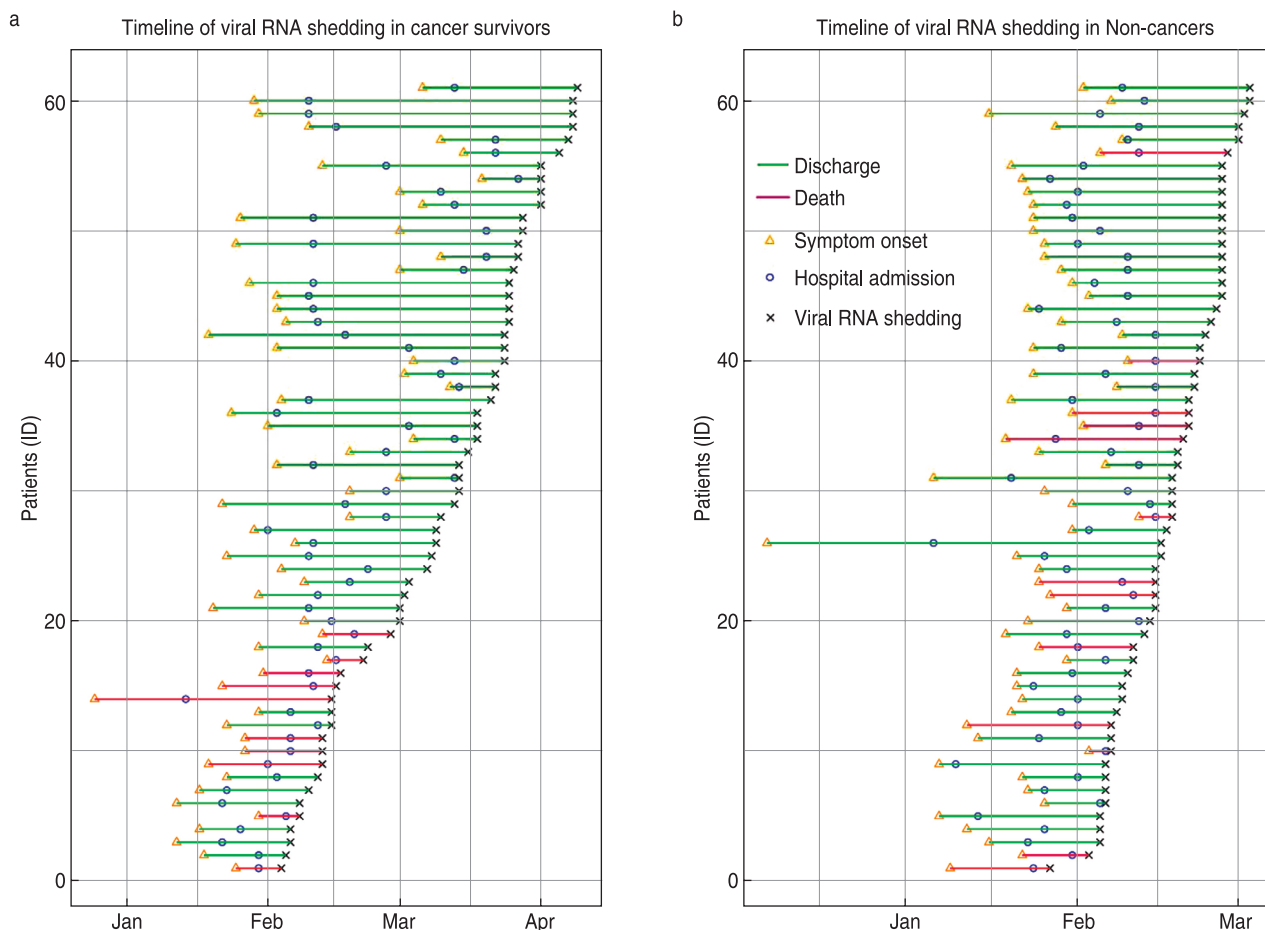


Fig. 2 Timelines of viral RNA shedding of the cancer survivors (a) and the non-cancer patients (b)

the non-cancer patients. In addition, it was found that the incidence of secondary infection was significantly higher in the cancer survivor cohort. These results were consistent with those of previous studies on respiratory

viral infections^[25–26], suggesting that immunosuppressive status may interfere with viral clearance and increase the risk of secondary infection.

Among the cancer survivors, 3 patients retested

positive in the RNA testing during the follow-up after discharge. The clinical significance of the nucleic acid re-positivity has not been determined. However, it is inferred that due to the immunocompromised status of cancer survivors, their ability to eliminate the virus has been weakened. Special attention should be paid to persistent viral carriage, recrudescence, and secondary infection.

It was found that, consistent with the data of the general population reported [17], the most prevalent symptom onset in cancer survivors was fever, followed by cough, myalgia, or fatigue; dyspnea was present in more than one-third of cancer survivors. These symptoms were more common in cancer survivors than in non-cancer patients. It is possible that cancer survivors are more concerned about their health conditions and more sensitive to physical changes; hence, they tend to report their symptoms earlier and more frequently and are more likely to seek medical care. Current research suggests that early recognition and medical intervention may improve the prognosis of COVID-19 patients [27]; therefore, early medical attention may contribute to the outcome of cancer survivors infected with COVID-19.

The median age of the cancer survivor cohort was 64 years, while a study of 1,099 patients showed a median age of 47.0 years in COVID-19 patients, suggesting that cancer patients tend to be older, which is consistent with previous studies [10]. Among the cancer survivors, 37 (60.7%) were women and 26 (42.7%) had a history of thyroid and breast cancer. Both types of cancer exhibit a good prognosis, and the patients' nutritional and physical status are less affected. Cancer survivors in the study had a median body mass index of 24 and a median albumin concentration of 36.6 g/L, indicating that most cancer survivors included had recovered from the disease and sequelae of anti-cancer treatments.

In terms of laboratory testing, compared to the cancer survivors, the non-cancer patients had a higher proportion of lymphopenia, higher levels of aspartate transferase, LDH, hs-CRP, and d-dimer, all of which were considered to be associated with adverse outcomes [17, 19, 28]. Among cancer survivors, 21.3% received chemotherapy and radiation, and anemia was more common in this cohort because of the long-lasting toxicity of the bone marrow [29–30]. Although the incidence of anemia was higher in the cancer survivor cohort, the median concentration of hemoglobin was 120 g/L (IQR, 112.0–128.0), and no increase in severe disease or mortality was observed in patients with mild anemia. Thus, mild anemia demonstrated less impact on the development of COVID-19 disease. Accumulated evidence has suggested that the cytokine storm syndrome (CRS) may be an important cause of a critical disease course or death in COVID-19 patients. Such a cytokine storm may destroy

the adaptive immunity against SARS-CoV-2 [31], leading to fulminant and fatal multiorgan failure. We found that patients in the cancer survivor cohort had relatively low levels of pro-inflammatory cytokines including IL-6, IL-10, and IL-1b. These trends suggest that cancer survivors had lower or at least similar levels of inflammation compared to non-cancer patients. Impaired cellular immunity in cancer survivors may suppress excessive inflammation, preventing the development of CRS [32]. Therefore, in the case of hyperinflammation, a certain degree of immunosuppression may serve as a protective factor [33]. In summary, the immunosuppressive state may be a double-edged sword for cancer survivors with COVID-19, and which factor dominates the outcome still needs further investigation.

Although the study of Liang et al. revealed a worse outcome in cancer patients infected with COVID-19 [5], there was no distinction between cancer survivors and cancer patients, which may reduce representativeness of the findings. We believe that there are differences between cancer survivors and cancer patients. The immune function and nutritional status of cancer patients were significantly impaired by anti-cancer therapy or disease progression, while most cancer survivors have recovered to varying degrees. Nevertheless, cancer survivors comprise a heterogeneous group, and different tumor types, anti-cancer treatment methods, and durations after diagnosis of cancer would affect the immune status of patients, thus affecting their survival and RNA shedding. To date, little is known about SARS-CoV-2, and more research is needed to determine which factors drive inflammation and which groups are at high risk.

Limitations

Our study has several limitations. First, this study was a retrospective cohort study using propensity score matching methods, which could not represent all cancer survivors. Therefore, prospective controlled studies with larger sample sizes should be carried out to clarify differences among cancer survivors, cancer patients, and non-cancer patients. Second, although this study was a multicenter study, all the centers were located in mainland China. Due to the global spread of COVID 19, international multi-center investigation needs to be considered.

Conclusions

The severe events and mortality risk of cancer survivors with COVID-19 were comparable to those of non-cancer patients, but the viral RNA shedding duration was longer and the incidence of secondary infection was higher. Based on our results, it is helpful for clinicians to take tailored measures to treat cancer survivors with

COVID-19. Although continuous follow-up should be carried out to determine the long-term prognosis of cancer survivors infected with COVID-19, we suggest that the comprehensive care plan of cancer survivors with COVID-19 should take longer viral RNA shedding duration into consideration and pay more attention to such patients than non-cancer patients to prevent development of secondary infections.

Conflicts of interest

The authors indicated no potential conflicts of interest.

References

- WHO COVID-19 Dashboard. Available at: <https://covid19.who.int/> (accessed 11 November 2020).
- Bray F, Ferlay J, Soerjomataram I, *et al.* Global cancer statistics 2018: GLOBOCAN estimates of incidence and mortality worldwide for 36 cancers in 185 countries. *CA Cancer J Clin*, 2018, 68: 394–424.
- MKuderer NM, Choueiri TK, Shah DP, *et al.* COVID-19 and Cancer Consortium. Clinical impact of COVID-19 on patients with cancer (CCC19): a cohort study. *Lancet*, 2020; 395: 1907–1918.
- Lee LY, Cazier JB, Starkey T, *et al.* UK Coronavirus Cancer Monitoring Project Team. COVID-19 mortality in patients with cancer on chemotherapy or other anticancer treatments: a prospective cohort study. *Lancet*, 2020, 395: 1919–1926.
- Liang W, Guan W, Chen R, *et al.* Cancer patients in SARS-CoV-2 infection: a nationwide analysis in China. *Lancet Oncol*, 2020, 21: 335–337.
- Wu Z, McGoogan JM. Characteristics of and important lessons from the Coronavirus disease 2019 (COVID-19) outbreak in China: Summary of a report of 72314 cases from the Chinese center for disease control and prevention. *JAMA*, 2020, 323: 1239–1242.
- Zhang L, Zhu F, Xie L, *et al.* Clinical characteristics of COVID-19-infected cancer patients: A retrospective case study in three hospitals within Wuhan, China. *Ann Oncol*, 2020, 31: 894–901.
- Yu J, Ouyang W, Chua MLK, *et al.* SARS-CoV-2 transmission in patients with cancer at a tertiary care hospital in Wuhan, China. *JAMA Oncol*, 2020, 6: 1108–1110.
- Zeng H, Chen WQ, Zheng RS, *et al.* Changing cancer survival in China during 2003–15: a pooled analysis of 17 population-based cancer registries. *Lancet Glob Health*, 2018, 6: e555–e567.
- Miller KD, Nogueira L, Mariotto AB, *et al.* Cancer treatment and survivorship statistics, 2019. *CA Cancer J Clin*, 2019, 69: 363–385.
- Dai MY, Liu DB, Liu M, *et al.* Patients with cancer appear more vulnerable to SARS-COV-2: a multi-center study during the COVID-19 outbreak. *Cancer Discov*, 2020, 10: 783–791.
- Moser EC, Meunier F. Cancer survivorship: A positive side-effect of more successful cancer treatment. *EJC Suppl*, 2014, 12: 1–4.
- Jin YH, Zhan QY, Peng ZY, *et al.* Chemoprophylaxis, diagnosis, treatments, and discharge management of COVID-19: An evidence-based clinical practice guideline (updated version). *Mil Med Res*, 2020, 7: 41.
- Force ADT, Ranieri VM, Rubenfeld GD, *et al.* Acute respiratory distress syndrome: the Berlin Definition. *JAMA*, 2012, 307: 2526–2533.
- Khwaja A. KDIGO clinical practice guidelines for acute kidney injury. *Nephron Clin Pract*, 2012, 120: 179–184.
- Huang CL, Wang YM, Li XW, *et al.* Clinical features of patients infected with 2019 novel coronavirus in Wuhan, China. *Lancet*, 2020, 395: 497–506.
- Zhou F, Yu T, Du RH, *et al.* Clinical course and risk factors for mortality of adult inpatients with COVID-19 in Wuhan, China: a retrospective cohort study. *Lancet*, 2020, 395: 1054–1062.
- Chen T, Wu D, Chen HL, *et al.* Clinical characteristics of 113 deceased patients with coronavirus disease 2019: retrospective study. *BMJ*, 2020, 368: m1091.
- Ruan QR, Yang K, Wang WX, *et al.* Clinical predictors of mortality due to COVID-19 based on an analysis of data of 150 patients from Wuhan, China. *Intensive Care Med*, 2020, 46: 846–848.
- Ward EM, Flowers CR, Gansler T, *et al.* The importance of immunization in cancer prevention, treatment, and survivorship. *CA Cancer J Clin*, 2017, 67: 398–410.
- Kawakita D, Abdelaziz S, Chen YJ, *et al.* Adverse respiratory outcomes among head and neck cancer survivors in the Utah Cancer Survivors Study. *Cancer*, 2020, 126: 879–885.
- Fossa SD, Gilbert E, Dores GM, *et al.* Noncancer causes of death in survivors of testicular cancer. *J Natl Cancer Inst*, 2007, 99: 533–544.
- Shree TY, Li Q, Glaser SL, *et al.* Impaired immune health in survivors of diffuse large B-cell lymphoma. *J Clin Oncol*, 2020, 38: 1664–1675.
- Xu KJ, Chen YF, Yuan J, *et al.* Factors associated with prolonged viral RNA shedding in patients with COVID-19. *Clin Infect Dis*, 2020, 71: 799–806.
- Wang YM, Guo Q, Yan Z, *et al.* Factors associated with prolonged viral shedding in patients with avian influenza A (H7N9) virus infection. *J Infect Dis*, 2018, 217: 1708–1717.
- Hijano DR, Maron G, Hayden RT. Respiratory viral infections in patients with cancer or undergoing hematopoietic cell transplant. *Front Microbiol*, 2018, 9: 3097.
- Sun Q, Qiu HB, Huang M, *et al.* Lower mortality of COVID-19 by early recognition and intervention: experience from Jiangsu Province. *Ann Intensive Care*, 2020, 10: 33.
- Chen G, Wu D, Guo W, *et al.* Clinical and immunologic features in severe and moderate Coronavirus Disease 2019. *J Clin Invest*, 2020, 30: 2620–2629.
- Eytan DF, Blackford AL, Eisele DW, *et al.* Prevalence of comorbidities among older head and neck cancer survivors in the United States. *Otolaryngol Head Neck Surg*, 2019, 160: 85–92.
- Skuli SJ, Sheng JY, Bantug ET, *et al.* Survivorship care visits in a high-risk population of breast cancer survivors. *Breast Cancer Res Treat*, 2019, 173: 701–708.
- Mehta P, McAuley DF, Brown M, *et al.* COVID-19: consider cytokine storm syndromes and immunosuppression. *Lancet*, 2020, 395: 1033–1034.
- Schreiber RD, Old LJ, Smyth MJ. Cancer immunoediting: integrating immunity's roles in cancer suppression and promotion. *Science*, 2011, 331: 1565–1570.
- Seminari E, Colaneri M, Sambo M, *et al.* SARS Cov2 infection in a renal transplanted patients. A case report. *Am J Transplant*, 2020, 20: 1882–1884.

DOI 10.1007/s10330-020-0469-9

Cite this article as: Peng H, Wang S, Mei Q, *et al.* Comparable outcomes but higher risks of prolonged viral RNA shedding duration and secondary infection in cancer survivors with COVID-19: A multi-center, matched retrospective cohort study. *Oncol Transl Med*, 2020, 6: 237–246.

Identification of potential immune-related prognostic biomarkers of lung cancer using gene co-expression network analysis*

Aixia Chen¹, Shengnan Zhao², Fei Zhou¹, Hongying Lv¹, Donghai Liang¹, Tao Jiang¹, Rui Liu¹, Lijin Zhu¹, Jingyu Cao³, Shihai Liu⁴, Hongsheng Yu¹ (✉)

¹ Department of Radiation Oncology, The Affiliated Hospital of Qingdao University, Qingdao 266000, China

² Department of Medicine Oncology, Qinghai University Affiliated Hospital, Qinghai 810000, China

³ Department of Hepatobiliary and Pancreatic Surgery, The Affiliated Hospital of Qingdao University, Qingdao 266000, China

⁴ Department of Central Laboratory, The Affiliated Hospital of Qingdao University, Qingdao 266000, China

Abstract

Objective The objective of this study was to identify new carcinogenetic hub genes and develop the integration of differentially expressed genes to predict the prognosis of lung cancer.

Methods GSE139032 microarray data packages were downloaded from the Gene Expression Omnibus for planning, testing, and review of data. We identified KRT6C, LAMC2, LAMB3, KRT6A, and MYEOV from a key module for validation.

Results We found that the five genes were related to a poor prognosis, and the expression levels of these genes were associated with tumor stage. Furthermore, Kaplan-Meier plotter showed that the five hub genes had better prognostic values. The mean levels of methylation in lung adenocarcinoma (LUAD) were significantly lower than those in healthy lung tissues for the hub genes. However, gene set enrichment analysis (GSEA) for single hub genes showed that all of them were immune-related.

Conclusion Our findings demonstrated that KRT6C, LAMC2, LAMB3, KRT6A, and MYEOV are all candidate diagnostic and prognostic biomarkers for LUAD. They may have clinical implications in LUAD patients not only for the improvement of risk stratification but also for therapeutic decisions and prognosis prediction.

Key words: lung adenocarcinoma (LUAD); bioinformatics; gene expression omnibus; gene expression profiling interactive analysis (GEPIA); prognosis; methylation

Abbreviations: LUAD, lung adenocarcinoma; GSEA, gene set enrichment analysis; NSCLC, non-small-cell lung cancer; WGCNA, weighted gene co-expression network analysis; MEs, module eigengenes; GS, gene significance; MS, module significance; KEGG, Kyoto Encyclopedia of Genes and Genomes; GO, gene ontology; CC, cellular component; MF, molecular function; BP, biological process; GEPIA, gene expression profiling interactive analysis; HPA, Human Protein Atlas; TIMER, Tumor Immune Estimation Resource; TCGA, The Cancer Genome Atlas; OS, overall survival; PF, first progression; PPS, post-progression survival; IHC, immunohistochemical

Received: 15 June 2020

Revised: 13 October 2020

Accepted: 8 November 2020

Lung cancer is the most frequently diagnosed type of cancer, accounting for 11.6% of all cancer cases, and is a leading cause of cancer morbidity, representing 18.4% of all cancer-related deaths [1]. Non-small cell lung cancer (NSCLC) is the most prevalent type of lung cancer, and lung adenocarcinoma (LUAD) is the most common subtype of NSCLC, representing almost half of

lung cancer diagnoses [2]. Standard treatment for LUAD is surgical resection and chemotherapy, which improves survival rates by 5%–10% [3]. Many treatment options exist for LUAD; however, appropriate treatment usually depends on the stage of LUAD. Five-year survival rates are low and stage-dependent [3]. It has been reported that the number of CD133+ cells, which can increase drug

✉ Correspondence to: Hongsheng Yu. Email: qdyuhs@126.com

* Supported by a grant from the Chinese Society of Clinical Oncology (No. Y-HR2018-293 and Y-HR2018-294).

© 2020 Huazhong University of Science and Technology

resistance and the likelihood of tumor recurrence, are enhanced by the chemotherapeutic agent, cisplatin [4]. Early identification of LUAD through the discovery of relevant tumor biomarkers is urgently needed to improve prognoses [5-6].

A weighted gene co-expression network analysis (WGCNA) was used to identify correlations in gene patterns. We constructed a free-scale gene co-expression network to discover modules with highly correlated genes. Accordingly, we discuss here potential biomarkers of lung cancer to improve patient prognosis via a systematic biological method using WGCNA.

Materials and methods

Data procession and construction of co-expression network

Gene expression dataset GSE139032 (<https://www.ncbi.nlm.nih.gov/geo/query/acc.cgi?acc=GSE139032>), including 77 lung adenocarcinomas and 77 matched non-malignant lung samples (Illumina HumanMethylation27 BeadChip), were downloaded from the Gene Expression Omnibus [7]. Sangerbox (<http://www.sangerbox.com>), a free online tool for data analysis, was utilized to analyze sample information and dataset matrices. The top 50% of the most variable genes (7239) from the dataset (14 477 genes) were chosen by analysis of variance. Sangerbox was used to perform WGCNA, and study-specific parameters and WGCNA rationale are as follows [8].

First, a co-expression network was constructed with Pearson correlation coefficients i and j representing the expression levels of the i th and j th genes, respectively.

$$S_{ij} = |1 + \text{cor}(x_i + y_j)/2|$$

Second, the co-expression similarity was transformed into the adjacency according to the following equation:

$$a_{ij} = |(1 + \text{cor}(x_i + y_j)/2)|^\beta$$

β : soft thresholding, which revealed the adjacency of a signed network [9]. We selected a soft threshold parameter power of $\beta = 7$ to build an approximately scale-free network to balance the scale-free network properties.

Third, the topological overlap measure (TOM) transformation was calculated from the adjacency matrix using

$$TOM = (\sum_{\mu \neq ij} \alpha_{ij}^{\alpha_{ij} + \alpha_{\mu}}) / (\min(\sum_{\mu} \alpha_{ij}^{\alpha_{ij} + \alpha_{\mu}} + \sum_{\mu} \alpha_{\mu}^{\alpha_{ij}}) + 1 - \alpha_{ij})$$

to further convert the adjacency matrix of the 7239 genes from the co-expression network to the screening function module [10].

Screening of clinically significant modules

Module eigen genes (MEs) represent all genes in a specific module, which were screened for the identification of clinically relevant modules that correlate to a specific cancer type. Clinical traits, such as tumor stage and tumor grade, were calculated for each ME. Gene significance

(GS) was utilized in the linear regression to quantify the relevance of the gene and clinical features [8]. The average absolute GS in a specific module was measured using module significance.

Functional enrichment analysis of gene ontology and KEGG

DAVID (<https://david.ncifcrf.gov/>), an online public web server, was used to characterize and manipulate gene lists by mining high-throughput genomic data and performing gene ontology (GO) and KEGG signaling pathway enrichment analysis. Cellular component (CC), molecular function (MF), and biological process (BP) were the three categories included in the ontology. A P -value < 0.05 was considered statistically significant.

Hub gene selection and validation

Gene connectivity was measured using the absolute value of Pearson's correlation, defined by module connectivity (cor. Gene module membership > 0.8) and clinical connectivity (cor. genetrail significance > 0.2). Gene expression profiling interactive analysis (GEPIA) was utilized to validate the central hub genes of LUAD. Immunohistochemistry of the five genes identified was performed using the Human Protein Atlas (HPA) (<http://www.proteinatlas.org>), which showed that the genes were upregulated in tumors.

Methylation analyses of hub genes

The human disease methylation database (DiseaseMeth version 2.0, <http://biobigdata.hrbmu.edu.cn/diseasemeth/>) contains methylome information from high-throughput microarray and sequencing studies of human methylation and shows DNA methylation abnormalities for human diseases in a case-control or disease-disease format [11-12].

Differences in the methylation levels of hub genes in cancerous lung tissues were compared with those in healthy lung tissues using the cBioPortal for Cancer Genomics (<https://www.cbioportal.org/>). Genetic changes associated with the hub genes were investigated to explore the associations between mRNA expression and DNA methylation in lung cancer using a large-scale cancer genome database.

Evaluation of the immunological infiltrate

To study the relationship between hub gene expression and immune cell infiltration, we used the online TIMER tool [13-14]. Samples (10 897) from a wide variety of cancers available from The Cancer Genome Atlas (TCGA) were used to study the interaction between hub gene expression and immune cell tumor infiltration.

Gene set enrichment analysis of hub genes

GSEA 3.0 software was used to analyze the hub genes

associated with immune infiltration of a variety of biological function gene sets in lung cancer.

Statistical analysis

WGCNA was performed using the Sangerbox platform (version 1.0.9) based on R software version 3.4.3. We utilized the Kaplan-Meier method to perform survival analysis using the log-rank test. The independent samples *t*-test for data comparison was performed by GEPIA. *P*-values < 0.05 (two-sided) were considered statistically significant.

Results

Weighted co-expression network building and key modules recognition

The coefficient and average association of Pearson's correlation were used to cluster the GSE139032 sample based on the WGCNA packages in R (Fig. 1 and 2). After transforming the co-expression similarity matrix, we computed the TOM to identify modules utilizing the dynamic tree cut method (Fig. 2c). WGCNA was performed to collect information for a co-expression network [9]. The soft threshold parameter power of $\beta =$

7 was selected to balance the scale-free nature of the network for a network that will be approximately scale-free (Fig. 2a and 2b). Using the average hierarchical linkage, 11 modules were identified. The turquoise module was selected as the clinically meaningful unit

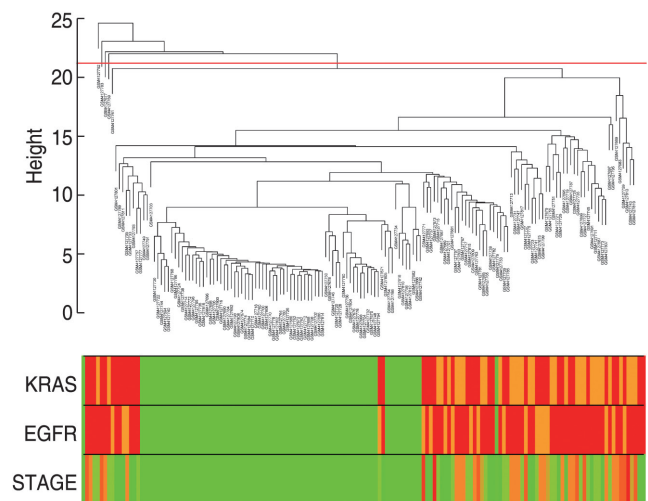


Fig. 1 Clustering dendrogram of 152 samples

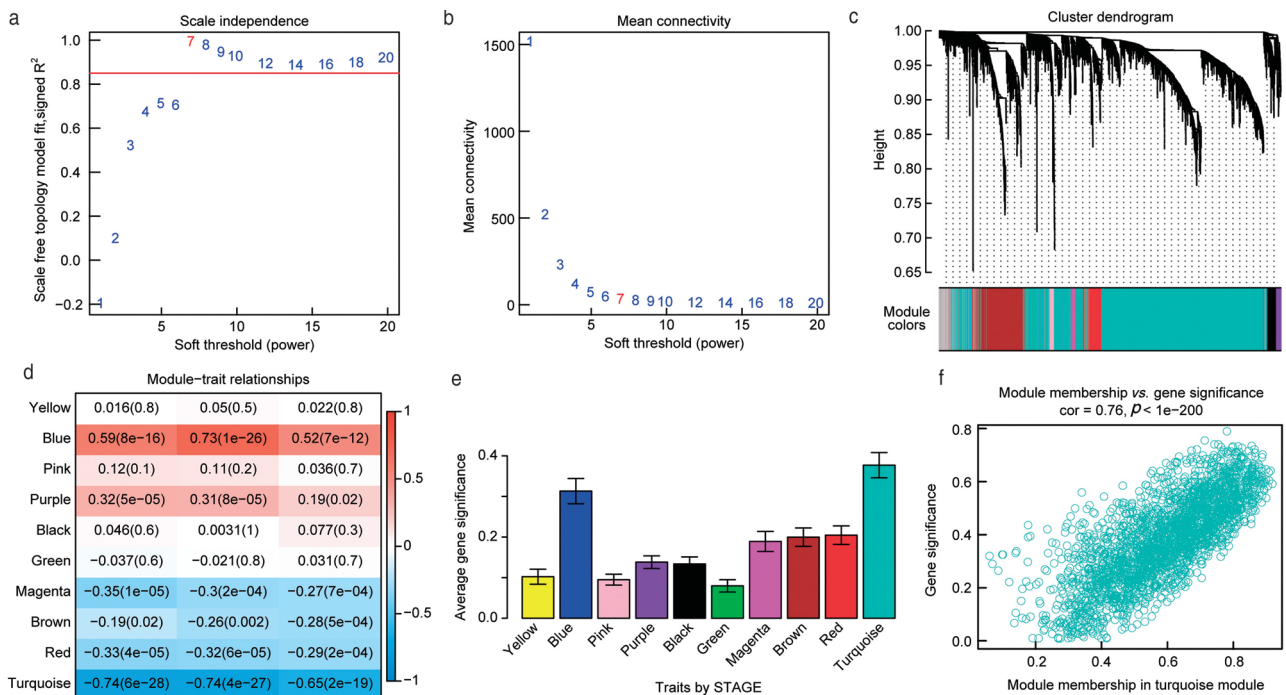


Fig. 2 Identification of modules related to clinical traits of LUAD through WGCNA. (a) Scale-free fit index analysis for a variety of soft threshold strengths (β). (b) Mean connectivity study for a number of soft thresholds. All modules were related to the respective LUAD clinical characteristics that were screened. (c) Gene dendrogram of differentially expressed genes obtained through clustering as a measure of dissimilarity (1-TOM). Each branch represents a single gene in the dendrogram. A specific color signifies a single module containing closely conserved genes. (d) Connection of the clinical phenotype of LUAD and consensus module eigengenes. (e) Bar graphs indicating the importance and errors of the individual modules across all modules associated with the LUAD tumor stage. (f) Scatter plot for the relationship between the significance of the gene and the membership of the gene module in the turquoise module. Every circle is a gene

owing to its close interaction with tumor stage (Fig. 2d) and the highest tumor stage association (Fig. 2d).

Functional enrichment analysis

GO and KEGG pathway enrichment analyses were performed. Functional groups included three parts (CC, MP, and BP) to analyze GO enrichment. Enrichment of genes in the CC group from the turquoise module mainly included the extracellular region, extracellular space, integral component of the plasma membrane, extracellular exosome, plasma membrane, cornified envelope, intermediate filament, apical plasma membrane, and blood microparticle. The genes from the module in the MF group were chiefly enriched in structural molecule activity, iron ion binding, CC chemokine receptor binding, serine-type endopeptidase activity, serine-type peptidase activity, calcium ion binding, chemokine activity, serine-type endopeptidase inhibitor activity, cytokine activity,

and heme-binding. The BP group included clinically significant genes in the following modules: keratinization, immune response, peptide cross-linking, neutrophil chemotaxis, keratinocyte differentiation, innate immune response, monocyte chemotaxis, inflammatory response, epidermis development, and lymphocyte chemotaxis (Fig. 3). Hub genes from the turquoise module were enriched in the KEGG pathway as follows: cytokine receptor interaction, hematopoietic cell lineage, systemic lupus erythematosus, pancreatic secretion, carbohydrate digestion and absorption, neuroactive ligand-receptor interaction, complement and coagulation cascades, rheumatoid arthritis, fat digestion and absorption, and toll-like receptor signaling pathways.

Hub gene selection and validation

In terms of cut-off criteria $|MM| > 0.8$ and $|GS| > 0.2$, we identified 2496 hub genes from the turquoise unit. A

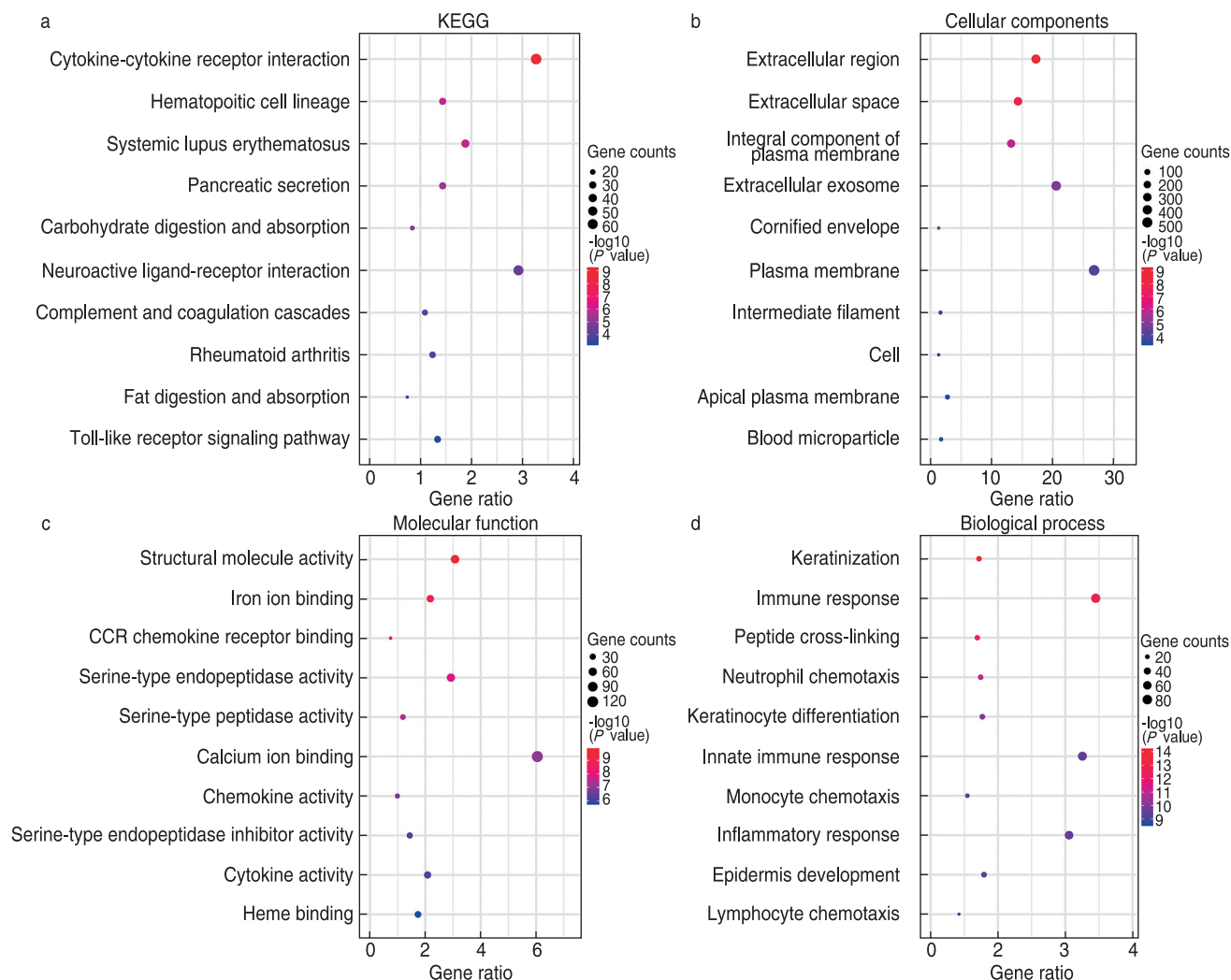


Fig. 3 The enrichment analyses of KEGG and GO pathways for all turquoise genes. An analysis of the (a) KEGG pathway of turquoise genes; (b) cellular components; (c) molecular function; and (d) biological process

Kaplan-Meier plotter was used to estimate the clinical prognostic significance of the hub genes. We found five genes (*MYEOV*, *LAMC2*, *LAMB3*, *KRT6C*, and *KRT6A*) that were negatively related to overall survival (OS) and first progression.

MYEOV, *LAMC2*, *KRT6C*, and *KRT6A* were associated with post-progression survival (PPS). *LAMB3* was not associated with PPS (Fig. 4). GEPIA revealed a substantially higher level of expression of these five genes in tumor tissues than innormal tissue (Fig. 5a–5e). However, in advanced tumor stages,

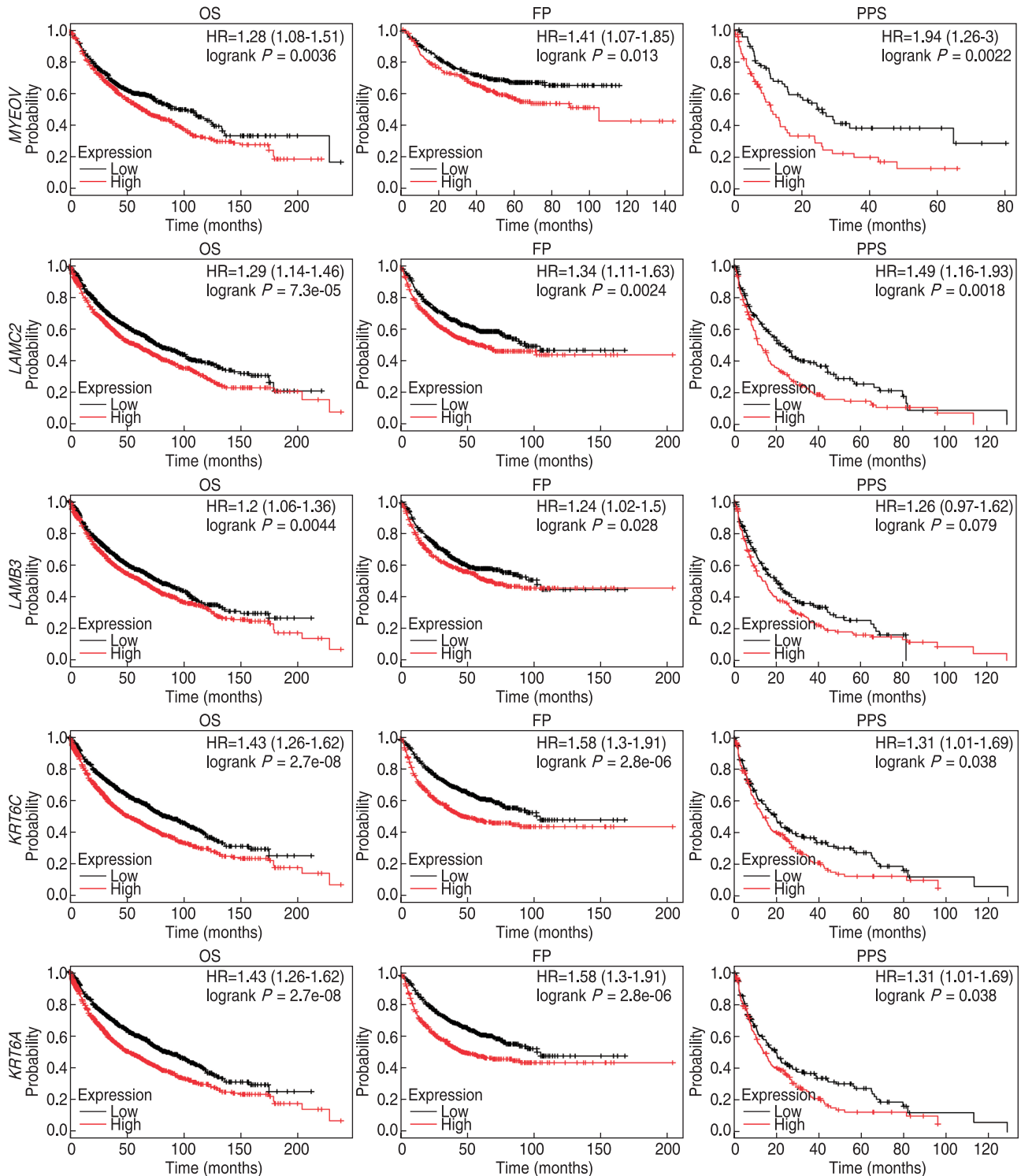


Fig. 4 Survival analysis using the Kaplan-Meier curve of *MYEOV*, *LAMC2*, *LAMB3*, *KRT6C*, and *KRT6A* in LUAD patients. HR, hazard ratio

based on a GEPIA cancer stage analysis, the expression levels of these five genes were found to be completely unregulated (Fig. 5f–5j). To estimate the expression of the proteins corresponding to the genes, the Protein Atlas

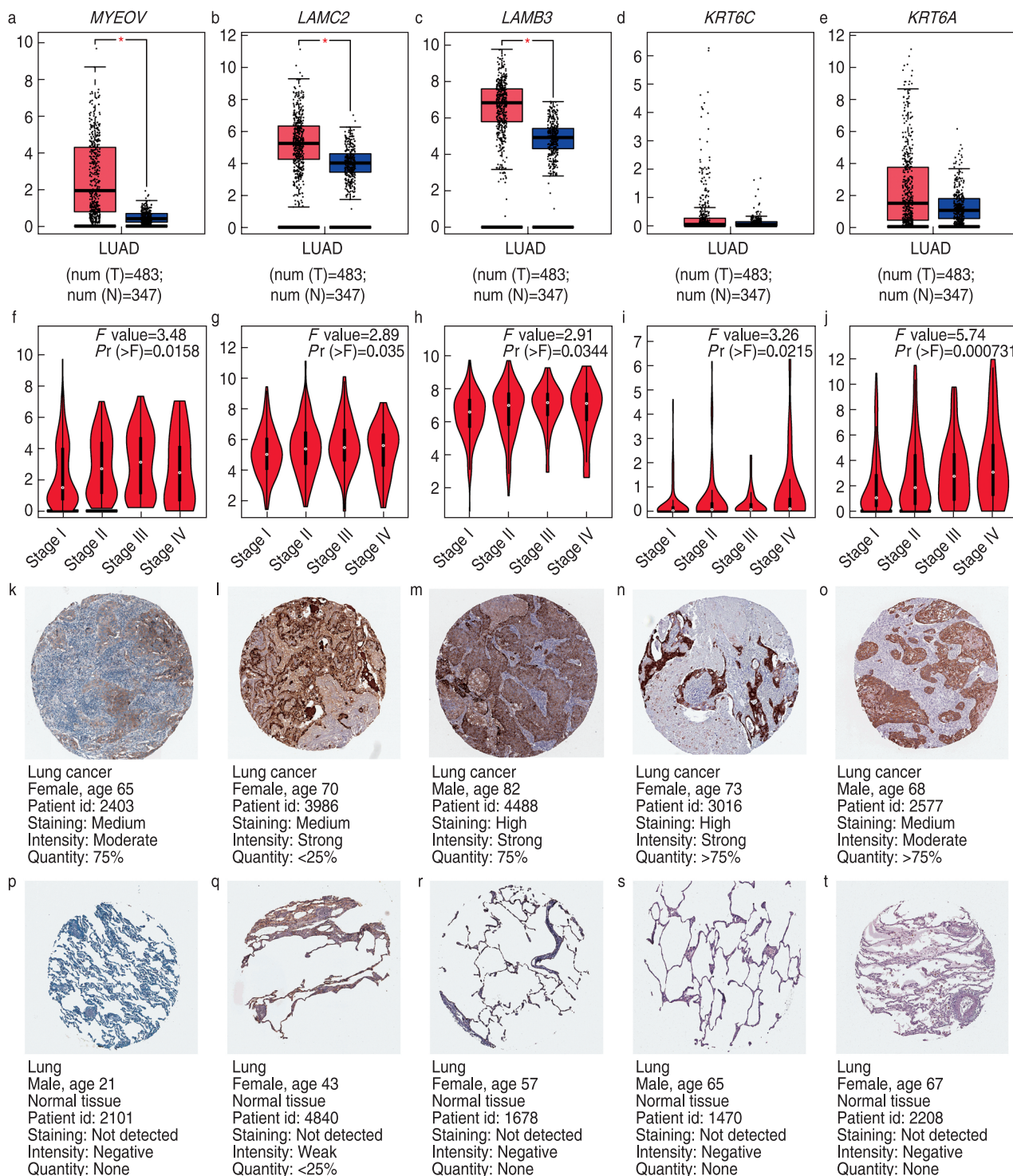


Fig. 5 (a–e) Expression of the five hub genes in LUAD and normal tissues ($P < 0.01$) from GEPIA. T: tumor, N: normal. (f–j) Correlation between expression of the five hub genes and tumor stage in LUAD using GEPIA. $P < 0.05$ represented a statistical difference. (k–t) Immunohistochemistry of the five hub genes in LUAD based on the Human Protein Atlas. (k and p) *MYEOV*; (l and q) *LAMC2*; (m and r) *LAMB3*; (n and s) *KRT6C*; (o and t) *KRT6A*. The top row is cancerous and the bottom row is normal lung tissue.

database (<https://www.proteinatlas.org/>) was used for immunohistochemistry (IHC) (Fig. 5k–5t).

Association between methylation and hub gene expression

The association between the expression of the five hub genes and their methylation status were analyzed to identify possible mechanisms for upregulation in lung tissues. A review of the human disease methylation

databases (DiseaseMeth version 2.0) revealed that the mean levels of methylation in LUAD were significantly lower than those in healthy lung tissue for *MYEOV*, *LAMC2*, *LAMB3*, *KRT6C*, and *KRT6A* (Fig. 6a–6e). Fig. 6f–6j shows the correlation between mRNA expression and DNA methylation expression in the TCGA LUAD patient dataset. The negative correlations between them indicated that mRNA expression levels of these genes were maintained by methylation (cBioPortal dataset

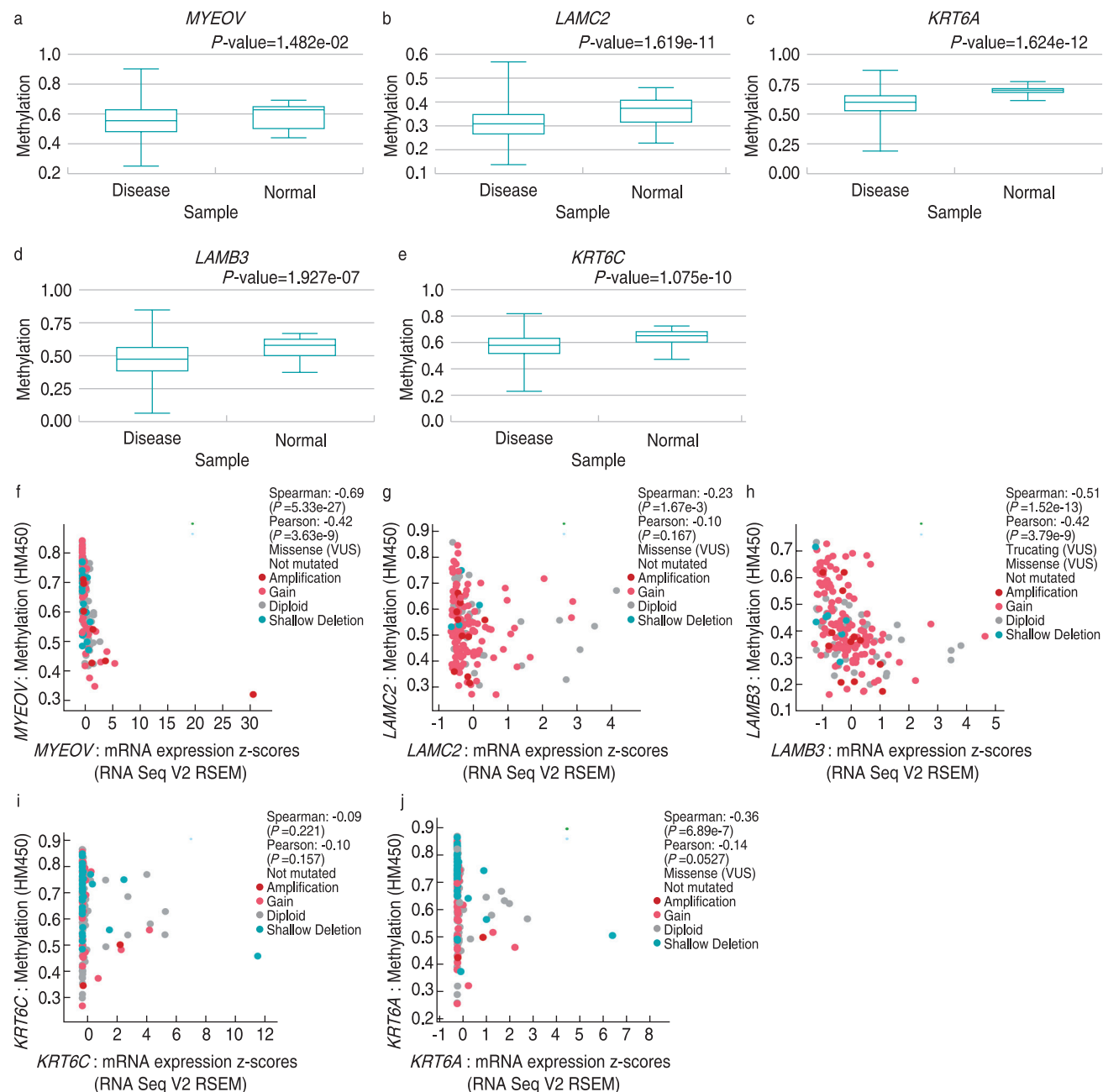


Fig. 6 Methylation analyses of the hub genes in LUAD. (a–e) The methylation levels of the genes in tumor and normal tissues. (a) *MYEOV*; (b) *LAMC2*; (c) *KRT6A*; (d) *LAMB3*; (e) *KRT6C*. (f–j) Relationship between mRNA expression and DNA methylation in the TCGA data set of hub genes. (f) *MYEOV*; (g) *LAMC2*; (h) *LAMB3*; (i) *KRT6C*; (j) *KRT6A*

<https://www.cbiportal.org/>).

Association between hub gene expression and immune infiltration

For the lung cancer hub genes, we used the TIMER platform to investigate possible associations between gene expression and immune infiltration. *MYEOV*, *LAMB3*, *LAMC2*, *KRT6C*, and *KRT6A* were positively correlated with tumor purity and B cells (Fig. 7). CD4+ T cells, CD8+ T cells, neutrophils, macrophages, and dendritic cells showed no or low correlation with *MYEOV*, *LAMB3*, *LAMC2*, *KRT6C*, and *KRT6A*.

Relationship between hub genes and immune signaling pathway

GSEA was performed to investigate the functions of *MYEOV*, *LAMB3*, *LAMC2*, *KRT6C*, and *KRT6A*. *KRT6A* was enriched in “peroxisome,” “FC epsilon RI signaling pathway,” and “complement and coagulation cascade” pathways (Fig. 8). *KRT6C* was enriched in “antigen processing and presentation,” “cytosolic and sensing pathway,” and “Toll-like receptor signaling pathway.” *LAMB3* was enriched in “calcium signaling pathway” and “FC epsilon RI signaling pathway.” *MYEOV* was enriched in “RIG-I-like receptor signaling pathway.” *LAMC2* was enriched in “dorsoventral axis formation”

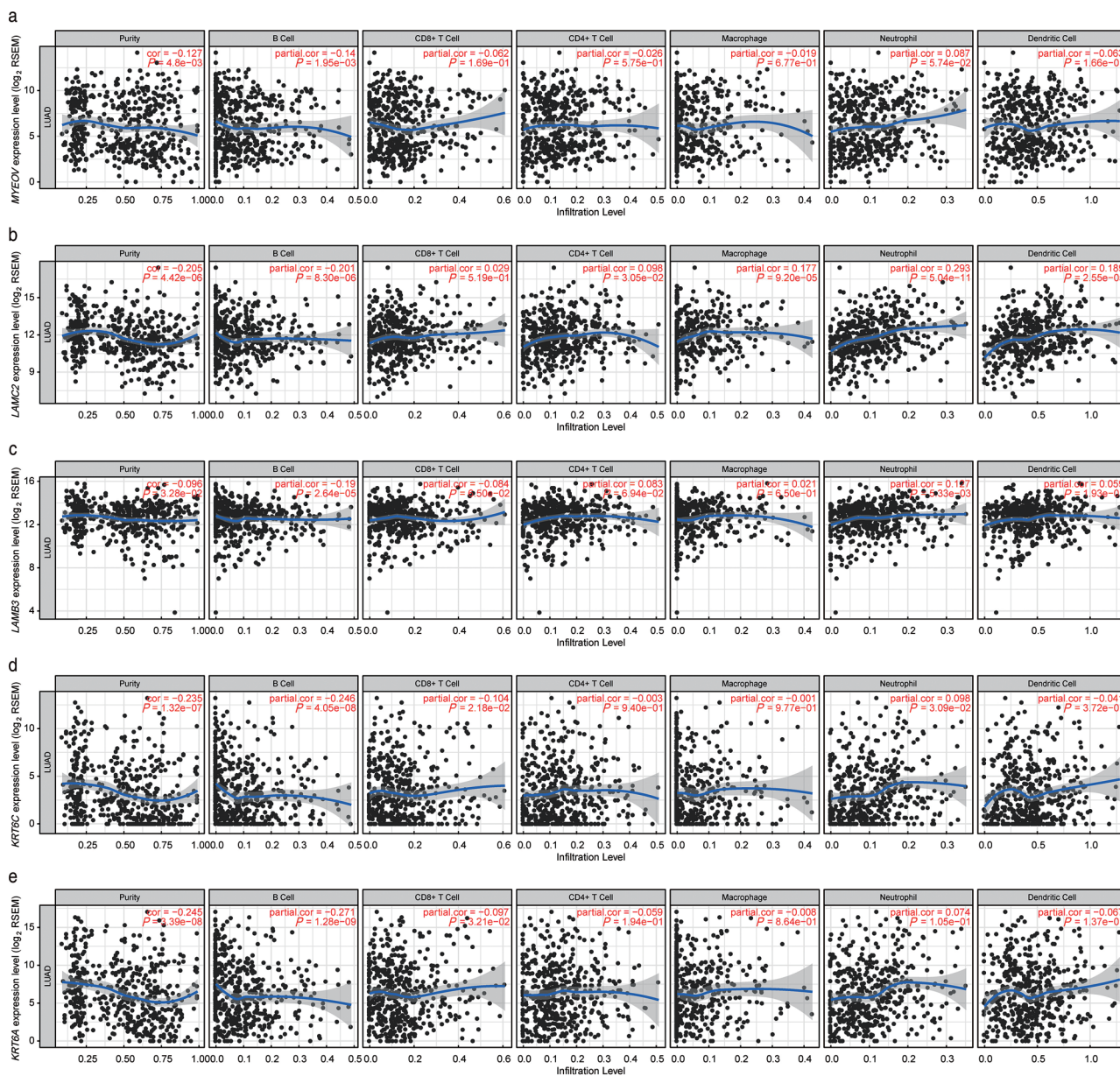


Fig. 7 LUAD immune infiltration connected with hub gene expression. (a) *MYEOV*; (b) *LAMC2*; (c) *LAMB3*; (d) *KRT6C*; (e) *KRT6A*. A P-value of < 0.05 was considered statistically significant. Each dot corresponds to a sample in the dataset of TCGA-PRAD

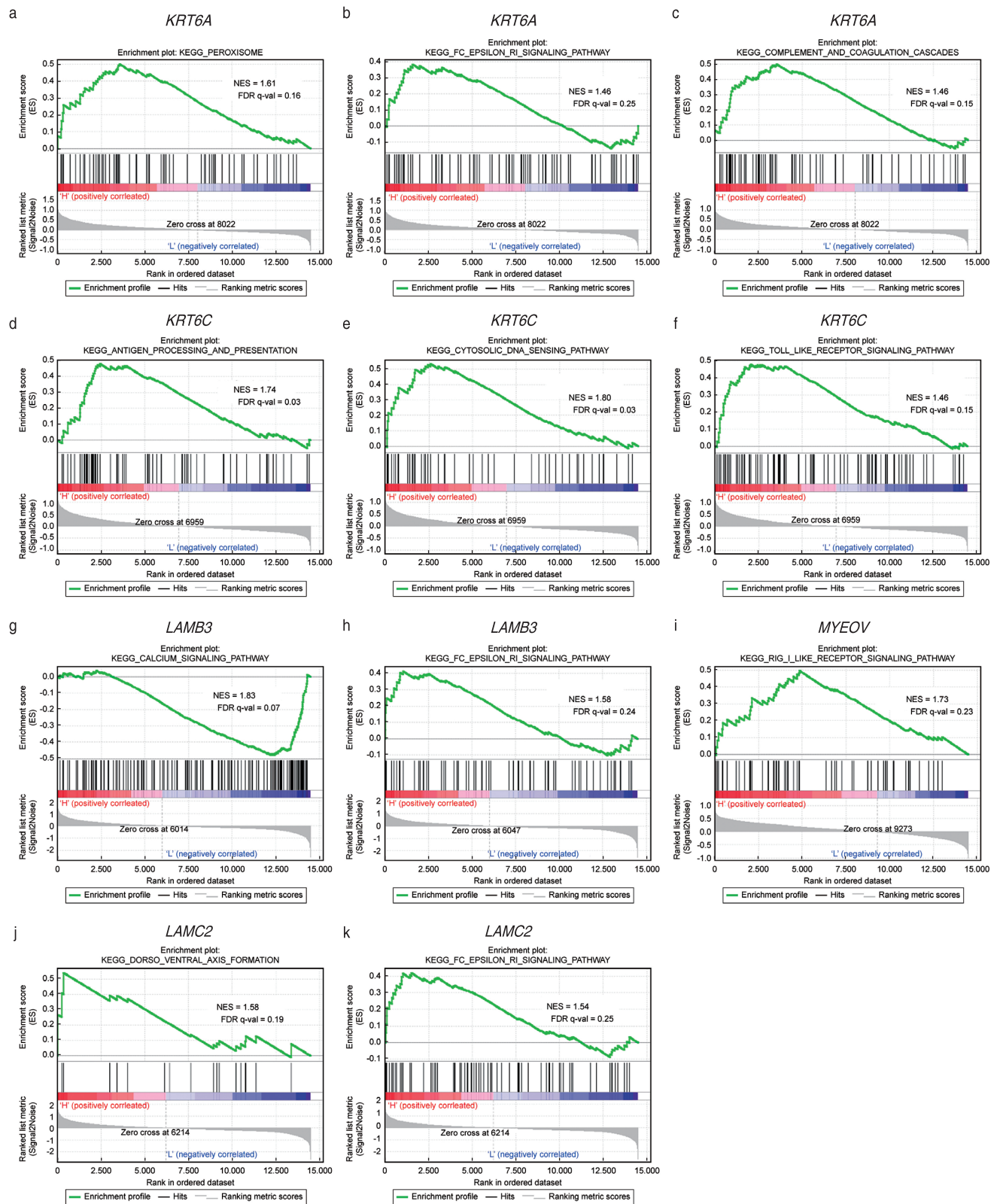


Fig. 8 Gene set enrichment analysis (GSEA) of significant gene sets in accordance with the GSEA enrichment score of the five hub genes. (a–c) KRT6A; (d–f) KRT6C; (g–h) LAMB3; (i) MYEOV; (j–k) LAMC2

and “FcEpsilonRI signaling pathway.”

Discussion

Survival after diagnosis of NSCLC improved from 2013 to 2016 in the United States and is related to the use of targeted therapies [15]. As a molecularly heterogeneous disease, understanding the biology is critical for the treatment of lung cancer. The treatment of lung cancer has transformed owing to the identification of targetable gene alterations and the utilization of individualized therapy resulting from tumor genotyping. In comparison to those without targeted therapies, the survival of patients who are treated with genotype-directed therapy has improved [16]. New diagnostic and prognostic markers that might support the treatment of lung cancer are crucial.

Our study used the WGCNA approach to construct co-expression modules of genes related to lung cancer. In comparison to traditional microarray expression profiling, WGCNA focused more on a batch of gene modules rather than on individual genes, which may avoid the drawbacks of treating genes separately and prevent missing the transcriptional molecular networks [17]. In our study, comprehensive bioinformatics analyses, including WGCNA, were used to screen five genes connected to the progression and prognosis of LUAD.

MYEOV is found in the chromosomal region (chr) 11q13.3, which is associated with carcinogenic amplification [18–19]. This region has been studied in various cancers, including colon [20], gastric [21], esophageal squamous cell [22], neuroblastoma [23], and multiple myeloma [24]. *MYEOV* is a prognostic factor in multiple myeloma [24]. The molecular mechanisms of carcinogenic amplification are still unclear.

Laminin-5 is a large molecule of $\alpha 3$, $\beta 3$, and $\mu 2$ chains encoded by *LAMA3*, *LAMB3*, and *LAMC2*, respectively, and is necessary for cancer diagnosis. Outcomes for patients with stage I LUAD correlated with dysregulated *LAMC2* protein expression [25–27]. Moreover, *LAMB3* cleavage by membrane type-1-matrix metalloproteinase (MT1-MMP) [28] and matrilysin [29] was associated with increased carcinoma cell migration. Our results implied that *LAMC2* and *LAMB3* expression are upregulated in tumor tissues compared to that in healthy tissues and are related to advanced tumor stage (Fig. 5f–5j). However, the influence of *LAMC2* and *LAMB3* overexpression in lung cancer is unclear.

The most common proteins in exhaled breath condensate samples are *KRT6C* and *KRT6A*, and their expression levels in lung cancer tissues are high [30]. We found that *KRT6C* and *KRT6A* overexpression were associated with poorer prognosis and advanced tumor stage in LUAD (Fig. 4 and Fig. 5f–5j).

Our study had several limitations. First, as with

most data mining methods, technical artifacts or tissue contaminations may have influenced our WGCNA results. Second, owing to HPA limitations, the immunohistochemical data shown were from an assortment of patient samples that may not be relevant for LUAD.

DiseaseMeth 2.0 and cBioPortal were also utilized to explore DNA methylation patterns that may have an aberrant expression in LUAD. In comparison to standard samples, *MYEOV*, *LAMB3*, *LAMC2*, *KRT6C*, and *KRT6A* were found to be hypomethylated and associated with the upregulation of the five hub genes observed in LUAD. DNA methylation abnormalities are significantly related to the oncogenic properties of alternative promoters [31]. Feinberg pointed out that DNA methylation is responsible for the occurrence of cancer progenitor cells [32]. DNA hypomethylation of promoter region melanoma-related CT antigen MAGE was associated with recrudescence in colorectal cancer and melanoma [33–34]. In breast and colorectal cancers, overexpression of P-cadherin is caused by hypomethylation of the promoter region of *CDH3* and promotes cell invasion, motility, and migration [35].

We used TIMER and GSEA for each hub gene to investigate biological functions. Tumor purity and B cells positively correlated with *MYEOV*, *LAMB3*, *LAMC2*, *KRT6C*, and *KRT6A*. In LUAD samples, no significant associations were found between these hub genes and other immune infiltrates. GSEA indicated that single hub genes were significantly enriched in immune pathways. Increased expression of T and B cells, such as adenocarcinoma B cells and CD8 cells, predicts OS in patients with LUAD [36]. Moreover, further research needs to be conducted to study the correlation between the hub genes and smokers carrying lung cancer, in terms of an increase in the development of squamous cell carcinoma. Deficient-type GSTM1 has been shown to increase the risk of squamous cell carcinoma development [37]. We believe that the five hub genes are mainly expressed in lung cancer cells and are related to B cell functions.

Conclusion

We identified five hub genes (*MYEOV*, *LAMB3*, *LAMC2*, *KRT6C*, and *KRT6A*) that were correlated with the development and prognosis of lung cancer and potentially regulated by epigenetic mechanisms. Additional research is required to demonstrate their contribution to the pathogenesis of lung cancer and confirm their utility as diagnostic and/or predictive biomarkers.

Acknowledgments

We thank the Gene Expression Omnibus and TCGA database for sharing large amounts of data.

Conflicts of interest

The authors indicated no potential conflicts of interest.

References

- Bray F, Ferlay J, Soerjomataram I, *et al.* Global cancer statistics 2018: GLOBOCAN estimates of incidence and mortality worldwide for 36 cancers in 185 countries. *CA Cancer J Clin*, 2018, 68: 394–424.
- Nesbitt JC, Putnam JB, Walsh GL, *et al.* Survival in early-stage non-small cell lung cancer. *Ann Thorac Surg*, 1995, 60: 466–472.
- Liang Y, Wakelee HA. Adjuvant chemotherapy of completely resected early stage non-small cell lung cancer (NSCLC). *Transl Lung Cancer Res*, 2013, 2: 403–410.
- Li JH, Jiang M, Zhao XT, *et al.* Cisplatin selects for CD133+ cells in lung cancer cells. *Oncol Transl Med*, 2020, 6: 16–20.
- Chan BA, Hughes BGM. Targeted therapy for non-small cell lung cancer: current standards and the promise of the future. *Transl Lung Cancer Res*, 2015, 4: 36–54.
- Francis H, Solomon B. The current status of targeted therapy for non-small cell lung cancer. *Intern Med J*, 2010, 40: 611–618.
- Edgar R, Domrachev M, Lash AE. Gene Expression Omnibus: NCBI gene expression and hybridization array data repository. *Nucleic Acids Res*, 2002, 30: 207–210.
- Langfelder P, Horvath S. WGCNA: an R package for weighted correlation network analysis. *BMC Bioinformatics*, 2008, 9: 559.
- Zhang B, Horvath S. A general framework for weighted gene co-expression network analysis. *Stat Appl Genet Mol Biol*, 2005, 4: Article 17. doi: 10.2202/1544-6115.1128. Epub 2005 Aug 12.
- Yip AM, Horvath S. Gene network interconnectedness and the generalized topological overlap measure. *BMC Bioinformatics*, 2007, 8: 22.
- Lv J, Liu HB, Su JZ, *et al.* DiseaseMeth: a human disease methylation database. *Nucleic Acids Res*, 2012, 40 (Database issue): D1030–D1035.
- Xiong YC, Wei YJ, Gu Y, *et al.* DiseaseMeth version 2.0: a major expansion and update of the human disease methylation database. *Nucleic Acids Res*, 2017, 45 (D1): D888–D895.
- Li B, Severson E, Pignon JC, *et al.* Comprehensive analyses of tumor immunity: implications for cancer immunotherapy. *Genome Biol*, 2016, 17: 174.
- Li TW, Fan JY, Wang BB, *et al.* TIMER: A web server for comprehensive analysis of tumor-infiltrating immune cells. *Cancer Res*, 2017, 77: e108–e110.
- Howlader N, Forjaz G, Mooradian MJ, *et al.* The effect of advances in lung-cancer treatment on population mortality. *N Engl J Med*, 2020, 383: 640–649.
- Herbst RS, Morgensztern D, Boshoff C. The biology and management of non-small cell lung cancer. *Nature*, 2018, 553: 446–454.
- Ivliev AE, Hoen PAC, Sergeeva MG. Coexpression network analysis identifies transcriptional modules related to proastrocytic differentiation and sprouty signaling in glioma. *Cancer Res*, 2010, 70: 10060–10070.
- Hui ABY, Or YYY, Takano H, *et al.* Array-based comparative genomic hybridization analysis identified cyclin D1 as a target oncogene at 11q13.3 in nasopharyngeal carcinoma. *Cancer Res*, 2005, 65: 8125–8133.
- Brown LA, Irving J, Parker R, *et al.* Amplification of EMSY, a novel oncogene on 11q13, in high grade ovarian surface epithelial carcinomas. *Gynecol Oncol*, 2006, 100: 264–270.
- Moss AC, Lawlor G, Murray D, *et al.* ETV4 and Myeov knockdown impairs colon cancer cell line proliferation and invasion. *Biochem Biophys Res Commun*, 2006, 345: 216–221.
- Leyden J, Murray D, Moss A, *et al.* Net1 and Myeov: computationally identified mediators of gastric cancer. *Br J Cancer*, 2006, 94: 1204–1212.
- Janssen JWG, Imoto I, Inoue J, *et al.* MYEOV, a gene at 11q13, is coamplified with CCND1, but epigenetically inactivated in a subset of esophageal squamous cell carcinomas. *J Hum Genet*, 2002, 47: 460–464.
- Takita J, Chen YY, Okubo J, *et al.* Aberrations of NEGR1 on 1p31 and MYEOV on 11q13 in neuroblastoma. *Cancer Sci*, 2011, 102: 1645–1650.
- Moreaux J, Hose D, Bonnefond A, *et al.* MYEOV is a prognostic factor in multiple myeloma. *Exp Hematol*, 2010, 38: 1189–1198. e3.
- Aumailley M, Bruckner-Tuderman L, Carter WG, *et al.* A simplified laminin nomenclature. *Matrix Biol*, 2005, 24: 326–332.
- Kagesato Y, Mizushima H, Koshikawa N, *et al.* Sole expression of laminin gamma 2 chain in invading tumor cells and its association with stromal fibrosis in lung adenocarcinomas. *Jpn J Cancer Res*, 2001, 92: 184–192.
- Moriya Y, Niki T, Yamada T, *et al.* Increased expression of laminin-5 and its prognostic significance in lung adenocarcinomas of small size. An immunohistochemical analysis of 102 cases. *Cancer*, 2001, 91: 1129–1141.
- Udayakumar TS, Chen ML, Bair EL, *et al.* Membrane type-1-matrix metalloproteinase expressed by prostate carcinoma cells cleaves human laminin-5 beta3 chain and induces cell migration. *Cancer Res*, 2003, 63: 2292–2299.
- Remy L, Trespeuch C, Bachy S, *et al.* Matrilysin 1 influences colon carcinoma cell migration by cleavage of the laminin-5 beta3 chain. *Cancer Res*, 2006, 66: 11228–11237.
- López-Sánchez LM, Jurado-Gómez B, Feu-Collado N, *et al.* Exhaled breath condensate biomarkers for the early diagnosis of lung cancer using proteomics. *Am J Physiol Lung Cell Mol Physiol*, 2017, 313: L664–L676.
- Takacs M, Banati F, Koroknai A, *et al.* Epigenetic regulation of latent Epstein-Barr virus promoters. *Biochim Biophys Acta*, 2010, 1799: 228–235.
- Feinberg AP, Ohlsson R, Henikoff S. The epigenetic progenitor origin of human cancer. *Nat Rev Genet*, 2006, 7: 21–33.
- Weber J, Salgaller M, Samid D, *et al.* Expression of the MAGE-1 tumor antigen is up-regulated by the demethylating agent 5-aza-2'-deoxycytidine. *Cancer Res*, 1994, 54: 1766–1771.
- Kim KH, Choi JS, Kim IJ, *et al.* Promoter hypomethylation and reactivation of MAGE-A1 and MAGE-A3 genes in colorectal cancer cell lines and cancer tissues. *World J Gastroenterol*, 2006, 12: 5651–5657.
- Paredes J, Albergaria A, Oliveira JT, *et al.* P-cadherin overexpression is an indicator of clinical outcome in invasive breast carcinomas and is associated with CDH3 promoter hypomethylation. *Clin Cancer Res*, 2005, 11: 5869–5877.
- Iglesia MD, Parker JS, Hoadley KA, *et al.* Genomic analysis of immune cell infiltrates across 11 tumor types. *J Natl Cancer Inst*, 2016, 108: djw144.
- Li JH, Zhang LN, Wang Y, *et al.* Association of genetic polymorphisms of GSTM1 and smoking status with lung cancer risk. *Oncol Transl Med*, 2019, 5: 249–256.

DOI 10.1007/s10330-020-0437-7

Cite this article as: Chen AX, Zhao SN, Zhou F, *et al.* Identification of potential immune-related prognostic biomarkers of lung cancer using gene co-expression network analysis. *Oncol Transl Med*, 2020, 6: 247–257.

Silencing Neuropilin 1 gene reverses TGF- β 1-induced epithelial mesenchymal transition in HGC-27 gastric cancer cell line*

Weiguo Xu¹ (✉), Xin Yang¹, Qiqi Zhan¹, Guanyi Ding¹, Shang Guo¹, Bing Zhu¹, Hong Xu², Xiangmei Liu^{1,3}

¹ Department of Surgical Oncology, North China University Of Science and Technology Affiliated Hospital, Tangshan 063000, China

² North China University of Science and Technology, Tang Shan 063000, China

³ Department of Gynaecology and Obstetrics, Liuyang Maternal and Child Health Care Hospital, Liu Yang 410300, China

Abstract

Objective The aim of this study was to determine Neuropilin 1 (NRP1) contribution to transforming growth factor β 1 (TGF- β 1)-induced epithelial mesenchymal transition (EMT) of HGC-27 gastric cancer cells and study its mechanism.

Methods In this study, TGF- β 1 was used to induce EMT in HGC-27 cells. Further, these cells were stably transfected with siRNA targeting NRP1. Wound healing and transwell assays were used to measure cell migration and invasion, respectively. NRP1 and EMT markers were measured using quantitative real time reverse transcription polymerase chain reaction and western blotting.

Results Exposure of TGF- β 1 conferred a fibroblastic-like shape to cancer cells and significantly increased the expression of NRP1 in HGC-27 cells. TGF- β 1 subsequently promoted migration and invasion of HGC-27 cells. Furthermore, silencing NRP1 inhibited the invasion and migration of TGF- β 1-induced cells undergoing EMT.

Conclusion Silencing NRP1 can inhibit cell migration, invasion, and metastasis and reverse the TGF- β 1-induced EMT process of gastric cancer.

Key words: Neuropilin1 (NRP1); epithelial-mesenchymal transition (EMT); gastric cancer; transforming growth factor- β 1

Received: 26 March 2020

Revised: 15 April 2020

Accepted: 20 May 2020

Gastric cancer (GC) is one of the most important cancers worldwide. It is the fifth most frequently diagnosed cancer and is the third leading cause of cancer death in patients [1].

Epithelial-mesenchymal transition (EMT) is perceived as a significant phenotypic transformation that occurs during early-stage development [2]. It has become progressively certain that EMT has significant roles in malignancy, diminishes the affectability of disease cells to therapeutics, and advances malignant cell growth and metastasis [3]. Lost E-cadherin articulation, which is recognized in gastrointestinal malignancies, is related to a poor prognosis with faster disease progress [4]. The articulation and initiation of the EMT-prompting

interpretation factors result as a response to different signaling pathways, including those that are interceded by transforming growth factor β (TGF- β), Wnt, Sonic Hedgehog (Shh), platelet-derived growth factor (PDGF), fibroblast growth factor (FGF), epidermal growth factor (EGF), bone morphogenetic protein (BMP), Notch and integrin [5–10]. During EMT, cells lose their epithelial attributes with a rise in mesenchymal phenotype before entering systemic circulations during metastasis [11].

Neuropilins are single-pass transmembrane proteins. Neuropilin 1 (NRP1) was described in 1987 as the first member of the family, and later, in 1997, neuropilin 2 (NRP2) was insulated by Chen *et al* [12–13]. In 1998, Soker *et al.* isolated NRP1 from endothelial cells and tumor

✉ Correspondence to: Weiguo Xu. Email: mimimay860@gmail.com

* Supported by grants from Returning Overseas Students (No. CY201721).

©2020 Huazhong University of Science and Technology

tissues^[14]. Indeed, NRP expression is not just restricted to intra-tumoral vessels, but a vast majority of cancer cells are reported to express NRPs^[15]. Since its discovery, NRP1 has been widely used as a selective tumor targeting agent in both preclinical and human studies, and NRPs have rapidly become recognized as key regulators of angiogenesis, lymphangiogenesis, EMT, and tumor progression^[16]. Clinical-pathological data seem to indicate a correlation between the increased expression of NRPs and the advanced stage of tumors with poor prognosis, and they are more broadly observed in a large variety of diverse tumor types and the generation of cancer stem cells^[17-20]. Non-small cell lung cancer (NSCLC) patients with a high articulation of NRP1 have a shorter disease-free and endurance rate^[21]. NRP1 upregulation in gastrointestinal carcinomas appears to correlate with invasive behavior and metastatic potential^[22]. It has been shown that NRPs interact with TGF- β , hepatocyte growth factor (HGF), and signal PDGF^[23-26].

Few ecological signs have been found to control the NRP's articulation of tumor cells *in vitro*. It is not completely understood how NRPs can control such a wide scope of various signaling receptors. The mechanism by which NRP1 impacts tumorigenesis is not yet thoroughly characterized. In this study, we hypothesized that NRP1 contributes to the responsiveness of the TGF- β -induced EMT pathway in the HGC-27 cells, which is important for the progression and metastasis of tumors. We also hypothesized the anticipated cure for GC by targeting NRP-1.

Materials and methods

Cell culture

The human GC cell line HGC-27 was bought from the cell bank of the Chinese Academy of Sciences (China). The cells were cultured in RPMI 1640 (Gibco, USA) complemented with 10% fetal bovine serum (FBS) (Jiangsu Ke Te Biological Co., Ltd., China), 100 μ g/mL streptomycin, and 100 U/mL of penicillin (Invitrogen, USA) at 37 °C in a humidified atmosphere containing 5% CO₂.

Establishment of TGF- β 1-induced EMT model

Recombinant human TGF- β 1 (Invitrogen Biotechnology Co., Ltd., USA) was used to initiate EMT in HGC-27 cells. Cells were simmered for 24 h and seeded in 6-well plates for TGF- β 1 incentive, and these cells were cultured with RPMI 1640 accompanied with 2% FBS comprising 5 ng/mL TGF- β 1 every 2 d until 7 d in 37 °C incubator with 5% CO₂ to achieve the EMT state. Cell morphology changes were observed using quantitative real-time reverse transcription-polymerase chain reaction (qRT-PCR) and western blotting to find the mRNA and protein

expression of NRP1, E-cadherin, Vimentin, and Snail, respectively, and to screen out the best TGF- β 1-induced EMT model.

Gene expression knockdown by RNA interference of HGC-27 cells

In tumor cells, NRP1 expression was suppressed by transfecting targeted siRNA sequences with Lipofectamine 2000 (Invitrogen, USA). The NRP1 siRNA (si-NRP1) and negative control siRNA (si-NC) were purchased from RiboBio (Suzhou RiboBio Co., Ltd., China). The target arrangement was used to down-regulate NRP1 *in vitro*. A nontarget siRNA sequence was utilized as a depressing control. Cells were then grouped and transfected as the CON group (blank control, transfected with the phosphate-buffered saline; PBS), NC group (transfected with the negative control siRNA), and si-NRP1 group (transfected with the NRP1 siRNA). Lipofectamine 2000 were transfected when the cell intensity reached 30% to 50%. Later, cells were handled with the mixed solution and cultivated for 4 to 6 h at 37 °C with 5% CO₂. After incubation, cells were transported to a complete medium and cultivated for 48 h to 72 h. The qRT-PCR and western blotting validated knockdown efficiency.

Wound healing assay

HGC-27 cells were cultured in a 6-well plate at a final density of 1×10^6 cells/well and incubated overnight for adhesion. When the confluence reached 95%, a 200 μ L micropipette tip was used to create a vertical linear scratch on the cell monolayer in the 6-well plate. Next, the wells were washed twice with PBS to remove any loose cells, and cells were continuously cultured in medium supplemented with 2% FBS under the standard conditions. The images were taken at different time points, including 0 h, 24 h, and 48 h after the scratch. Using Image J software, the wound closure was analyzed. The 24 h (or 48 h) relative percent of wound closure = (the width at 0 h - the width at 24 h (or 48 h))/the width at 0 h.

Cell migration and invasion assays

For the cell invasion assay, transwell chambers were coated with Matrigel (dilution 1:8; Becton, Dickinson and Company, USA) on the upper side of the membrane and incubated at 37 °C overnight before starting the invasion assay. Three wells per test group were assayed. In the meantime, at a final density of 1×10^5 cells/mL, trypsin-digested cells were combined with RPMI 1640. Then, 600 μ L of RPMI 1640 containing 10% FBS were added into the lower chamber, whereas 200 μ L of the cell suspension were transferred to the upper chamber. After 24 h of culture, cells that did not enter through the membrane were removed with cotton swabs and detached from the

culture plate. Transferred cells were then fixed with 4% polyformaldehyde for 15 min, then with a 0.1% crystal violet solution for 15 min, and finally cleaned with PBS. Lastly, we observed cells under the microscope. For cell migration, the invasion assay was performed the same as described above, except chambers were not coated with Matrigel. Cell migration and invasion were defined by counting the marked cells in 5 randomly selected fields with a light microscope, and the number of cells was computed with ImageJ software.

qRT-PCR

Using Trizol (Invitrogen, USA) reagent, total RNA was extracted from HGC-27 cell lines. After confirming the concentration and purity of the RNA, a Reverse Transcription Kit (ZR102-1, Zeman Biotechnology Co., Ltd. China) was used for the reverse transcription of 2 µg RNA to cDNA with 20 µL of the reverse transcription system according to the manufacturer. qRT-PCR was directed with a 2 × SYBR qPCR Mix. The sequences of primers are given below: NRP1 (Forward: 5'- GATCTACCCCGAGAGAGCCA -3' Reverse: 5'- TGAGCTGGAAGTCATCACCTG -3'), E cadherin (Forward: 5'- GGCTGGACCGAGAGAGTTTC -3' Reverse: 5'- CAAAATCCAAGCCCGTGGTG -3'), Vimentin (Forward: 5'- TCCGCACATTTCGAGCAAAGA -3' Reverse: 5'- TGAGGGCTCCTAGCGGTTTA -3'), Snail (Forward: 5'- CGGCTTTTGCAGTGGACATC -3' Reverse: 5'- CGGCTTTTGCAGTGGACATC -3'), and GAPDH (Forward: 5'- ACCCAGAAGACTGTGGATGG -3' Reverse: 5'- TCTAGACGGCAGGTCAGGTC -3'). The mRNA level of the target genes was normalized by the GAPDH mRNA level to quantify gene expression. The gene expression was analyzed using the $2^{-\Delta\Delta CT}$ approach (formula: $\Delta\Delta CT = \Delta CT_{\text{experimental group}} - \Delta CT_{\text{control group}}$, $\Delta CT = CT_{\text{target gene}} - CT_{\text{internal reference}}$).

Western blotting analysis

Overall proteins were mined from cells. PBS-washed cells were lysed with RIPA lysis buffer, which contained 1% phenylmethylsulfonyl fluoride (PMSF) at 4 °C. The whole-cell lysate obtained was centrifuged at 12,000 rpm for 15 min. The protein intensities were calculated using bicinchoninic acid (BCA) method. 30 µg protein were separated by 10% sodium dodecyl sulfate-polyacrylamide gel electrophoresis (10% polyacrylamide) at 90 V and moved to a polyvinylidene fluoride membrane at 120 V for 100 min. The membrane was closed with PBS containing 5% skimmed milk powder for 1 h and incubated with primary antibodies at 4 °C overnight with anti-NRP1 (diluted at 1:1500, ARG59279), anti-E cadherin (diluted at 1:700, A11492), anti-Vimentin (diluted at 1:1000,

ARG69199), anti-Snail (diluted at 1:1000, A5544), and anti-Tubulin (diluted at 1:200, GTX11270). The membrane was washed with TBST 5 times. Afterward, the membrane was incubated with the anti-rabbit (1:5000) secondary antibodies for 1 h at 37 °C. Washing thrice with TBST for 5 min each afterward, the membrane was incubated with the enhanced chemiluminescence solution, followed by X-film exposure and photographing. The intensities of protein bands were analyzed using Image J software. Gray values of the target bands were normalized with those of the internal reference band (Tubulin). Protein expression was calculated between the target and the internal criteria band.

Statistical analysis

All data were statistically analyzed using IBM SPSS Statistics for Windows (version 20.0; IBM Corp. Armonk, USA). Values were expressed as the mean ± SD. An ANOVA was used for multiple groups, while pairwise evaluations were completed using Student's *t*-tests. All the experiments were repeated in triplicate. *P* < 0.05 was considered significant.

Results

TGF-β1 induced EMT in the GC HGC-27 cells

Through EMT, HGC-27 cells can undergo a phenotypic, reversible switch to fibroblast-like cells. TGF-β1 exposure led to the formation of spindle-shaped cells with elongated cellular processes and diminished cell-to-cell contacts, characteristics of EMT, as compared to the TGF-β1 negative group (Fig. 1a). TGF-β1-induced EMT led to upregulation of migration and invasion of HGC-27 cells (Fig. 1b and 1c). Furthermore, TGF-β1 reduced protein expression of epithelial markers (E-cadherin) and increased expression of Vimentin, Snail and NRP1 (Fig. 1d). qRT-PCR was performed to examine the mRNA levels of EMT-related molecules in HGC-27 cells at 0, 2, 3, 4, and 7 d (Fig. 1e). In conclusion, TGF-β1 could be used to stimulate the HGC-27 cell line to implement the TGF-β1-induced EMT model for further studies.

NRP1 expression and stable knockdown in the GC HGC-27 cell lines

Following the transfection result, qRT-PCR demonstrated that *NRP1* gene expression was significantly downregulated in the siNRP1 group compared to the NC and CON groups, and the differences were statistically significant (*P* < 0.05). Western blotting clearly showed that NRP1 protein was suppressed 0.47-fold in HGC-27 cells transfected with NRP1-siRNA (Fig. 2).

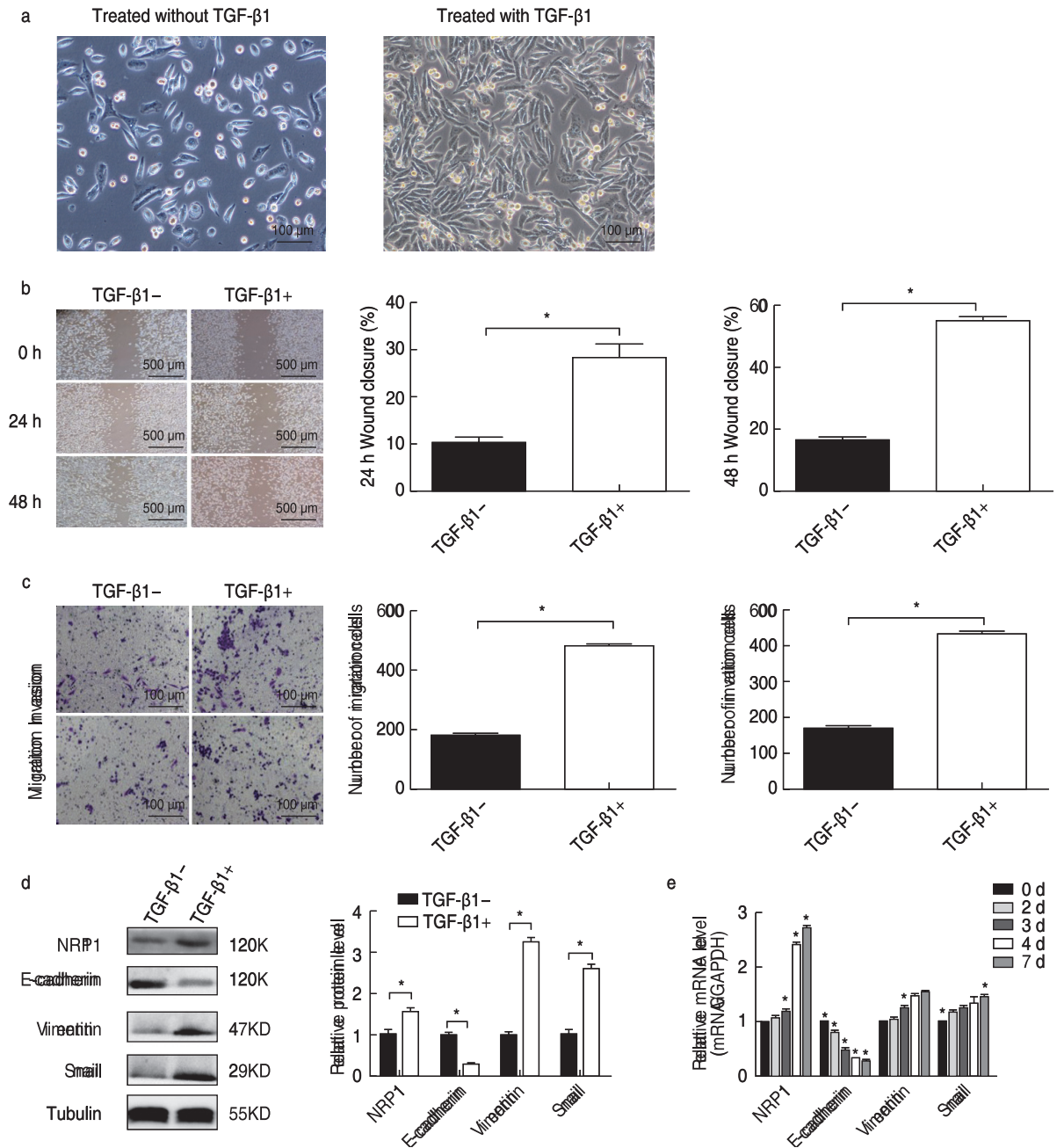


Fig. 1 TGF-β1 induces EMT in HGC-27 cells. (a) Morphological changes. At 200× magnification, scale bar = 100 μm; (b) The results of the wound healing assay. At 40 × magnification, scale bar = 500 μm; (c) The results of the transwell assay. At 100× magnification, scale bar = 100 μm; (d) Western blot analysis; (e) qRT-PCR analysis. The cells were treated with 5 ng/mL TGF-β1 for 0 to 7 d. Data were presented as the mean ± SD; **P* < 0.05 vs TGF-β1 negative group

Silencing NRP1 diminishes the ability of invasion and migration of HGC-27 via inhibition of TGF-β1-induced EMT

To examine the potential effect of NRP1 on TGF-β1-induced EMT in HGC-27 cells, experiments were divided into four groups: (1) blank group (without treatment), (2) TGF-β1 + CON group (cells treated with TGF-β1 and

transfected with the PBS), (3) TGF-β1 + NC group (cells treated with TGF-β1 and transfected with the negative control siRNA), and (4) TGF-β1 + siNRP1 group (cells treated with TGF-β1 and transfected with NRP1-siRNA). As presented in Fig. 3a and 3b, 24 and 48 h after the scratch, the wound of TGF-β1 + siNRP1 group exhibited significant closure, and the number of migratory and

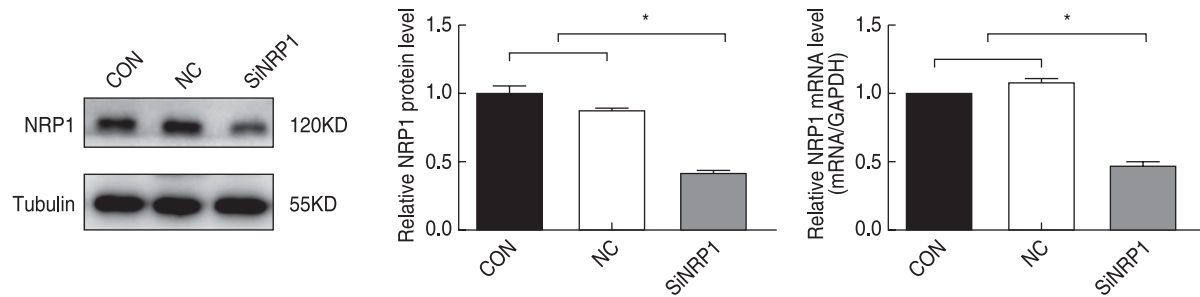


Fig. 2 The NRP1 expression in HGC-27 transfected with siRNA was assessed with Western blotting qRT-PCR. Data were presented as the mean \pm SD; $P < 0.05$

invasive cells in TGF- β 1+ siNRP1 group was significantly reduced. These results demonstrated that treatment with TGF- β 1 promoted HGC-27 cell invasion and migration, and those effects were greatly weakened after silencing NRP1, which indicates that low expression of NRP1 attenuates TGF- β 1-induced cell invasion and migration.

NRP1 contributes to the TGF- β 1-induced EMT in GC cells

HGC-27 cells were first treated with 5 ng/mL of TGF- β 1 for 96 h to initiate EMT and further treated with siNRP1. Western blot results showed that in the TGF- β 1 + siNRP1 group, E-cadherin level was increased to a great extent, the expression of Snail and Vimentin decreased ($P < 0.05$); conversely, no changes were observed in protein expression levels between the TGF- β 1 + CON and TGF- β 1 + NC groups ($P \geq 0.05$). Therefore, TGF- β 1-induced EMT was reversed by silencing NRP1 in HGC-27 cells (Fig. 3c). qRT-PCR detected mRNA expression alterations similar to the western blot trend (Fig. 3d). The loss of NRP1 may efficiently reverse EMT produced by TGF- β 1. The outcome expressed that the initiation of EMT markers produced by TGF- β 1 was reduced later in epithelial cells by NRP silencing, demonstrating that the NRP1 signaling pathways could be liable for TGF- β 1-negotiated EMT. Western blot and qRT-PCR were utilized to identify protein and mRNA expression alterations of NRP1 in the TGF- β 1/NRP1 signaling pathway during EMT, respectively. Results indicated that on exposure with 5 ng/mL TGF- β 1, the protein expression of NRP1 steadily reduced, which was considerably lower in TGF- β 1+SiNRP1group ($P < 0.05$), and no major change in these protein expression were seen between the TGF- β 1+NC and TGF- β 1+ CON groups ($P \geq 0.05$) (Fig. 3c and Fig. 3d). Silencing NRP1 may reverse the EMT process by regulating the TGF- β 1/NRP1 signaling pathway, indicating that NRP1 acted downstream of the TGF- β 1 pathway.

Discussion

Without activating oncogenes, EMT may struggle for a subsistence benefit for cancer cells^[27]. Cancer cell invasion, migration, resistance to apoptosis, therapy resistance, and metastasis involves EMT^[28-32]. In distant sites of metastasis, the mesenchymal cells coalesce and repolarize through a reverse process known as “the mesenchymal to epithelial transition (MET) form secondary epithelial cells”^[33]. Thus, through EMT at the primary site and with MET at secondary sites, the neoplastic epithelial cells gain (through evolution) the ability to invade surrounding tissues and, therefore, can spread to further locations^[34]. Interestingly, CD44 (high)/CD24 (low) cells, which are purified from normal and malignant breast cancer tissues, show features of EMT and exhibit stem cell-like properties along with increased metastatic potential^[35]. Since the mesenchymal-type cancer cells are more resistant to chemotherapeutic agents than the epithelial-type cancer cells^[36-37], the status of the EMT characteristics must, therefore, be reversed to overcome drug resistance, which in turn could lead to the sensitization of drug-resistant cancer cells to conventional chemotherapeutic agents. There is increasing evidence of an association between the acquired resistance to standard chemotherapeutic agents and EMT in gastrointestinal malignancies^[38]. In this study, the treatment of TGF- β 1 caused EMT in HGC-27 cells, further transfection with siRNA-NRP1 led to upregulation of E-cadherin and downregulation of mesenchymal markers at dissimilar stages, as tested by western blot analysis and qRT-PCR (Fig. 3c and Fig. 3d). On approachable epithelial cell types, EMT-inducing signals can disturb intercellular bond complexes and cause the intermediate loss of apical-basal polarity^[39]. Embryos require multiple steps under EMT and MET during complete gastrulation and primitive streak creation, which highlights the reversibility of this procedure^[40].

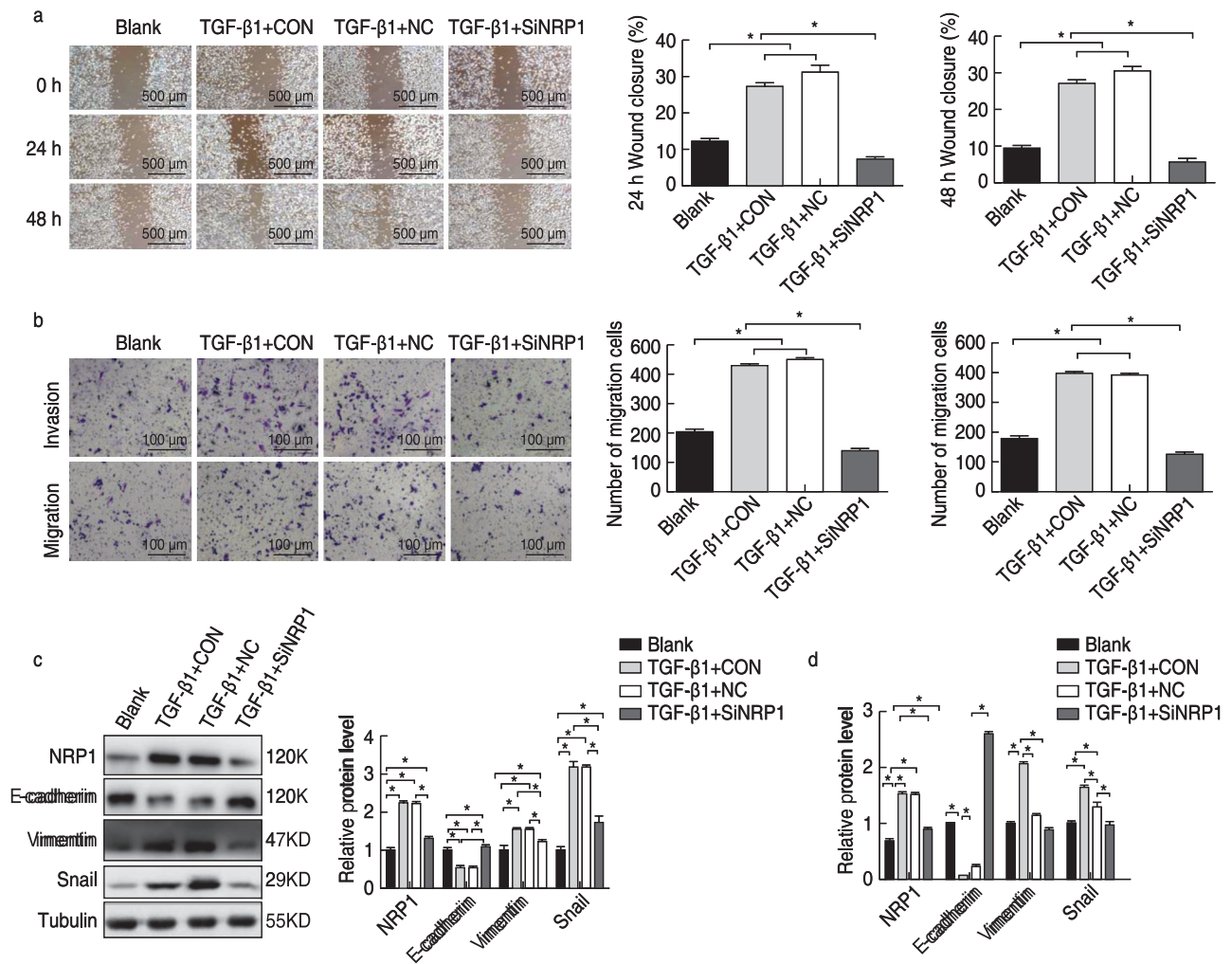


Fig. 3 The potential effect of knockdown NRP1 on TGF-β1-induced EMT in HGC-27 cells. (a) The results of the wound healing assay. At 40× magnification, scale bar = 500 μm; (b) The results of transwell assay, At 100 × magnification, scale bar = 100 μm; (c) Western blot analysis; (d) qRT-PCR analysis. Data were presented as the mean ± SD; *P < 0.05

NRP1 is a multifunctional protein that is essential for the development of both neural and vasculature systems.^[41] In most cases, NRP1 acts with a co-receptor and, at times, a multi-protein complex of VEGF and TGF-β, which results in a series of diverse biological roles that encompass angiogenesis, carcinoma, and immunity^[41-42]. Thus, NRP1 acts as a receptor hub present on the cell surface that promotes multiple signaling cascades^[43-44]. In some studies conducted, the NRP1-binding peptides or knockdown of NRP1 by siRNA inhibited cancer cell growth and increased the sensitivity of cells to chemotherapeutic agents (e.g., 5-FU, paclitaxel, and cisplatin)^[45]. Furthermore, the NRP1 may be a valuable target for therapy in glioblastoma, melanoma, and some in forms of leukemia^[46-48].

Since TGF-β1 promotes metastasis, this is extremely

relevant to cancer biology^[23]. Wu *et al*^[49] using a meta-analysis of the patients suffering from GC, reported a TGFβ-associated supermodule of stroma-related genes that are associated with diffuse-type histology and poor prognosis in patients with GC. Drugs that inhibit TGF-β1 signaling prevent EMT and block metastases in murine models^[50]. TGF-β plays an important role in EMT through regulating the expression of multiple genes and pathways, as recently reviewed by Fuxe *et al*^[51]. Upcoming studies, authenticating special NRP1-interfering molecules for this determination that is valid *in vivo* under preclinical models must be conducted. While NRP1 attenuates EMT via TGF-β1 pathway, the inhibition of NRP1 may contribute to a TGF-β1-independent EMT reversal.

Our outcomes recommend that NRP1 guides TGF-β1 constitutive signaling activation and endures a probable

role of NRP1 and TGF- β 1 under the EMT. To demonstrate our hypothesis that NRP1 persuades the constitutive activation of the TGF- β 1 pathway, we studied the impact of NRP1 on TGF- β 1 signaling. In this study, our data revealed that knockdown NRP1 overpowers the EMT and TGF- β 1 signaling pathway in GC cells by targeting many markers and proteins in the process. In future, we need *in vivo* experiments to confirm that TGF- β 1 promotes the growth of HGC-27 cells and that this effect was weakened on silencing NRP-1 expression. Resultantly, silencing NRP-1 may attenuate TGF- β 1-generated EMT in HGC-27 cells, indicating the prominence of the contribution of NRP-1 as a potential marker for GC therapy.

Conflicts of interest

The authors indicated no potential conflicts of interest.

References

- Bray F, Ferlay J, Soerjomataram I, *et al.* Global cancer statistics 2018: GLOBOCAN estimates of incidence and mortality worldwide for 36 cancers in 185 countries. *CA: a cancer journal for clinicians* 2018, 68: 394–424.
- Drees F, Pokutta S, Yamada S, *et al.* Alpha-catenin is a molecular switch that binds E-cadherin-beta-catenin and regulates actin-filament assembly. *Cell*, 2005, 123: 903–915.
- Fuchs BC, Fujii T, Dorfman JD, *et al.* Epithelial-to-mesenchymal transition and integrin-linked kinase mediate sensitivity to epidermal growth factor receptor inhibition in human hepatoma cells. *Cancer Res*, 2008, 68: 2391–2399.
- Natalwala A, Spychal R, Tselepis C. Epithelial-mesenchymal transition mediated tumorigenesis in the gastrointestinal tract. *World J Gastroenterol*, 2008, 14: 3792–3797.
- McCormack N, O'Dea S. Regulation of epithelial to mesenchymal transition by bone morphogenetic proteins. *Cellular Signal*, 2013, 25: 2856–2862.
- Espinoza I, Miele L. Deadly crosstalk: Notch signaling at the intersection of EMT and cancer stem cells. *Cancer Lett*, 2013, 341: 41–45.
- Gantao, Chen, Weiguo, *et al.* Targeting of RhoE inhibits epithelial-mesenchymal transition during colorectal cancer cell migration. *Oncol Transl Med*, 2016, 3: 119–126.
- Katoh Y, Katoh M. FGFR2-related pathogenesis and FGFR2-targeted therapeutics. *Int J Mol Med*, 2009, 23: 307–311.
- Taipale J, Beachy PA. The Hedgehog and Wnt signalling pathways in cancer. *Nature*, 2001, 411: 349–354.
- Yue J, Lv D, Wang C, *et al.* Epigenetic silencing of miR-483-3p promotes acquired gefitinib resistance and EMT in EGFR-mutant NSCLC by targeting integrin beta3. *Oncogene*, 2018, 37: 4300–4312.
- Nawshad A, Lagamba D, Polad A, *et al.* Transforming growth factor-beta signaling during epithelial-mesenchymal transformation: implications for embryogenesis and tumor metastasis. *Cells Tissues Organs*, 2005, 179: 11–23.
- Takagi S, Tsuji T, Amagai T, *et al.* Specific cell surface labels in the visual centers of *Xenopus laevis* tadpole identified using monoclonal antibodies. *Dev Biol*, 1987, 122: 90–100.
- Chen H, Chedotal A, He Z, *et al.* Neuropilin-2, a novel member of the neuropilin family, is a high affinity receptor for the semaphorins Sema E and Sema IV but not Sema III. *Neuron*, 1997, 19: 547–559.
- Soker S, Takashima S, Miao HQ, *et al.* Neuropilin-1 is expressed by endothelial and tumor cells as an isoform-specific receptor for vascular endothelial growth factor. *Cell*, 1998, 92: 735–745.
- Yaqoob U, Cao S, Shergill U, *et al.* Neuropilin-1 stimulates tumor growth by increasing fibronectin fibril assembly in the tumor microenvironment. *Cancer Res*, 2012, 72: 4047–4059.
- Grandclement C, Borg C. Neuropilins: a new target for cancer therapy. *Cancers*, 2011,3: 1899–1928.
- Ellis LM. The role of neuropilins in cancer. *Mol Cancer Ther*, 2006, 5: 1099–1107.
- Barr MP, Byrne AM, Duffy AM, *et al.* A peptide corresponding to the neuropilin-1-binding site on VEGF(165) induces apoptosis of neuropilin-1-expressing breast tumour cells. *Br J Cancer*, 2005, 92: 328–333.
- Bielenberg DR, Pettaway CA, Takashima S, *et al.* Neuropilins in neoplasms: expression, regulation, and function. *Exp Cell Res*, 2006, 312: 584–593.
- Guttmann-Raviv N, Kessler O, Shraga-Heled N, *et al.* The neuropilins and their role in tumorigenesis and tumor progression. *Cancer Letters*, 2006, 231: 1–11.
- Hong TM, Chen YL, Wu YY, *et al.* Targeting neuropilin 1 as an antitumor strategy in lung cancer. *Clin Cancer Res*, 2007, 13: 4759–4768.
- Hansel DE, Wilentz RE, Yeo CJ, *et al.* Expression of neuropilin-1 in high-grade dysplasia, invasive cancer, and metastases of the human gastrointestinal tract. *Am J Surg Pathol*, 2004, 28: 347–356.
- Glinka Y, Stoilova S, Mohammed N, *et al.* Neuropilin-1 exerts co-receptor function for TGF-beta-1 on the membrane of cancer cells and enhances responses to both latent and active TGF-beta. *Carcinogenesis*, 2011, 32: 613–621.
- Nasarre P, Gemmill RM, Potiron VA, *et al.* Neuropilin-2 Is upregulated in lung cancer cells during TGF-beta1-induced epithelial-mesenchymal transition. *Cancer Res*, 2013, 73: 7111–7121.
- Evans IM, Yamaji M, Britton G, *et al.* Neuropilin-1 signaling through p130Cas tyrosine phosphorylation is essential for growth factor-dependent migration of glioma and endothelial cells. *Mol Cell Biol*, 2011, 31: 1174–1185.
- Banerjee S, Sengupta K, Dhar K, *et al.* Breast cancer cells secreted platelet-derived growth factor-induced motility of vascular smooth muscle cells is mediated through neuropilin-1. *Mol Carcinog*, 2006, 45: 871–880.
- Singh A, Greninger P, Rhodes D, *et al.* A gene expression signature associated with “K-Ras addiction” reveals regulators of EMT and tumor cell survival. *Cancer Cell*, 2009, 15: 489–500.
- Zheng X, Zhang Y, Liu Y, *et al.* HIF-2alpha activated lncRNA NEAT1 promotes hepatocellular carcinoma cell invasion and metastasis by affecting the epithelial-mesenchymal transition. *J Cell Biochem*, 2018, 119: 3247–3256.
- Yang F, Gu Y, Zhao Z, *et al.* NHERF1 suppresses lung cancer Cell migration by regulation of epithelial-mesenchymal transition. *Anticancer Res*, 2017, 37: 4405–4414.
- Buhrmann C, Shayan P, Kraehe P, *et al.* Resveratrol induces chemosensitization to 5-fluorouracil through up-regulation of intercellular junctions, epithelial-to-mesenchymal transition and apoptosis in colorectal cancer. *Biochem Pharmacol*, 2015, 98: 51–68.

31. Lovisa S, LeBleu VS, Tampe B, *et al.* Epithelial-to-mesenchymal transition induces cell cycle arrest and parenchymal damage in renal fibrosis. *Nat Med*, 2015, 21: 998–1009.
32. Du B, Shim JS. Targeting Epithelial-Mesenchymal Transition (EMT) to Overcome Drug Resistance in Cancer. *Molecules*, 2016, 21: 965.
33. Neelakantan D, Drasin DJ, Ford HL. Intratumoral heterogeneity: Clonal cooperation in epithelial-to-mesenchymal transition and metastasis. *Cell Adh Migr*, 2015, 9: 265–276.
34. Peng W, Zhang J, Liu J. URG11 predicts poor prognosis of pancreatic cancer by enhancing epithelial-mesenchymal transition-driven invasion. *Med Oncol*, 2014, 31: 64.
35. Kotiyal S, Bhattacharya S. Epithelial mesenchymal transition and vascular mimicry in breast cancer stem cells. *Crit Rev Eukaryot Gene Expr*, 2015, 25: 269–280.
36. Hendijani F, Javanmard SH, Sadeghi-aliabadi H. Human Wharton's jelly mesenchymal stem cell secretome display antiproliferative effect on leukemia cell line and produce additive cytotoxic effect in combination with doxorubicin. *Tissue Cell*, 2015, 47: 229–234.
37. Kitahara H, Hirai M, Kato K, *et al.* Eribulin sensitizes oral squamous cell carcinoma cells to cetuximab via induction of mesenchymal-to-epithelial transition. *Oncol Rep*, 2016, 36: 3139–3144.
38. Toden S, Okugawa Y, Jascur T, *et al.* Curcumin mediates chemosensitization to 5-fluorouracil through miRNA-induced suppression of epithelial-to-mesenchymal transition in chemoresistant colorectal cancer. *Carcinogenesis*, 2015, 36: 355–367.
39. Meyer-Schaller N, Heck C, Tiede S, *et al.* Foxf2 plays a dual role during transforming growth factor beta-induced epithelial to mesenchymal transition by promoting apoptosis yet enabling cell junction dissolution and migration. *Breast Cancer Res*, 2018, 20: 118.
40. Nieto MA. Epithelial plasticity: a common theme in embryonic and cancer cells. *Science*, 2013, 342: 1234850.
41. Guo HF, Vander Kooi CW. Neuropilin functions as an essential cell surface receptor. *J Biol Chem*, 2015, 290: 29120–29126.
42. Roy S, Bag AK, Singh RK, *et al.* Multifaceted role of neuropilins in the immune system: potential targets for immunotherapy. *Front Immunol*, 2017, 8: 1228.
43. Vadasz Z, Attias D, Kessel A, *et al.* Neuropilins and semaphorins - from angiogenesis to autoimmunity. *Autoimmun Rev*, 2010, 9: 825–829.
44. Yasmin T, Ali MT, Haque S, *et al.* Interaction of quercetin of onion with axon guidance protein receptor, NRP-1 plays important role in cancer treatment: an in silico approach. *Interdiscip Sci*, 2017, 9: 184–191.
45. Kamarulzaman EE, Vanderesse R, Gazzali AM, *et al.* Molecular modelling, synthesis and biological evaluation of peptide inhibitors as anti-angiogenic agent targeting neuropilin-1 for anticancer application. *J Biomol Struct Dyn*, 35: 1–49.
46. Zhang G, Chen L, Sun K, *et al.* Neuropilin-1 (NRP-1)/GIPC1 pathway mediates glioma progression. *Tumour Biol*, 2016, 37: 13777–13788.
47. Bai J, Zhang Z, Li X, *et al.* MicroRNA-365 inhibits growth, invasion and metastasis of malignant melanoma by targeting NRP1 expression. *Cancer Biomark*, 2015, 15: 599–608.
48. Abaza HM, Alfeky MAA, Eissa DS, *et al.* Neuropilin-1/CD304 expression by flow cytometry in pediatric precursor B-Acute lymphoblastic leukemia: a minimal residual disease and potential prognostic marker. *J Pediatr Hematol Oncol*, 2018, 40: 200–207.
49. Wu Y, Grabsch H, Ivanova T, *et al.* Comprehensive genomic meta-analysis identifies intra-tumoural stroma as a predictor of survival in patients with gastric cancer. *Gut*, 2013, 62: 1100–1111.
50. Spender LC, Ferguson GJ, Liu S, *et al.* Mutational activation of BRAF confers sensitivity to transforming growth factor beta inhibitors in human cancer cells. *Oncotarget*, 2016, 7: 81995–82012.
51. Vincent CT, Fuxe J. EMT, inflammation and metastasis. *Semin Cancer Biol*, 2017, 47: 168–169.

DOI 10.1007/s10330-020-0412-2

Cite this article as: Xu WG, Yang X, Zhan QQ, *et al.* Silencing Neuropilin 1 gene reverses TGF- β 1-induced epithelial mesenchymal transition in HGC-27 gastric cancer cell line. *Oncol Transl Med*, 2020, 6: 258–265.

Influence of lymph node micrometastasis on the staging system for gastric cancer*

Lixiong Gao¹ (✉), Xiankun Ren¹, Guiquan Li¹, Benhua Wu¹, Xuan Chen²

¹ Department of Gastroenterology, Medical Center Hospital of Qionglai, Qionglai 611530, China

² Department of Gastroenterology, The Affiliated Hospital of Southwest Medical University, Luzhou 646000, China

Abstract

Objective The aim of this study was to investigate the effect of lymph node micrometastasis on the prognosis of patients with gastric cancer and the necessity of integrating it into the gastric cancer staging system.

Methods In total, 241 patients with gastric cancer were included. Hematoxylin and eosin staining of lymph nodes was performed, and negative lymph nodes were evaluated by immunohistochemistry to detect micrometastases. Differences in survival rates between stages were evaluated.

Results (1) A total of 78 patients (32.4%) had lymph node micrometastases. Compared with the group without micrometastases, the overall recurrence rate, lymph infiltration, vascular invasion, and nerve invasion rate in the micrometastasis group were significantly higher ($P < 0.05$). (2) According to the standard N staging system, the rates of disease-free survival (DFS) for the N0, N1, N2, N3a, and N3b groups were 96.0%, 84.0%, 67.6%, 59.0%, and 21.7%, respectively. There was no significant difference in survival between N2 and N3a. The cumulative survival curves for N2 and N3a intersected. (3) The N stage of 38 patients (15.8%) differed between the traditional system and the new N staging system reflecting micrometastasis. The DFS for N0, N1, N2, N3a, and N3b were 97.0%, 86.3%, 74.2%, 65.4%, and 29.2%, respectively. There was no significant difference in survival between N2 and N3a, but the cumulative survival curves for N2 and N3a did not intersect. (4) Based on a Cox multivariate analysis, various independent risk factors for recurrence were identified ($P < 0.05$).

Conclusion Lymph node micrometastasis is an important risk factor for gastric cancer recurrence. Lymph node micrometastasis should be considered in TNM staging to determine prognosis and optimal treatment strategies.

Key words: gastric cancer; lymph node micrometastasis; TNM stage

Received: 12 May 2020

Revised: 20 June 2020

Accepted: 15 July 2020

In gastric cancer, lymph node metastasis is recognized as the most important determinant of prognosis^[1]. As a special form of lymph node metastasis, the clinical value of micrometastasis is still controversial. Its significance was described in the seventh edition of the TNM classification^[2-3]. Many previous studies have supported the prognostic value of lymph node micrometastasis in gastric cancer; however, it is not clear whether it should be considered in the lymph node staging system for gastric cancer^[4-5]. In this study, we performed a prospective analysis of 241 patients with gastric cancer, including immunohistochemical (IHC) staining of lymph nodes, analyses of clinical pathological data, and a comparison

between the new lymph node staging system incorporating micrometastasis with the traditional lymph node staging system. Our findings provide a basis for determining the significance of lymph node micrometastasis in gastric cancer staging.

Materials and methods

Patient origin and immunohistochemical staining

From February 2010 to December 2016, 241 patients who underwent radical gastrectomy in the Department

✉ Correspondence to: Lixiong Gao. Email: huahua2200@163.com

* Supported by a grant from the scientific research project of Sichuan Health Committee (No. 19pj045)

© 2020 Huazhong University of Science and Technology

of Gastrointestinal Surgery, Qionglai Medical Center Hospital were selected as the study subjects. Surgical specimens were maintained in the Department of Pathology of our hospital. The patients were divided into two groups according to the detection of lymph node micrometastasis. Clinical and pathological results were obtained, including age, sex, tumor size, WHO classification, Lauren classification, average number of lymph nodes dissected, average number of metastatic lymph nodes, lymph node infiltration, vascular infiltration, peripheral infiltration, and TNM stage (7th AJCC). Clinical pathological results and recurrence rates were compared between the two groups.

Definition of lymph node micrometastasis

Lymph node micrometastasis includes two forms: isolated tumor cells (ITC) and micrometastasis. ITC refers to a single tumor cell with a diameter of less than 0.2 mm [6]. At present, there is no evidence that ITC contributes to tumor metastasis. Therefore, micrometastasis in this study refers to a tumor cell cluster with a size of 0.2–2.0 mm, excluding ITCs.

Immunohistochemical staining

Specimens were stained with hematoxylin & eosin (HE) before anti-CAM5.2 IHC staining. The CAM5.2 antibody can recognize low-molecular-weight cytokeratin expressed in tumor cells and can detect micrometastasis in surgical specimens [7]. To improve the micrometastasis detection rate, two or more lymph node sections were used for IHC staining. Brownish-yellow staining indicated micrometastasis in lymph nodes. The lymph nodes with positive HE staining were defined as macrolymph node metastasis or micrometastasis.

Follow-up

The 3-year disease-free survival (DFS) rates were evaluated according to the N stage determined by AJCC stage 7 and the new staging standard. In the new staging system, lymph node micrometastasis was defined as positive lymph nodes, and the number of metastatic lymph nodes was calculated by the sum of macrometastasis and micrometastasis lymph nodes. DFS was defined as the time from randomization to relapse or death for any reason.

Statistical analysis

All data were analyzed using SPSS 20.0. Counts are presented as the number of cases and were evaluated by the chi-squared test. Measurement data are presented as means \pm standard deviation and were evaluated by the *t*-test. The Kaplan–Meier method and log rank test were used for the survival analysis. Factors with statistically significant differences in a single-factor survival analysis

were included in a multivariate Cox regression analysis. $P < 0.05$ was considered statistically significant.

Results

Comparison of demographic characteristics and clinicopathological parameters

The average age of 241 patients was 59.3 ± 13.4 years (25–87 years). There were 163 males (67.6%) and 78 females (32.4%). The mean follow-up time was (76.8 ± 2.3) months (2.3–106.8 months), and the 3-year DFS rate was 78.9%. A total of 78 patients (32.4%) had lymph node micrometastasis and 163 (67.6%) had no lymph node micrometastasis. There were significant differences in tumor size, WHO classification, Lauren classification, average number of lymph nodes, average number of metastatic lymph nodes, T stage, and N stage between the two groups ($P < 0.05$). There were no significant differences in age and gender between the two groups (Table 1).

Comparison of recurrence and metastasis between groups

Compared with the group without micrometastasis, the overall recurrence rate was significantly higher in the micrometastasis group ($P < 0.05$). The most common types of recurrence were peritoneal, hematogenous, and local lymph nodes in the micrometastasis group and hematogenous, peritoneal, and local lymph nodes in the non-micrometastasis group. The incidences of lymphatic invasion, vascular invasion, and nerve invasion in the micrometastasis group were significantly higher than those in the non-micrometastasis group ($P < 0.05$; Table 2).

Immunohistochemical staining of lymph node metastasis

Micrometastasis was detected by CAM5.2 immunohistochemistry. The macrometastasis and micrometastases were brownish-yellow on IHC staining. There were significant brownish-yellow masses in the macroscopic metastases and scattered and single cell clusters in the micrometastases (Fig. 1).

Survival curve for the traditional N staging system

According to the traditional N staging standard of AJCC 7th edition, the DFS of patients with N0, N1, N2, N3a, and N3b disease were 96.0%, 84.0%, 67.6%, 59.0%, and 21.7%, respectively. A log rank test showed that the differences between N0 and N1, N1 and N2, and N3a and N3b were statistically significant. However, there was no significant difference between N2 and N3a. In the conventional staging system, the cumulative survival

Table 1 demographic characteristics and clinicopathological results

Index	Microtransmission group (n = 78)	No-Microtransmission group (n = 163)	t/ χ^2	P
Age	59.6 ± 12.4	59.8 ± 14.2	-0.106	0.915
male	49	114	1.221	0.269
Tumor diameter (cm)	6.5 ± 3.3	4.3±3.1	5.047	0.000
WHO classification			20.148	0.001
well-differentiated	15	57		
moderately differentiated	39	46		
poorly differentiated	10	21		
mamillary	3	26		
Myxoid carcinoma	4	6		
signet ring cell cancer	7	7		
Lauren classification			10.687	0.001
Intestinal	26	91		
diffuse	52	72		
Operation type			15.611	0.000
Subtotal gastrectomy	45	133		
Total gastrectomy	33	30		
Dissected lymph nodes	44.6 ± 17.2	36.8 ± 17.5	3.255	0.001
Metastatic lymph nodes	11.3 ± 13.6	3.5 ± 11.4	4.661	< 0.001
T stage			72.857	< 0.001
T1	10	109		
T2	7	18		
T3	4	2		
T4a	53	31		
T4b	4	3		
N stage			53.646	< 0.001
N0	10	101		
N1	14	19		
N2	18	14		
N3a	16	15		
N3b	20	14		

Table 2 Comparison of recurrence and metastasis rate between the two groups

Index	Microtransmission group (n = 78)	No-Microtransmission group (n = 163)	χ^2	P
Lymphatic invasion	40	39	17.916	< 0.001
Vascular invasion	32	25	19.279	0.001
Perineural invasion	5	10	0.007	0.934
Recurrence (%)	32 (41.0)	21 (12.8)	24.355	< 0.001
Peritoneal	13	8		
Hematogenous	11	9		
Local lymph node	8	4		

curves for N2 and N3a intersected (Fig. 2).

Survival curve for the N staging system reflecting micrometastasis

The N stages for 38 patients (15.8%) changed with the new N staging system. In addition, 8 cases (3.3%) experienced two or more n-phase increases. In this system, the DFS of patients with N0, N1, N2, N3a, and N3b were 97.0%, 86.3%, 74.2%, 65.4%, and 29.2%, respectively. The differences in survival between N0 and N1, N1 and N2, and N3a and N3b were statistically significant. There

was no significant difference in survival between N2 and N3a stages; however, in the new staging system, the cumulative survival curves for N2 and N3a did not cross (Fig.3).

Multivariate analysis of prognostic factors for DFS

Based on univariate analyses, a Cox multivariate analysis showed that the combination of nerve infiltration, pathological T stage, number of lymph nodes dissected, and macrometastasis and micrometastasis of lymph nodes

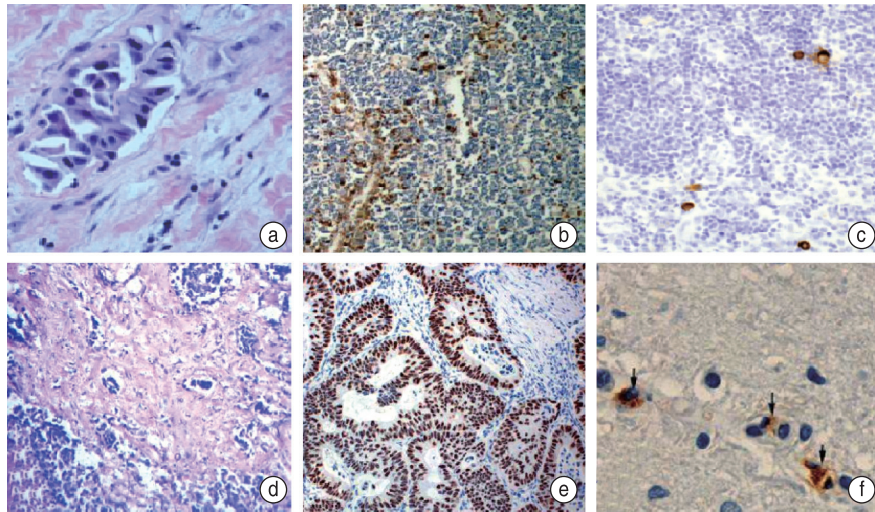


Fig. 1 Immunohistochemical staining of metastases. (a, d) negative staining (a: x200, d: x400); (b, e) positive macroscopic metastasis of lymph nodes (b: x200, e: x400); (c, f) positive micrometastasis of lymph nodes (c: x200, f: x400)

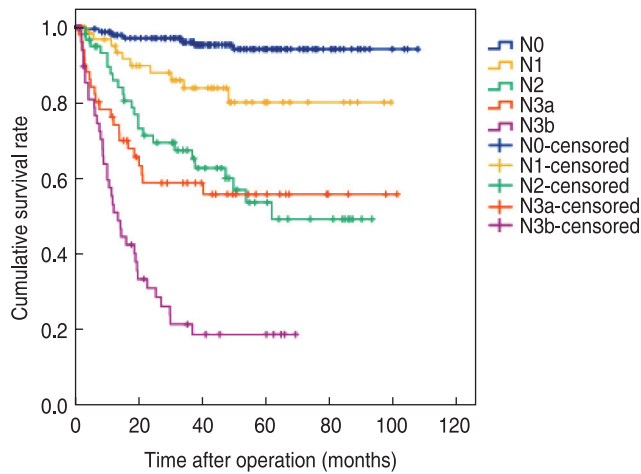


Fig. 2 survival curve of traditional N stage

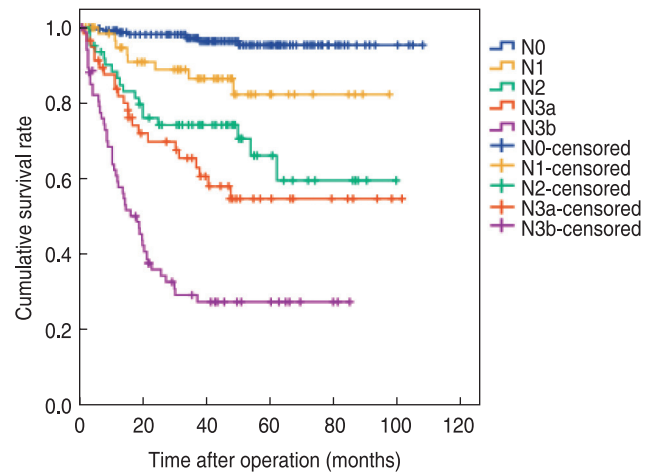


Fig. 3 survival curve of N stage reflecting micrometastasis

were independent risk factors for the recurrence of gastric cancer ($P < 0.05$; Table 3).

Discussion

Many studies have explored the clinical effect of lymph node micrometastasis on pN0 gastric cancer by routine pathological examination, focusing on its role in the minimally invasive treatment of early gastric cancer, such as sentinel lymph node navigation surgery and endoscopic submucosal cleaning surgery^[8]. In this prospective study, we focused on the effect of micrometastasis on N-staging. In particular, we evaluated the significance of lymph node micrometastasis in gastric cancer staging. ITCs were also detected by immunohistochemistry but were excluded from analyses owing to the lack of clinical evidence that

they affect prognosis^[9].

The recurrence rate of micrometastases is related to demographic and clinicopathological factors^[10-11]. We hypothesized that lymph node micrometastasis has the same clinical value as lymph node metastasis and constructed a new staging system. By comparing the performance of the traditional N-staging system with that of the new N-staging system, the advantages and disadvantages of each were evaluated. With respect to the performance of staging systems, Ueno proposed three criteria^[12-13]: (1) intragroup homogeneity, (2) heterogeneity between group, and (3) monotonicity of the correlation gradient between groups. Compared with the traditional staging system, the new system was more discriminative for the prognosis of each N-phase, and DFS showed more significant differences between

Table 3 multivariate analysis of prognostic factors of DFS

Index	univariate analysis			multivariable analysis		
	HR	95%CI	P	HR	95%CI	P
Age	1.654	1.354–5.124	0.458	—	—	—
Male	0.968	0.074–1.587	0.500	—	—	—
Tumor diameter	2.865	1.652–4.998	< 0.001	1.018	0.946–1.096	0.652
Operation type	2.144	1.021–3.897	< 0.001	1.033	0.619–1.746	0.912
WHO classification	1.104	0.631–1.934	0.730	—	—	—
Lauren classification	0.658	0.357–1.225	0.189	—	—	—
Lymphatic invasion	3.153	1.398–6.874	< 0.001	1.354	0.438–1.249	0.266
Vascular invasion	3.356	1.287–6.538	< 0.001	1.117	0.679–1.830	0.293
Perineural invasion	4.159	1.874–7.698	< 0.001	2.069	1.190–3.551	0.011
T stage						
T1	1	—	< 0.001	1	—	< 0.001
T2	2.884	1.987–4.521	0.158	3.191	0.697–14.617	0.136
T3	17.654	9.687–36.3254	< 0.001	12.800	3.079–53.654	< 0.001
T4a	35.954	18.554–54.335	< 0.001	30.668	9.879–95.654	< 0.001
T4b	107.632	68.147–198.35	< 0.001	72.697	19.547–276.325	< 0.001
Dissected lymph nodes	1.015	0.236–2.987	0.003	0.971	0.955–0.986	< 0.001
Metastatic lymph nodes	1.035	0.257–2.148	< 0.001	1.049	0.013–1.089	< 0.001
Microtransmission	1.098	0.336–1.987	< 0.001	1.068	1.024–1.179	0.002

different N-phases.

Generally speaking, prognosis is better for stage N3a than for N2. In the conventional N staging system evaluated in this study, the DFS curves for N2 and N3a intersected, suggesting that the survival rate for patients classified as N3a continues to exceed that of patients classified as N2 over time, and the difference grows. This phenomenon may be explained by the inability to detect micro-transfer, which the traditional staging system does not reflect. To account for this difference, we designed a new hypothetical staging system, including the total number of macrometastatic and micrometastatic lymph nodes. In the new N staging system, the survival curves for N2 and N3a no longer crossed. Stages N2 and N3a had stronger discrimination ability with respect to prognosis, and their correlation showed a more monotonous trend.

The inclusion of lymph node micrometastasis in the N staging system would influence treatment strategies; the reclassification of stages will lead to changes in adjuvant treatment, especially radiotherapy and chemotherapy^[14–15]. In this study, because the number of metastatic lymph nodes increased with the number of micrometastasis lymph nodes, the N stage for 38 patients (15.8%) was higher in the new system than in the traditional system, and the corresponding TNM stage was adjusted to a later stage. Considering previous reports on micrometastasis proliferation, this phenomenon should not simply be considered an “overestimation” of stages by the new staging system. On the contrary, it can be regarded as an “underestimation” by the traditional staging system. Therefore, in these cases, more aggressive treatment may

be needed. In particular, when considering minimally invasive surgery, the operator should cautiously consider the influence of lymph node micrometastasis. Jee *et al*^[9] have reported that if endoscopic mucosal resection or ESD is performed according to traditional staging criteria, metastatic lymph nodes may be missed. If micrometastasis is not considered in staging, patients may be at risk of lymph node metastasis after endoscopic mucosal resection or ESD.

To sum up, the results of this study showed that lymph node micrometastasis is an important risk factor for gastric cancer recurrence. Lymph node micrometastasis should be considered in TNM staging to determine prognosis and the best treatment strategy. However, this study had some limitations. (1) The sample size was small. (2) It was a single-center study, and there may be sampling bias. (3) The detection method for micrometastasis needs to be further improved; in the future, RT-PCR with higher sensitivity and specificity can be used.

Conflicts of interest

The authors indicated no potential conflicts of interest.

References

1. Link H, Angele M, Schüller M, *et al*. Extra-capsular growth of lymph node metastasis correlates with poor prognosis and high SOX9 expression in gastric cancer. *Bmc Cancer*, 2018, 18: 483.
2. Hiroki O, Hiroshi K, Toshiyuki Y, *et al*. Clinical impact of Epstein-Barr virus status on the incidence of lymph node metastasis in early gastric cancer. *Dig Endosc*, 2020, 32: 316–322.

3. Jin J, Deng J, Liang H, *et al.* Analysis of risk factor of perioperative complications in patients with radical gastrectomy for gastric cancer and its influence on prognosis. *Chin J Gastrointest Surg*, 2018, 21: 53–60.
4. Toshifumi S, Tetsuji H, Makoto A, *et al.* A Case of recurrent gastric cancer with No. 13 lymph node metastasis treated with surgical resection. *Gan to kagaku ryoho*, 2018, 45: 2363–2365.
5. Chi J, Xie Q, Jia J, *et al.* Prognostic value of albumin/globulin ratio in survival and lymph node metastasis in patients with cancer: a systematic review and Meta-analysis. *J Cancer*, 2018, 9: 2341–2348.
6. Zhou Y, Zhang GJ, Wang J, *et al.* Current status of lymph node micrometastasis in gastric cancer. *Oncotarget*, 2017, 8: 357–359.
7. Pang T, Fang GE, Luo TH, *et al.* The related factors study of lymph node metastasis in 212 patients with early gastric cancer. *Chin J Pract Surg (Chinese)*, 2010, 2: 36–38.
8. Chung H W, Jang S, Kim H, *et al.* Combined targeting of high-mobility group box-1 and interleukin-8 to control micrometastasis potential in gastric cancer. *Int J Cancer*, 2015, 137: 1598–1609.
9. Kamiya S, Takeuchi H, Nakahara T, *et al.* Auxiliary diagnosis of lymph node metastasis in early gastric cancer using quantitative evaluation of sentinel node radioactivity. *Gastric Cancer*, 2016, 19: 1080–1087.
10. Zhang C, Hu X, Liu X Y, *et al.* Effect of tumor-associated macrophages on gastric cancer stem cell in omental milky spots and lymph node micrometastasis. *Int J Clin Exp Pathology*, 8: 13795–13805.
11. Zeng YJ, Zhang CD, Dai DQ. Impact of lymph node micrometastasis on gastric carcinoma prognosis: A meta-analysis. *World J Gastroenterol*, 2015, 21: 1628.
12. Blouhos K, Boulas K A, Tsalis K, *et al.* Recurrence of a pT2N0cM0 lower third gastric cancer with No. 6 lymph node micrometastasis after R0 extended surgery. Should adjuvant therapy be performed in conventionally node-negative but micrometastasis-positive pT2 gastric cancer? *J Gastrointest Cancer*, 2017, 48: 89–93.
13. Jeuck T L A, Wittekind C. Gastric carcinoma: stage migration by immunohistochemically detected lymph node micrometastases. *Gastric Cancer*, 2015, 18: 100–108.
14. Wang Y, Wang D, Xie G, *et al.* MicroRNA-152 regulates immune response via targeting B7-H1 in gastric carcinoma. *Oncotarget*, 2017, 8: 28125–28134.
15. Natsugoe S, Arigami T, Uenosono Y, *et al.* Novel surgical approach based on the sentinel node concept in patients with early gastric cancer. *Ann Gastroenterol Surg*, 2017, 1: 180–185.

DOI 10.1007/s10330-020-0429-9

Cite this article as: Gao LX, Ren XK, Li GQ, *et al.* Influence of lymph node micrometastasis on the staging system for gastric cancer. *Oncol Transl Med*, 2020, 6: 266–271.

Salvage treatments for prostate-specific antigen relapse of cT₃N₀M₀ prostatic adenocarcinoma after radical prostatectomy combined with neoadjuvant androgen deprivation

Lufang Zhang¹, Dongliang Pan² (✉), Ludong Liu¹, Yunjiang Zang¹, Ningchen Li²

¹ Department of Urology, Weifang People's Hospital, Shandong 261000, China

² Department of Urology, Peking University Shougang Hospital; Wujieping Urology Medical Center of Peking University, Beijing 100144, China

Abstract

Objective The aim of the study was to evaluate the efficiency of salvage treatments for prostate specific antigen (PSA) relapse of cT₃N₀M₀ prostatic adenocarcinoma (PCa) after radical prostatectomy (RP) combined with neoadjuvant androgen deprivation (ADT).

Methods A total of 332 patients with cT₃N₀M₀ PCa were enrolled in the prospective study and received RP and pelvic lymph node dissection with neoadjuvant ADT for 3 months. All patients with PSA relapse were treated with salvage external beam radiation therapy (RT) and ADT for 6 months.

Results The 5-year postoperative PSA relapse rate was 40.96% (136/332). The patients have been divided into the PSA relapse and PSA relapse-free groups in order to compare patient characteristics. The ratio of patients with Gleason score ≥ 8 and positive surgical margin in the PSA relapse group were significantly higher than those of in the PSA relapse-free group ($P = 0.01$). The mean duration between the start of operative treatment and PSA relapse was 31 months. Salvage treatment to all 136 PSA relapse patients led to favorable outcomes. PSA relapse was not observed after salvage treatment by the end of follow-up. The 5-year overall survival rates of the PSA relapse and PSA relapse-free groups were 94.9% and 93.9%, respectively.

Conclusion In pursuit of curative treatment, our study showed that RP combined with neoadjuvant ADT is an aggressive multimodality strategy associated with lower PSA relapse and better survival outcomes for stage cT₃N₀M₀ PCa patients. Patients with PSA relapse after RP may benefit from early aggressive salvage RT combined with short-term ADT.

Key words: prostatic adenocarcinoma (PCa); radical prostatectomy (RP); neoadjuvant androgen deprivation (ADT); external beam radiation therapy; salvage treatment; prostate specific antigen (PSA) relapse

Received: 4 May 2020

Revised: 14 July 2020

Accepted: 3 September 2020

T₃N₀M₀ prostatic adenocarcinoma (PCa) is a locally advanced disease characterized by tumors having various properties, with some exhibiting remarkably malignant behavior. To date, no standard treatment for the disease can be defined in the absence of level 1 evidence. A multimodal therapy comprising local treatment combined with a systemic one provides the best outcome, provided the patient is ready and fit enough to receive both. Nevertheless, the optimal local treatment is still a

matter of debate.

There are many local treatment opinions as well as discussions about the use of operative procedures and radiation; however, most curative procedures are based on multidisciplinary strategies combined with androgen deprivation therapy (ADT). Surgery for locally advanced PCa as part of a multimodal therapy has been reported [1–3]. A prospective phase III RCT (SPCG-15) comparing radical prostatectomy (RP) with or without adjuvant

✉ Correspondence to: Dongliang Pan. Email: dongliangpan@hotmail.com

© 2020 Huazhong University of Science and Technology

or salvage external beam radiation therapy (EBRT) against primary EBRT and ADT among patients with T₃ PCa is currently recruiting [4], and RP and laparoscopic techniques are continuously developing [5]. However, the comparative oncological effectiveness of RP as part of a multimodality treatment strategy versus upfront EBRT with ADT for T₃ PCa remains unknown.

We treated T₃ PCa patients with RP combined with neoadjuvant ADT from 2005 to 2014. When prostate-specific antigen (PSA) relapse occurred, these patients were treated with salvage EBRT and ADT. Outcomes for T₃N₀M₀ PCa patients from two hospitals were reported.

Patients and methods

Patients

A total of 332 patients with cT₃N₀M₀ PCa were diagnosed and treated at two investigative hospitals in China between 2005 and 2014. All patients had been initially diagnosed as having PCa and had not received any prior Gn-RH analogue or hormonal treatment. Their outcomes were documented in the present study after obtaining their informed consent and ethical approval of hospitals. Records of patient outcomes were completed by the end of 2019. The classification of stages was performed according to the National Comprehensive Cancer Network guidelines [6]. Pretreatment biopsy consisted of 12 cores that were performed via the perineal route, and the pathological findings were classified using the Gleason grading system with the ISUP 2005 modification [7]. Ultrasonography, magnetic resonance imaging, computed tomography, and whole-body bone scan were performed in all patients. Their mean age was 73.2 years (range: 61–80 years) and their total PSA values were 12.15–28.53 ng/mL.

Methods

Open or laparoscopic retroperitoneal RP and pelvic lymph node dissection were performed with neoadjuvant ADT for 3 months. ADT consisted of a luteinizing hormone-releasing hormone analog with daily dose of 50 mg bicalutamide. Total PSA was measured every month after RP and then every 3 months from the second year. PSA relapse was defined as a linear increase in PSA of more than 0.1 ng/mL. Before the PSA level rose to > 0.5 ng/mL, all PSA relapse patients were treated with salvage EBRT and ADT for 6 months. EBRT was performed with total doses of 66–78 Gy. The clinical target volume was defined as the surgical bed of the entire prostate. After EBRT, total PSA was monitored similarly as during postoperative monitoring.

Statistical analyses

The SPSS statistical computer program (IBM SPSS V26.0; USA) was used to calculate PSA relapse and overall survival rate. The Cox proportional hazard model and multivariate analysis were used to evaluate the difference among clinical factors and outcomes. *P* values of ≤ 0.05 were considered significant. The follow-up time was calculated from the start date of treatment initiation up to the end of 2019.

Results

The 5-year postoperative PSA relapse rate in all patients was 40.96% (136/332). All 332 patients had been assigned into either the PSA relapse group or PSA relapse-free group in order to compare patient characteristics.

Some patient characteristics, such as the age, preoperative PSA value, and ratio of stage T_{3a} and T_{3b}, were similar between the two groups (Table 1). The ratio of patients with a Gleason score ≥ 8 was significantly higher in the PSA relapse group (42.0%) than in the PSA relapse-free group (32.7%; *P* = 0.01). However, there were no significant difference in the ratios of patients with Gleason scores ≤ 6 and 7 between these two groups.

According to the histological examination of operative specimens, cancerous tissues were found at the edge of the cutting surfaces in 7 patients of the PSA relapse group, whereas no patients in the PSA relapse-free group exhibited positive surgical margins (*P* = 0.001). No metastases were detected in regional lymph nodes. The

Table 1 Patient characteristics and outcomes [*n* (%)]

Characteristic	PSA relapse (<i>n</i> = 136)	PSA relapse-free (<i>n</i> = 196)
Age (year)	72.4 (61–79)	74 (61–80)
PSA (ng/mL)	24.6 (12.8–28.53)	21.13 (12.15–27.2)
Stage		
T _{3a}	113 (83.0%)	167 (85.2%)
T _{3b}	23 (17.0%)	29 (14.8%)
Gleason score		
≤ 6	56 (41.1%)	89 (45.4%)
= 7	23 (16.9%)	43 (21.9%)
≥ 8	47 (42.0%)	64 (32.7%)
Positive surgical margin	7	0
Positive lymph node	0	0
Postoperative PSA relapse	136 (40.9%)	0
Duration* (month)	31 (9–37)	–
Salvage treatment	136	–
PSA relapse after salvage treatment	0	–
Death		
Prostate Ca	0	0
Other	7 (5.1%)	12 (6.1%)

Note: Statistical significance of PSA relapse vs no relapse-positive surgical margin: *P* = 0.001; Gleason score ≥ 8: *P* = 0.01; * Start of relapse

extension of tumors through the prostate capsule was considered low in most of the patients, thus no adjuvant treatments were immediately scheduled.

The mean duration between the start of operative treatment and PSA relapse was 31 months. After relapse, good treatment compliance was observed and the salvage treatment in all 136 patients led to favorable outcomes. After the salvage treatment, no PSA relapse was observed until the end of follow-up.

The 5-year overall survival rates of the PSA relapse and PSA relapse-free groups were 94.9% and 93.9%, respectively. Deaths that occurred during the follow-up were not directly from prostate cancer. No detectable adverse effects were observed in the patients who underwent salvage treatment.

Discussion

Irrespective of the pT stage, between 27% and 53% of all PCa patients undergoing RP or RT increasingly develop PSA relapse. Moreover, between 5% and 20% continue to have detectable or persistent PSA after RP^[8-9]. PSA relapse has been reported to occur in 60% of patients with stage T₃ PCa, 5 years after the start of treatment, which suggests a mortality rate of 70%–80% thereafter. ISUP score > 2 or patients classified as pT₃ pN₀ after RP due to positive margins, capsule rupture, and/or invasion of the seminal vesicles are at high risk of relapse; this risk can be as high as 50% after five years^[10]. In another study, patients with stage T₃ PCa have been surgically examined to confirm negative regional lymph glands, then treated with RT; 64% of these patients experienced PSA relapse^[11]. These findings indicate that RP or RT alone did not completely suppress subsequent disease progression. Therefore, numerous multimodality strategies are already being discussed to improve the survival of stage T₃ PCa patients.

RP with neoadjuvant ADT have been performed for several months in some studies^[12-13], resulting in a decrease in the stage and a reduction of marginal invasion observed in the prostate specimen. Moreover, histological changes resulting from ADT have already been confirmed^[14]. However, these improvements did not continue according to longer-term observations^[15-17]. Some stage T₃ PCa patients exhibit postoperative PSA relapse, with the histological findings on the cancer tissues exhibiting a high Gleason pattern^[18]. In our study, a similar pattern was also observed. The ratio of patients with Gleason score ≥ 8 in the PSA relapse group was significantly higher (42.0%) than in the PSA relapse-free group (32.7%; $P = 0.01$).

PSA relapse after RP may result from persistent local disease, pre-existing metastases, or residual benign prostate tissue. On the other hand, persistent PSA after RP is associated with more advanced disease (such as

positive surgical margins, pathologic stage > T_{3a}, positive nodal status, and/or pathologic ISUP grade > 3). However, not all patients with persistent PSA after RP experience disease recurrence. Xiang *et al* showed a 50% 5-year biochemical relapse-free survival for patients who had persistent PSA level > 0.1 ng/mL, but < 0.2 ng/mL at 6–8 weeks after RP^[19].

The timing and treatment modality for PSA-only relapse after RP remain controversial because of limited evidence. Active surveillance is the first choice for patients when their PSA levels are > 0.1 ng/mL but < 0.2 ng/mL. Salvage RT (SRT) is usually decided on the basis of biochemical relapse without histological proof of local recurrence, but only when the PSA level is < 0.5 ng/mL. Nevertheless, more than 60% of patients who have been treated before the PSA level rises to > 0.5 ng/mL achieved an undetectable PSA level^[20-23], corresponding to an 80% chance of being progression-free five years later^[24].

Early SRT provides the possibility of cure for patients with an increasing PSA after RP. Boorjian *et al*^[25] reported a 75% reduced risk of systemic progression with SRT, when comparing 856 SRT patients with 1801 non-SRT patients. Wiegel *et al*^[26] showed that following SRT to the prostate bed, patients with a detectable PSA after RP had significantly worse oncological outcomes when compared with those who achieved an undetectable PSA. Their 10-year metastasis-free survival was 67% vs. 83%, and their overall survival was 68% vs. 84%, respectively. Recent data from Preisser *et al*^[27] also compared oncological outcomes in patients with persistent PSA who received SRT versus those who did not. In the subgroup of patients with persistent PSA, after 1:1 propensity score matching between patients with SRT vs. no RT, the 10-year overall survival rates after RP were 86.6% vs. 72.6% in the entire cohort ($P < 0.01$), 86.3% vs. 60.0% in patients with positive surgical margin ($P = 0.02$), 77.8% vs. 49.0% in pT_{3b} disease ($P < 0.001$), 79.3% vs. 55.8% in ISUP grade 1 disease ($P < 0.01$), and 87.4% vs. 50.5% in pN₁ disease ($P < 0.01$), for SRT and no RT, respectively. Moreover, the 10-year CSS rates after RP were 93.7% vs. 81.6% in the entire cohort ($P < 0.01$), 90.8% vs. 69.7% in patients with positive surgical margin ($P = 0.04$), 82.7% vs. 55.3% in pT_{3b} disease ($P < 0.01$), 85.4% vs. 69.7% in ISUP grade 1 disease ($P < 0.01$), and 96.2% vs. 55.8% in pN₁ disease ($P < 0.01$), for SRT and no RT, respectively. In multivariable models, after 1:1 propensity score matching, SRT was associated with a lower risk of death (HR: 0.42, $P = 0.02$) and lower cancer-specific death (HR: 0.29, $P = 0.03$). These survival outcomes for patients with persistent PSA who underwent SRT suggest that they benefit from the treatment; however, outcomes are still worse for patients experiencing biochemical relapse. Choo *et al* report that the addition of 2-year ADT to immediate RT in the prostate bed of patients with pathologic T₃

disease and/or positive surgical margins after RP may improve progression-free survival^[28]. The GETUG-22 trial comparing RT with RT plus short-term ADT for post-RP PSA persistence (0.2–2.0 ng/mL) also reported good tolerability of the combined treatment; however, their oncological end-points are yet to be published^[29]. In our present study, we reported that SRT and 6 months of ADT was associated with favorable results. Our findings suggest that patients with PSA relapse after RP may benefit from early aggressive multi-modality treatment such as SRT combined with short-term ADT.

Conclusion

In the pursuit of curative treatment for stage cT₃N₀M₀ healthy PCa patients, our findings show that RP combined with neoadjuvant ADT is one of the aggressive multimodality strategies associated with lower PSA relapse and better survival outcomes. Patients with PSA relapse after RP may benefit from early aggressive SRT combined with short-term ADT.

Conflicts of interest

The authors indicated no potential conflicts of interest.

References

- Donohue JF, Bianco FJ Jr, Kuroiwa K, *et al.* Poorly differentiated prostate cancer treated with radical prostatectomy: long-term outcome and incidence of pathological downgrading. *J Urol*, 2006, 176: 991–995.
- Yossepowitch O, Eggener SE, Bianco FJ Jr, *et al.* Radical prostatectomy for clinically localized, high risk prostate cancer: critical analysis of risk assessment methods. *J Urol*, 2007, 178: 493–499.
- Bastian PJ, Gonzalgo ML, Aronson WJ, *et al.* Clinical and pathologic outcome after radical prostatectomy for prostate cancer patients with a preoperative Gleason sum of 8 to 10. *Cancer*, 2006, 107: 1265–1272.
- Akre O. Surgery versus radiotherapy for locally advanced prostate cancer (SPCG-15). U.S. National library of Medicine. 2014, NCT02102477.
- Pan DL. Prophylaxis and management of perioperative hemorrhage in retropubic radical prostatectomy. *Oncol Transl Med*, 2017, 3: 171–175.
- Mohler JL, Kantoff PW, Armstrong AJ, *et al.* Prostate cancer, version 1.2014. *J Natl Compr Canc Netw*, 2013, 11: 1471–1479.
- Epstein JI, Allsbrook WC Jr, Amin MB, *et al.* The 2005 international society of urological pathology (ISUP) consensus conference on Gleason grading of prostatic carcinoma. *Am J Surg Pathol*, 2005, 29: 1228–1242.
- Ploussard G, Staerman F, Pierrelvein J, *et al.* Predictive factors of oncologic outcomes in patients who do not achieve undetectable prostate specific antigen after radical prostatectomy. *J Urol*, 2013, 190: 1750–1756.
- Wiegel T, Bartkowiak D, Bottke D, *et al.* Prostate-specific antigen persistence after radical prostatectomy as a predictive factor of clinical relapse-free survival and overall survival: 10-year data of the ARO 96-02 trial. *Int J Radiat Oncol Biol Phys*, 2015, 91: 288–294.
- Hanks GE. External-beam radiation therapy for clinically localized prostate cancer: patterns of care studies in the United States. *NCI Monogr*, 1988, (7): 75–84.
- Suzuki N, Shimbo M, Amiya Y, *et al.* Outcome of patients with localized prostate cancer treated by radiotherapy after confirming the absence of lymph node invasion. *Jpn J Clin Oncol*, 2010, 40: 652–657.
- Witjes WP, Schulman CC, Debruyne FM. Preliminary results of a prospective randomized study comparing radical prostatectomy versus radical prostatectomy associated with neoadjuvant hormonal combination therapy in T₂₋₃N₀M₀ prostatic carcinoma. The European study group on neoadjuvant treatment of prostate cancer. *Urology*, 1997, 49 (3A Suppl): 65–69.
- Schulman CC, Debruyne FM, Forster G, *et al.* 4-Year follow-up results of a European prospective randomized study on neoadjuvant hormonal therapy prior to radical prostatectomy in T₂₋₃N₀M₀ prostate cancer. European study group on neoadjuvant treatment of prostate cancer. *Eur Urol*, 2000, 38: 706–713.
- Selli C, Montironi R, Bono A, *et al.* Effects of complete androgen blockade for 12 and 24 weeks on the pathological stage and resection margin status of prostate cancer. *J Clin Pathol*, 2002, 55: 508–513.
- Klotz LH, Goldenberg SL, Jewett MA, *et al.* Long-term follow up of a randomized trial of 0 versus 3 months of neoadjuvant androgen ablation before radical prostatectomy. *J Urol*, 2003, 170: 791–794.
- Kumar S, Shelley M, Harrison C, *et al.* Neo-adjuvant and adjuvant hormone therapy for localised and locally advanced prostate cancer. *Cochrane Database Syst Rev*, 2006, (4): CD006019.
- Shelley MD, Kumar S, Coles B, *et al.* Adjuvant hormone therapy for localised and locally advanced prostate carcinoma: a systematic review and meta-analysis of randomised trials. *Cancer Treat Rev*, 2009, 35: 540–546.
- Hegemann NS, Morcinek S, Buchner A, *et al.* Risk of biochemical recurrence and timing of radiotherapy in pT_{3a}N₀ prostate cancer with positive surgical margin: a single center experience. *Strahlenther Onkol*, 2016, 192: 440–448.
- Xiang CH, Liu XY, Chen SL, *et al.* Prediction of biochemical recurrence following radiotherapy among patients with persistent PSA after radical prostatectomy: a single-center experience. *Urol Int*, 2018, 101: 47–55.
- Stish BJ, Pisansky TM, Harmsen WS, *et al.* Improved metastasis-free and survival outcomes with early salvage radiotherapy in men with detectable prostate-specific antigen after prostatectomy for prostate cancer. *J Clin Oncol*, 2016, 34: 3864–3871.
- Pfister D, Bolla M, Briganti A, *et al.* Early salvage radiotherapy following radical prostatectomy. *Eur Urol*, 2014, 65: 1034–1043.
- Siegmann A, Bottke D, Faehndrich J, *et al.* Salvage radiotherapy after prostatectomy – what is the best time to treat? *Radiother Oncol*, 2012, 103: 239–243.
- Ohri N, Dicker AP, Trabulsi EJ, *et al.* Can early implementation of salvage radiotherapy for prostate cancer improve the therapeutic ratio? A systematic review and regression meta-analysis with radiobiological modelling. *Eur J Cancer*, 2012, 48: 837–844.
- Wiegel T, Lohm G, Bottke D, *et al.* Achieving an undetectable PSA after radiotherapy for biochemical progression after radical prostatectomy is an independent predictor of biochemical outcome – results of a retrospective study. *Int J Radiat Oncol Biol Phys*, 2009, 73: 1009–1016.
- Boorjian SA, Karnes RJ, Crispen PL, *et al.* Radiation therapy after radical prostatectomy: impact on metastasis and survival. *J Urol*, 2009, 182: 2708–2714.
- Wiegel T, Bartkowiak D, Bottke D, *et al.* Prostate-specific antigen

- persistence after radical prostatectomy as a predictive factor of clinical relapse-free survival and overall survival: 10-year data of the ARO 96-02 trial. *Int J Radiat Oncol Biol Phys*, 2015, 91: 288–294.
27. Preisser F, Chun FKH, Pompe RS, *et al*. Persistent prostate-specific antigen after radical prostatectomy and its impact on oncologic outcomes. *Eur Urol*, 2019, 76: 106–114.
28. Choo R, Danjoux C, Gardner S, *et al*. Prospective study evaluating postoperative radiotherapy plus 2-year androgen suppression for post-radical prostatectomy patients with pathologic T3 disease and/or positive surgical margins. *Int J Radiat Oncol Biol Phys*, 2009, 75: 407–412.
29. Guerif SG, Latorzeff I, Roca L, *et al*. The acute toxicity results of the GETUG-AFU 22 study: A multicenter randomized phase II trial comparing the efficacy of a short hormone therapy in combination with radiotherapy to radiotherapy alone as a salvage treatment for patients with detectable PSA after radical prostatectomy. *J Clin Oncol*, 2017, 35 (6 Suppl): 16.

DOI 10.1007/s10330-020-0424-4

Cite this article as: Zhang LF, Pan DL, Liu LD, *et al*. Salvage treatments for prostate-specific antigen relapse of cT₃N₀M₀ prostatic adenocarcinoma after radical prostatectomy combined with neoadjuvant androgen deprivation. *Oncol Transl Med*, 2020, 6: 272–276.

Intervention for oxaliplatin-induced hypersensitivity in China: a cross-sectional internet-based survey*

Min Li¹, Wei Li¹, Yue Wang², Xiaofang Shangguan³, Rui Huang³, Dong Liu¹,
Chengliang Zhang¹ (✉)

¹ Department of Pharmacy, Tongji Hospital, Tongji Medical College, Huazhong University of Science and Technology, Wuhan 430030, China

² Statistical Department, Tongji Hospital Affiliated with Tongji Medical College, Huazhong University of Science and Technology, Wuhan 430030, China

³ School of Pharmacy, Tongji Medical College, Huazhong University of Science and Technology, Wuhan 430030, China

Abstract

Objective This cross-sectional study aimed at investigating the intervention status and the influence of oncologists on oxaliplatin-induced hypersensitivity reactions (OIHR).

Methods Snowball sampling was used to send questionnaires to oncologists in various provinces and cities in China, via the internet, to collect data on their socio-demographic characteristics, the occurrence of OIHR, and the current status of interventions. One-way ANOVA and T-test of geographic samples were used to explore the relationship between the incidence of OIHR and intervention measures.

Results A total of 401 valid questionnaires were collected, most respondents were 30–40 years old, and most oncologists had 5 years of working experience. The proportions of glucocorticoid and H1 receptor antagonist use for OIHR prevention were 67.83% and 38.65%, respectively. The proportion of oncologists with longer working years and higher professional titles who used glucocorticoids for OIHR prevention was higher, and the observed OIHR incidence was lower. Pretreatment with glucocorticoids may be an effective preventive measure and can reduce the incidence of the OXA allergic reactions ($P < 0.05$).

Conclusion The risk awareness of junior oncologists to OIHR prevention should be strengthened, and clinical efficacy evaluation of glucocorticoids in OIHR prevention should be further promoted.

Key words: oxaliplatin; hypersensitivity reactions; intervention; cross-sectional survey

Received: 28 June 2020

Revised: 16 July 2020

Accepted: 23 August 2020

Oxaliplatin (OXA), the third-generation platinum-containing chemotherapeutic agent, is widely used for the treatment of colorectal cancers [1]. Its primary side effect is sensory neurotoxicity, and hematological and gastrointestinal toxicities. The high frequency of OXA use in gastrointestinal cancer patients has resulted in an increase in the reports of oxaliplatin-induced hypersensitivity reactions (OIHR), with the incidence increasing from < 1% to 23.8% [2–3]. Hypersensitivity reactions during oxaliplatin infusion can result in treatment discontinuation, which prolongs hospital stay

and may be life threatening [4].

However, there are no optimal measures and suggestions for the prevention of such reactions. Furthermore, the exact mechanism of the pathophysiology of OIHR remains unclear. Glucocorticoids and H1 receptor antagonists have been the main drugs used to prevent this allergic reactions [5–6]; however, their effect remains unelucidated. Therefore, the present study aimed at investigating the current status of drug intervention for OIHR by oncologists, using questionnaires, and at providing references for clinicians.

✉ Correspondence to: Chengliang Zhang. Email: clzhang@tjh.tjmu.edu.cn

*Supported by grants from the Hubei Center for Adverse drug reaction Monitoring (No. 20160422), the funding for research-oriented clinician plan of Tongji Medical College, Huazhong University of Science and Technology (No. 5001540076), and the Health Research Fund of Hubei Province (No. WJ2019M117).

© 2020 Huazhong University of Science and Technology

Materials and methods

Subjects

According to the principle that the selected subjects should be representative, this study distributed questionnaires to doctors engaged in tumor treatment in all provinces and cities of China through the Internet using snowball sampling, from September 1, 2019 to November 30. This study was approved by the Medical Ethics Committee of Tongji Hospital, Tongji Medical College, Huazhong University of Science and Technology.

Methods

Data Measures

Self-designed questionnaires were designed by two experienced oncology pharmacists via literature review and clinical interviews on OIHR interventions. The questionnaire was comprised of three major sections. The first section provided to the participants the study purpose and method for filling the survey. The second section comprised of five items about the subject demographic characteristics, including age, gender, level of education, title, and working years. The third part enquired about specific usage of glucocorticoids and H1 receptor antagonists, and the incidence of OIHR observed by subjects. The incidence of OIHR was assigned 1, 2, 3, 4, and 5 points for “ $\leq 1\%$ ”, “1%–3%”, “3%–5%”, “5%–10%”, and “ $\geq 10\%$ ”, respectively, and the mean value was calculated. The statistical results were expressed as ($\bar{x} \pm SD$) values, and a higher value meant a higher incidence.

Statistical analysis

Epi Data version 3.1 (USA) was used for data entry, and the data collected were analyzed using IBM Statistical Package for Social Sciences version 19.0 (SPSS Inc., Chicago, IL, USA). Both descriptive and inferential statistics were applied for data analyses. We describe the demographic characteristics of oncologists, premedication for OIHR, and the average score for OIHR incidence. Besides, the Chi-square test, One-way ANOVA, and T-test were used to analyze the association between OIHR preventive drug use and OIHR occurrence. All tests were two-sided, and a P value < 0.05 was considered statistically significant.

Results

Study subject characteristics and prophylactic medication status

A total of 416 questionnaires were issued and 401 valid questionnaires were collected from 31 provinces or administrative regions of China, except Qinghai, Ningxia, and Taiwan, with a response rate of 96.39%. Women accounted for a large proportion (61.10%) of the 401 oncologists.

Approximately 32.92% of the subjects were under 30 years old, 176 (43.89%) were 30–40 years old, and 93 (23.19%) were over 40 years old. Among them, 52.12% of the oncologists had been engaged in tumor work for less than 5 years, 19.20% had been engaged for 5–10 years, and 28.68% had been engaged for more than 10 years. A total of 217 persons had bachelor's degrees or less (54.11%), 159 had master degrees (39.65%), and 25 had doctorates (6.24%); 106 (26.43%) oncologists were juniors, 217 (54.11%) were intermediates, and 78 (19.46%) were seniors (Table 1).

Among the respondents, 272 oncologists (67.83%) used glucocorticoids for OIHR prevention, 155 (38.65%) used H1 receptor antagonists for intervention, 29.92% used both glucocorticoids and H1 receptor antagonists, and 23.44% administered no preventive therapy. Oncologists with more than 10 years ($P = 0.015$) experience and at least senior titles ($P = 0.040$), tended to use glucocorticoids as intervention for OIHR, whereas those with junior titles tended to use H1 receptor antagonists (Table 1).

Subject demographic characteristics and OIHR incidence

There were no statistically significant differences between the gender, age, and educational level of the participating oncologists and the observed OIHR incidence ($P = 0.225, 0.765, \text{ and } 0.784$, respectively). However, the working years and professional title of the medical staff significantly affected the observed incidence ($P = 0.009, 0.041$, respectively) (Table 2).

Interventions and OIHR incidence

The average score of the above mentioned conditions and the OIHR incidence were statistically analyzed among oncologists who used glucocorticoids and H1 receptor antagonists alone for OIHR prevention, as well as the combination or no drug intervention. The results showed that the P values of the combination of both drugs, or glucocorticoids and H1 receptor antagonists alone, were 0.043, 0.044, and 0.096, respectively, compared with no preventive drug use (Table 3). The results demonstrated that premedication with glucocorticoids before chemotherapy, either alone or in combination with H1 receptor antagonists, could reduce the incidence of OXA allergic reaction to a certain extent.

Discussion

OXA, a third-generation platinum drug, is extensively used for the treatment of gastrointestinal cancers and other tumors, due to its low toxicity and broad anti-tumor spectrum^[7]. Nevertheless, OIHR can lead to chemotherapy discontinuation and a poor quality of life, thus posing a potential threat to cancer patients^[8]. Symptoms of

Table 1 Study subject characteristics and OIHR prophylactic medication status

Characteristics (n)	The usage of glucocorticoids			The usage of H1 receptor antagonists		
	n (%)	χ^2	P	n (%)	χ^2	P
Gender						
Male (156)	100 (64.10)	0.024	0.877	55 (35.26)	0.656	0.418
Female (245)	172 (70.20)			100 (40.82)		
Age (years)						
≤ 30 (132)	90 (68.18)	2.652	0.266	48 (36.36)	1.056	0.590
30–40 (176)	125 (71.02)			73 (41.48)		
≥ 40 (93)	57 (61.29)			34 (36.56)		
Working years						
≤ 5 (209)	130 (62.20)	8.373	0.015*	82 (39.23)	0.741	0.690
5–10 (77)	54 (70.13)			32 (41.56)		
≥ 10 (115)	88 (76.52)			41 (35.65)		
Educational level						
Bachelor and below (217)	140 (64.52)	3.285	0.194	96 (44.24)	0.726	0.696
Masters (159)	112 (70.44)			54 (33.96)		
Doctor (25)	20 (80)			5 (20)		
Title						
Junior and below (106)	63 (59.43)	6.437	0.040*	41 (38.68)	0.726	0.696
Intermediate (217)	151 (69.59)			87 (40.09)		
Senior (78)	58 (74.36)			27 (34.62)		

* P < 0.05

OIHR range from cutaneous reactions such as flushing, pruritus, and urticarial, to life-threatening respiratory and cardiovascular conditions such as anaphylactic shock,

acute hemolysis, and thrombocytopenia [9].

Currently, the mechanism of OIHR remains unelucidated. However, the mechanism underlying hypersensitivity to OXA is reportedly associated with immunoglobulin E (IgE)-mediated hypersensitivity [10–11]. Domestic and foreign literature have reported that OIHR often occurs after multi-cycle chemotherapy [12–13], and that a few patients develop allergic reactions at first OXA infusion. This suggests that OIHR can occur at any chemotherapy cycle. At present, there are no effective measures for preventing and treating OIHR. Premedication, prolonged OXA infusion time, and desensitization therapy may reduce the occurrence of these reactions [14–15]. Most physicians use glucocorticoids and histamine receptor antagonists for OIHR prevention [16–17]. Glucocorticoid is the most important stress-regulating hormone in the body, and is also the most widely clinically used and effective anti-inflammatory and immunosuppressant agent. Dexamethasone is the most common glucocorticoid used for hypersensitivity intervention. H1 receptor antagonists mainly prevent histamine production by acting on target cells through reversible competition for histamine receptor sites on cells, thus blocking H1 receptors to play an anti-allergy role. Additionally, promethazine and diphenhydramine are the most commonly used histamine receptor antagonists.

However, the current situation of drug intervention for OIHR prevention in China remains unknown. This

Table 2 Subject basic information and average OIHR score

Demographic characteristics (n)	Average score of OXA allergic reaction rate ($\bar{x} \pm SD$)	F/t	P
Gender			
Male (156)	2.41 ± 0.90	0.858	0.225
Female (245)	2.33 ± 0.91		
Age (years)			
≤ 30 (132)	2.40 ± 0.84	0.260	0.765
30–40 (176)	2.36 ± 0.91		
≥ 40 (93)	2.31 ± 0.99		
Working years			
≤ 5 (209)	2.49 ± 0.84	4.788	0.009*
5–10 (77)	2.17 ± 0.90		
≥ 10 (115)	2.25 ± 0.99		
Educational level			
Bachelor and below (217)	2.38 ± 0.93	0.243	0.784
Masters (159)	2.32 ± 0.88		
Doctor (25)	2.44 ± 0.82		
Title			
Junior and below (106)	2.45 ± 0.77	4.277	0.041*
Intermediate (217)	2.21 ± 0.98		
Senior (78)	2.14 ± 0.96		

* P < 0.05

Table 3 Interventive measures and OIHR incidence

Interventive measures	n (%)	Average score of OXA allergic reaction rate ($\bar{x} \pm SD$)	F/t	P	P ^a
Combination of glucocorticoid and H1 receptor antagonist	120 (29.92)	2.26 ± 0.96			0.043*
Glucocorticoid alone	152 (37.90)	2.27 ± 0.92	2.056	0.015	0.044*
H1 receptor antagonist alone	35 (8.73)	2.50 ± 0.71			0.906
No drug intervention	94 (23.44)	2.52 ± 0.97			

Compared with no drug intervention, * $P < 0.05$

cross-sectional study involved the distribution of a survey to clinical oncologists on the current status of OIHR interventions. The study also analyzed the factors that may affect the incidence of these reactions, so as to provide references for oncologists. The results showed that 76.56% of oncologists had adopted interventions: 67.83% used glucocorticoids for OIHR prevention, while 38.65% used H1 receptor antagonists. Moreover, a few oncologists used both drugs. Additionally, oncologists with longer working years and a higher professional title better adapted to intervention with glucocorticoid, and observed a lower incidence of OXA allergic reactions. Therefore, it is necessary to strengthen risk awareness training for less experienced oncologists with lower titles, to enhance their knowledge on OIHR prevention.

Some oncologists used a combination of both drugs for prevention. Thus, the difference between the effects of glucocorticoids and H1 receptor antagonists alone and that of the combination in OIHR prevention, were analyzed. The analysis showed that glucocorticoids might effectively reduce the incidence of allergic reactions. We concluded that oncologists in China were not only inclined to use glucocorticoids for OIHR prevention, but that the observed incidence of the reactions was lower with their use, indicating premedication with glucocorticoids might be an effective way of preventing OIHR.

Although this study analyzed the intervention status of OIHR and the potential effect, it had the following limitations. First, although we collected 401 questionnaires which can be reflective of the situation in the country to some extent, some provinces were not covered, and there were differences in the number of questionnaires completed by each provinces, inevitably introducing bias. Furthermore, the study investigated OIHR incidence via the personal experiences of the respondents, rather than the real clinical incidence of OIHR, introducing bias owed to subjectivity. Further, different strains of glucocorticoids and H1 receptor antagonists are used for prevention, and the doses and frequency used by each oncologist may be different. Therefore, this paper failed to properly evaluate the different treatment strategies applied by oncologists. These establish the need for further analytical research with a larger sample size.

In conclusion, this paper investigated the OIHR

interventions of oncologists in China, which can reflect their knowledge and application of OIHR treatment options to some extent. Furthermore, it provides reference for physicians for the need to further enhance their cognition of OIHR treatment and prevention, to enhance safe clinical OXA use.

Conflicts of interest

The authors indicated no potential conflicts of interest.

References

- Vyskocil J, Tucek S, Kiss I, *et al.* Type II hypersensitivity reactions after oxaliplatin rechallenge can be life threatening. *Int Immunopharmacol*, 2019, 74: 105728
- Parel M, Ranchon F, Nosbaum A, *et al.* Hypersensitivity to oxaliplatin: clinical features and risk factors. *BMC Pharmacol Toxicol*, 2014, 15: 1.
- Phull P, Quillen K, Hartshorn KL. Acute oxaliplatin-induced hemolytic anemia, thrombocytopenia, and renal failure: case report and a literature review. *Clin Colorectal Cancer*, 2017, S1533-0028: 30259–30256.
- Rogers BB, Cuddahy T, Briscella C, *et al.* Oxaliplatin: detection and management of hypersensitivity Reactions. *Clin J Oncol Nurs*, 2019, 23: 68–75.
- Nozawa H, Muto Y, Yamada Y. Desensitization to oxaliplatin with two stages of premedication in a patient with metastatic rectal cancer. *Clin Ther*, 2008, 30: 1160–1165.
- Lee SY, Kang HR, Song WJ, *et al.* Overcoming oxaliplatin hypersensitivity: different strategies are needed according to the severity and previous exposure. *Cancer Chemother Pharmacol*, 2014, 73: 1021–1029.
- Khurana A, Mitsis D, Kowligi GN, *et al.* Atypical presentation of fever as hypersensitivity reaction to oxaliplatin. *J Oncol Pharm Pract*, 2014, 22: 319–324.
- Shao YY, Hu FC, Liang JT, *et al.* Characteristics and risk factors of oxaliplatin-related hypersensitivity reactions. *J Formos Med Assoc*, 2010, 109: 362–368.
- Madrigal-Burgaleta R, Berges-Gimeno MP, Angel-Pereira D, *et al.* Desensitizing oxaliplatin-induced fever: a case report. *J Investig Allergol Clin Immunol*, 2013, 23: 435–447.
- Bano N, Najam R, Qazi F, *et al.* Clinical features of oxaliplatin induced hypersensitivity reactions and therapeutic approaches. *Asian Pac J Cancer Prev*, 2016, 17: 1637–1641.
- Aroldi F, Prochilo T, Bertocchi P, *et al.* Oxaliplatin-induced hypersensitivity reaction: underlying mechanisms and management. *J Chemother*, 2015, 27: 63–66.
- Park SJ, Lee KY, Park WS, *et al.* Clinical outcomes of reintroducing

- oxaliplatin to patients with colorectal cancer after mild hypersensitivity reactions. *Oncology*, 2013, 85: 323-327.
13. Ohta H, Hayashi T, Murai S, *et al.* Comparison between hypersensitivity reactions to cycles of modified FOLFOX6 and XELOX therapies in patients with colorectal cancer. *Cancer Chemother Pharmacol*, 2017, 79: 1021–1029.
 14. Rose PG, Metz C, Link N. Desensitization with oxaliplatin in patients intolerant of carboplatin desensitization. *Int J Gynecol Cancer*, 2014, 24: 1603–1606.
 15. Cercek A, Park V, Yaeger R, *et al.* Faster FOLFOX: Oxaliplatin can be safely infused at a rate of 1 mg/m²/min. *J Oncol Pract*, 2016, 12: e548–e553.
 16. Park HJ, Lee JH, Kim SR, *et al.* A new practical desensitization protocol for oxaliplatin-induced immediate hypersensitivity reactions: A necessary and useful approach. *J Investig Allergol Clin Immunol*, 2016, 26: 168–176.
 17. Yamauchi H, Goto T, Takayoshi K, *et al.* A retrospective analysis of the risk factors for allergic reactions induced by the administration of oxaliplatin. *Eur J Cancer Care*, 2015, 24: 111–116.

DOI 10.1007/s10330-020-0443-3

Cite this article as: Li M, Li W, Wang Y, *et al.* Intervention for oxaliplatin-induced hypersensitivity in China: a cross-sectional internet-based survey. *Oncol Transl Med*, 2020, 6: 277–281.



中国科技核心期刊

(中国科技论文统计源期刊)

收录证书

CERTIFICATE OF SOURCE JOURNAL
FOR CHINESE SCIENTIFIC AND TECHNICAL PAPERS AND CITATIONS

ONCOLOGY AND TRANSLATIONAL MEDICINE

经过多项学术指标综合评定及同行专家
评议推荐，贵刊被收录为“中国科技核心期
刊”（中国科技论文统计源期刊）。

特颁发此证书。

中国科学技术信息研究所

Institute of Scientific and Technical Information of China

北京复兴路 15 号 100038

www.istic.ac.cn

2019年11月





Call For Papers

Oncology and Translational Medicine

(CN 42-1865/R, ISSN 2095-9621)

Dear Authors,

Oncology and Translational Medicine (OTM), a peer-reviewed open-access journal, is very interested in your study. If you have unpublished papers in hand and have the idea of making our journal a vehicle for your research interests, please feel free to submit your manuscripts to us via the Paper Submission System.

Aims & Scope

- Lung Cancer
- Liver Cancer
- Pancreatic Cancer
- Gastrointestinal Tumors
- Breast Cancer
- Thyroid Cancer
- Bone Tumors
- Genitourinary Tumors
- Brain Tumor
- Blood Diseases
- Gynecologic Oncology
- ENT Tumors
- Skin Cancer
- Cancer Translational Medicine
- Cancer Imageology
- Cancer Chemotherapy
- Radiotherapy
- Tumors Psychology
- Other Tumor-related Contents

Contact Us

Editorial office of Oncology and
Translational Medicine
Tongji Hospital
Tongji Medical College
Huazhong University of Science
and Technology
Jie Fang Da Dao 1095
430030 Wuhan, China
Tel.: 86-27-69378388
Email: dmedizin@tjh.tjmu.edu.cn;
dmedizin@sina.com

Oncology and Translational Medicine (OTM) is sponsored by Tongji Hospital, Tongji Medical College, Huazhong University of Science and Technology, China (English, bimonthly).

OTM mainly publishes original and review articles on oncology and translational medicine. We are working with the commitment to bring the highest quality research to the widest possible audience and share the research work in a timely fashion.

Manuscripts considered for publication include regular scientific papers, original research, brief reports and case reports. Review articles, commentaries and letters are welcome.

About Us

- Peer-reviewed
- Rapid publication
- Online first
- Open access
- Both print and online versions

For more information about us, please visit:

<http://otm.tjh.com.cn>



Editors-in-Chief

Prof. Anmin Chen (Tongji Hospital, Wuhan, China)
Prof. Shiyong Yu (Tongji Hospital, Wuhan, China)